FUEL CELLS AS A BACKUP ENERGY SOURCE FOR HIGH AVAILABILITY NETWORK SERVERS

A Thesis

by

DANIEL ALAN HUMPHREY

Submitted to the Office of Graduate Studies of
Texas A&M University
in partial fulfillment of the requirements for the degree of

MASTER OF SCIENCE

August 2008

Major Subject: Electrical Engineering

FUEL CELLS AS A BACKUP ENERGY SOURCE FOR HIGH AVAILABILITY NETWORK SERVERS

A Thesis

by

DANIEL ALAN HUMPHREY

Submitted to the Office of Graduate Studies of
Texas A&M University
in partial fulfillment of the requirements for the degree of

MASTER OF SCIENCE

Approved by:

Chair of Committee,	Prasad Enjeti
Committee Members,	Hamid Toliyat
	Aniruddha Datta
	Emil Straube
Head of Department,	Costas Georghiades

August 2008

Major Subject: Electrical Engineering

ABSTRACT

Fuel Cells as a Backup Energy Source for High Availability Network Servers.

(August 2008)

Daniel Alan Humphrey, B.S., Texas A&M University

Chair of Advisory Committee: Dr. Prasad Enjeti

This thesis proposes an uninterruptible power supply, UPS for high availability servers with fuel cells as its back up energy source. The system comprises a DC to DC converter designed to accommodate the fuel cell's wide output voltage range. A server power supply is specified, designed and simulated for use with this UPS. The UPS interfaces internal to the server power supply, instead of providing standard AC power. This topology affords enhanced protection from faults and increases overall efficiency of the system by removing power conversions. The UPS is simulated with the designed power supply to demonstrate its effectiveness.

TABLE OF CONTENTS

CHAPTER Page

LIST OF FIGURES

Page

Page

Page

Page

LIST OF TABLES

Page

CHAPTER I

INTRODUCTION

1.1 Introduction

The role of computers and computer automation continue to expand; enabling more applications for all aspects of human life. This increasing role has led to the dependence of these applications and more specifically for the application's complete availability.

To minimize the impact of utility disturbances, computer administrators and users have employed many technologies. Some of these include:

- redundant, independent input power feeds
- backup generators
- uninterruptible power supplies

Redundant and independent input power feeds allow a single input power source to fault, without impacting the availability of the application computer system or server. Utilizing this solution requires the capital investment of bringing two independent utility sources to the application site, or datacenter; along with doubling the cost of internal distribution of the two source feeds. The application server must also support two independent online power supplies enabling the benefit of separate independent AC power feeds. Requiring the support of independent power supplies limits available server

---

This thesis follows the style of *IEEE Transactions on Power Electronics*.

product lines and also significantly decreases overall power conversion efficiency by lowering the nominal operating load point of each power supply.

In certain locations it is not practical or possible to bring independent utility sources to the datacenter. When this is the case on site generators can act as a second source of power. This can be implemented as the independent power source as was previously mentioned, or paralleled with a transfer switch. If the generators are implemented as an independent power source as previously discussed, the requirement for a server to support two power supplies and the need for redundant wiring still exists. Another possible solution would employ a transfer switch. These devices transfer the load from one power source to another. This would eliminate need for redundant power supplies and the parallel power distribution. A salient shortcoming to this solution is that without sufficient ride-through energy storage, the generators would need to run continuously to ensure no interruptions occur. This drawback is due to the significant amount of time a generator requires to transition from standby to online. To compensate a source of ride-through energy storage is needed to ride-through the time from fault to fully online backup generators.

Ride-through energy typically is provided by an uninterruptible power supply, or UPS. This term encompasses power supplies which will maintain sufficient energy for its load during interruptions of the primary power source.

1.2 Uninterruptible power supplies

Most uninterruptible power supply systems are very similar. The supplies monitor a primary power source and when a fault is detected, they convert energy stored

by their energy source into usable energy to supplement or replace the primary power source. Typical UPS implementations include:

- offline
- online double conversion
- line interactive

An offline UPS remains dormant until a line failure is detected. When the fault is detected the UPS powers on and begins supplying power. This power supply minimizes stand by power loss by remaining dormant until a fault condition occurs, but sacrifices reaction time to the fault conditions. This reaction time can be on the order of an entire AC cycle. This shortcoming requires that any server connected to an offline UPS must store enough energy internally to ride-through the offline UPS rise time.

Online UPS systems are the opposite of an offline UPS. These systems provide power to the loads continuously. During no fault conditions, the online UPS supplies power from the primary power source. When a primary power fault occurs, the UPS switches to backup energy storage. In doing this, online UPS systems minimize disturbances to the load, but there is a power loss due to the system continually generating the entire server load. This power loss is present during both fault and no fault conditions. The term double conversion applies to most online UPS systems. Most primary power sources are AC. Typical UPS energy storage devices provide their energy by DC. In order for the online UPS to output AC to the load, two conversions are required. The first is a rectification of the input power to DC and then an inversion back

to AC. This allows the energy from the backup energy source to be utilized more effectively and for charging of the energy source to occur.

Line interactive UPS systems condition and regulate the output power. During no fault conditions, power is routed through a conditioning stage, which is normally passive straight to the output. An inverter is typically connected to the energy storage devices and it maintains the output voltage between a set of predetermined values. This topology can save power over the double conversion online UPS during no fault conditions, but loses its ability to tightly regulate the output power.

All UPS systems have in common an energy storage element which they use to provide power while the primary source is in a fault condition. Some energy storage devices are:

- flywheels
- batteries
- capacitors
- fuel cells

Flywheels are mechanical energy storage devices. Their energy is stored in the rotational kinetic energy of a mass. A typical flywheel can act as a DC generator when the stored energy is needed. They do require energy to maintain momentum, but are typically in a vacuum to minimize the continual power loss. They are more environmentally favorable than other energy sources, but are limited in how much ride-through time they can store. Flywheels are best suited for ride-through times of a seconds or less.

Batteries are often the preferred choice of backup power. They have been used for quite some time in UPS applications, which has great appeal to the computing industry. Electrically, they are fairly easy to design for and provide reasonable power slew rates. Some drawbacks to batteries include:

- real estate
- maintenance
- environmental impact of manufacturing
- environmental impact of disposal

Capacitors are similar to batteries electrically, but there are significant differences and tradeoffs [1]-[2]. When comparing energy storage to batteries, capacitors weigh much less than their battery counterparts; however, their energy density is less than that of batteries [1]. Super capacitors can also be fully charged and discharged many more times than batteries, and allow for full discharges [1]. The capacitors require almost no maintenance until their life cycle has expired and replacement is needed [2]. Due to these considerations they are potentially better suited for shorter energy delivering requirements [2].

Batteries, flywheels and capacitors all hold a finite amount of energy. To increase the amount of energy stored, more components or larger components are required. Flywheels require an increased rotational speed or more mass. Increasing the capacity of batteries and capacitors requires purchasing more of them. Markedly different from all of these is the fuel cell. The fuel cell stores its energy in fuel, and then converts it as it is needed. With this, an increase in energy storage means only increasing

the amount of fuel on hand. This is similar to a backup generator, but without the negative environmental impacts.

1.3 Fuel cells

The fuel cell is a DC power source with very environmentally favorable exhaust. Fuel cells utilize chemical reactions to produce electricity. Hydrogen rich fuels are reacted such that during the reaction, the electron and protons of the hydrogen atom separate. The electrons are forced through an anode and cathode producing electricity. For polymer electrolyte membrane, PEM fuel cells the exhaust is water. Individual fuel cells produce very low voltage potentials, so in most applications they must be stacked in series.

Fuel cells require power conditioning due to severe voltage drops across their full load range. This voltage ratio can often be in the two to one range across the full load range for a given fuel cell stack. Also, do to the inherent nature of the fuel cell, slow power slew rates exist compared to other energy storage devices. A typical voltage to current plot for three different fuel cells is shown in Fig. 1 [3].

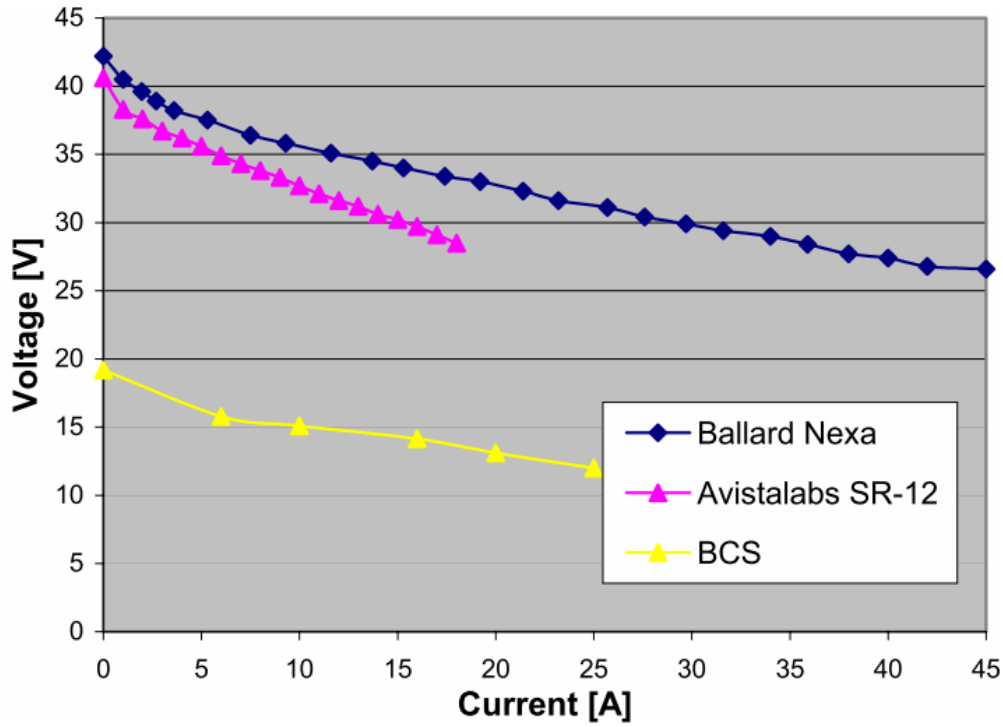

Fig. 1 Typical fuel cell voltage to current graph [3]

1.4 Fuel cell server applications

Fuel cells are a superior energy storage device for a UPS powering a small number of critical servers. Some salient benefits are:

- fuel capacity based energy storage
- cheaper storage requirements for fuel versus other options
- environmentally friendly exhaust
- no charge circuitry required

To increase ride-through time during fault conditions, alternate energy storage options require wiring large numbers of elements together. To accomplish this, a fuel

cell requires only a larger amount of fuel. The transfer of fuel from its tank to the fuel cell is lossless. With this, the fuel tank can be far away from the cell itself. This is a major benefit over other energy storage devices. Other energy storage options lose efficiency the further they are from the load due to resistive conduction losses.

Batteries require very strict environmental conditions. Fuel for fuel cells can typically be stored in much less controlled environment. This is a great advantage for all applications, especially any application requiring extended amounts of backup power usage.

The exhaust of PEM fuel cells is water. Environmentally there is no comparison between this and the manufacturing and disposal of all types of batteries.

The fuel cell does not require charge circuitry since it is effectively a generator. This eliminates the losses incurred from such a converter and also removes a point of failure in the UPS power system.

Two primary concerns arise when designing a fuel cell based UPS for servers. The first is in designing a wide input converter which meets output loads transient requirements and the fuel cells transient capabilities. The second issue comes in deciding where to incorporate the fuel cell into the overall server power delivery infrastructure.

1.5 Previous work

The selection of the best topology for the fuel cell converter depends greatly on the total load of the converter and the transient requirements of the load and source. The converter must also accommodate the fuel cell's wide input voltage range. There are several proposed topologies for step up DC to DC converters for fuel cells [4]-[9]. Two

approaches are generally used for fuel cell DC to DC converters. The first is a traditional single stage conversion [4]-[7]. The other is utilizing two conversion stages [8]-[9]. J.-T. Kim *et al.* [4] evaluated an active clamping current fed half bridge topology. M. Mohr and F.-W. Fuchs [5] explored using voltage and current fed full bridge converters as fuel cell converters. S.-R. Moon and J.-S. Lai [6] studied interleaving full bridge converters. S.-J. Jang *et al.* [7] analyzed a sepic and flyback hybrid converter. M. Harfman-Todorovic *et al.* [8] proposed cascaded paralleled boost converters with an isolated two inductor output stage. S.-G. Song *et al.* [9] introduced a cascaded buck and push-pull converter.

The backup power deliver topology depends greatly on ride-through requirements and the transient responses of the fuel cell with its converter. Fuel cell based UPS systems have been proposed [10]. W. Choi *et al.* [10] proposed a traditional UPS with backup energy provided by a fuel cell. This system outputs AC power to supply uninterruptible power as do traditional UPS systems. Q. Zhao *et al.* [11] discussed a battery based UPS specifically designed for network server applications. This proposed UPS outputs high voltage DC directly to the server [11].

1.6 Research objective

The thesis objective is to design and simulate a fuel cell based UPS for servers. The analysis and design involves designing a power supply for the server, followed by the design of a wide voltage input DC to DC converter for the fuel cell UPS.

A sample server power supply specification will be generated. The server power supply will be an interleaved two transistor forward converter along with a power factor

correcting boost converter. The two separate converters will be designed and tested alone. Once complete, the two converters will be simulated together and tested to meet the sample specification.

The fuel cell DC to DC converter will interact directly with the proposed fuel cell and be designed with the fuel cell's characteristics in mind. Exhaustive analysis and design will go into the converter followed by simulations. The DC to DC converter and fuel cell will compose the energy storage portion of the UPS.

Once the server power supply and the fuel cell converters are designed a sharing scheme will be designed into the simulations. This UPS will connect server power supply and the entire system will be simulated for robustness as a UPS.

1.7 Thesis outline

Chapter I of this thesis provides an overview of current industry solutions to provide maximum availability to servers. It explores the tradeoffs between existing solutions and explores current energy storage options. Fuel cells are introduced as an energy storage device for UPS applications. Attention is focused to some specific applications where fuel cells could be very useful for energy storage. The research objective is stated in the end.

Chapter II specifies a typical server power supply. A power supply solution is designed and simulated to meet the specification. At the end of the chapter the simulations are compared to actual waveforms from a server power supply.

Chapter III studies a PEM fuel cell and designs a power converter specifically for use as an energy backup to the power supply designed in the second chapter. A topology

review is carried out for this converter. A final topology is selected and the converter is designed and simulated. The converter will be tested with a fuel cell model as its power source.

Chapter IV designs and simulates using the fuel cell with its converter as a UPS for the server power supply. The UPS is first simulated in standalone with the server power supply to ensure the output specifications are met with the UPS as its power source. The UPS is then tested for robustness. The UPS is then compared to traditional approaches.

Chapter V provides a general conclusion of the work.

CHAPTER II

DESIGN OF A SERVER POWER SUPPLY

2.1 Introduction

Server power supplies come in a multitude of power levels and outputs. They accept AC and DC power and convert the power to the required voltages for the server in which they were intended. The vast majority of server power supplies today are AC powered since the majority of the world is on some form of an AC power grid. Server power architectures vary from server to server. Some servers require only a single input voltage, while others require many voltage outputs. Current high end servers use a single output voltage from their power supply to power the server. This simplifies the power supply design, reduces its form factor, and allows point of load modules to be sized specifically for its load. All of these increase the overall effectiveness and efficiency of the server power schemes. These high end servers are typically more reliable and their users would have more interest in increasing their server's availability. These users would be the target market for the UPS under investigation.

2.2 Sample specification

The following sections specify an 800 watt power supply which could be used in server computing systems. The specified server power supply will be designed and simulated for use in simulating the fuel cell converter in its actual application.

2.2.1 Input requirements

The server power supply shall operate under all input voltage and frequency conditions listed in Table I.

Table I Input voltage operating range

	Minimum	Maximum
Voltage	100 VRMS	240 VRMS
Frequency	50 Hz	60 Hz

The power supply shall maintain a true power factor greater than 0.95 for all input line conditions while supplying 800 watts of output power. The power supply shall operate uninterrupted while the input voltage varies through the entire input voltage range.

2.2.2 Output requirements

The server power supply shall provide a single output voltage with a set point listed in Table II.

Table II Output voltage set point

	Minimum	Typical	Maximum
Output Voltage at 1A Load	11.95 V	12.00 V	12.05 V

The minimum output capacitance of the power supply is 1,000 microfarads. The power supply must be unconditionally stable over all operating loads with a minimum

phase margin of 45 degrees and a minimum gain margin of 15 decibels when connected to the minimum specified output capacitance.

The static load output voltage must meet the requirements listed in Table III over all valid operating conditions.

Table III Static load output voltage regulation range

	Minimum	Maximum
Output Voltage	11.90 V	12.10 V

During transient loading conditions enumerated in Table IV the power supply must maintain dynamic output voltage regulation as listed in Table V. Transient loading slew rate will not exceed 0.5 amperes per microsecond.

Table IV Dynamic loading conditions

	Minimum	Maximum
Load Transient	0%	50%

Table V Dynamic output voltage regulation

	Minimum	Maximum
Output Voltage	10.8 V	13.2 V

The power supply must maintain dynamic regulation from Table V for at least 10 milliseconds during input voltage disturbances. This includes but is not limited to AC brownouts and AC dropouts.

The power supply output must meet ripple and noise requirements listed in Table VI.

Table VI Output ripple and noise specification

	Maximum
Voltage Ripple and Noise	120 mV (peak to peak)

2.3 Topology

The power conversion system to meet the power supply specification is shown in Fig. 2. The system comprises three distinct components. First, an input rectification stage with active power factor correction. Second, a DC-link stage containing enough

energy to support the specified holdup time for the system. Lastly, there is a DC to DC converter to generate the output voltage according to regulation specifications.

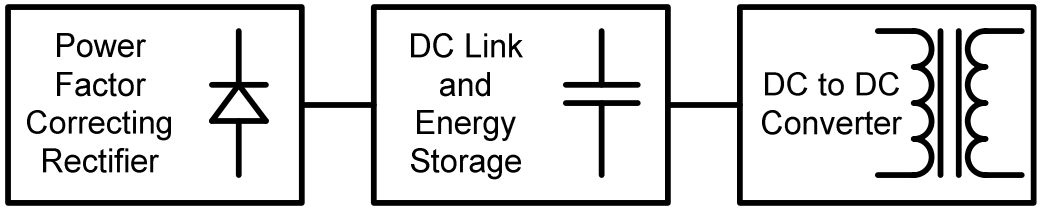

Fig. 2 Proposed power supply topology

The power factor correcting rectifier will be a full bridge rectifier followed by a boost converter. The DC link will be composed of electrolytic capacitors for ripple reduction, stability and energy storage. The output DC to DC converter will be an interleaved two transistor forward converter.

2.3.1 Power factor for datacenters

Power factor for datacenters deviates slightly from its mathematical definition. The datacenter is concerned with maximizing the fundamental frequency power factor as well as minimizing harmonic components in the current. When these two criteria are optimized, the lowest current levels are attained. This minimizes the volt amps for the datacenter and increases the number of servers a given component of the power infrastructure can support. Minimizing the apparent power saves infrastructure costs by not having to size the power delivery infrastructure any more than is necessary.

2.3.2 Power factor correction with a full bridge rectifier and boost converter

The power factor correcting boost converter serves two purposes. It must both regulate its output DC voltage and shape the input current to maximize fundamental frequency power factor while minimizing current harmonics. The basic schematic for the converter is shown in Fig. 3.

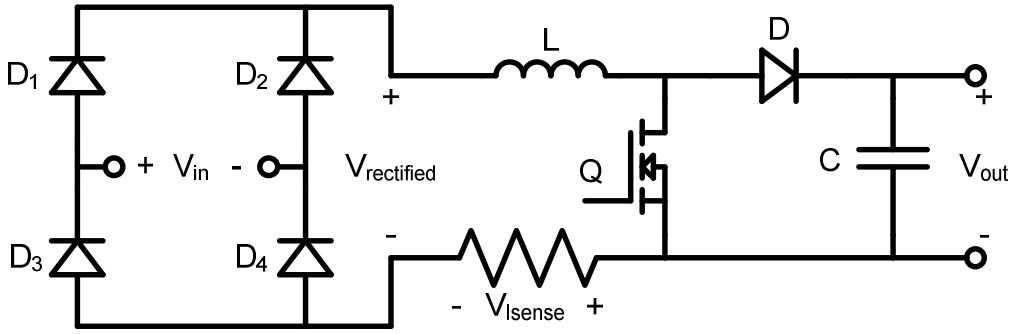

Fig. 3 Power factor correcting boost converter schematic

To serve its dual purpose, the boost converter must adjust its duty cycle based on the input current and the output voltage. Fig. 4 shows the control required to accomplish this.

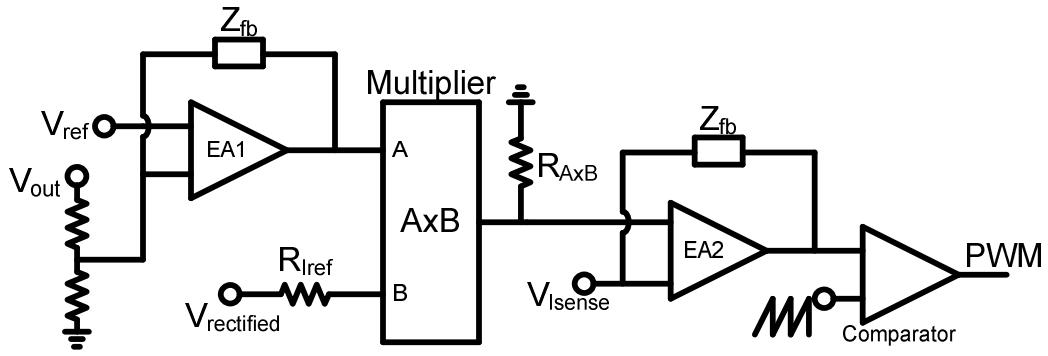

Fig. 4 Power factor correcting boost control schematic

The output voltage feedback is sent to an error amplifier and controlled to a reference voltage. The current reference comes from the rectified input voltage. The first error amplifier output along with the current reference is sent through a multiplier. The output of the multiplier is a full wave rectified voltage proportional to the output voltage error amplifier and the current reference waveform. To accommodate wide voltage inputs, the multiplier sometimes scales its output based on the amplitude of the input voltage. The multiplier output current creates a reference voltage signal through a resistor. The reference voltage signal and the current feedback voltage, via a current sense resistor are forced to equal through an error amplifier. The output of this error amplifier is used to generate the pulse width modulated waveform to control the boost converter. The boost converter must operate in continuous conduction mode to power factor correct properly.

2.3.3 Interleaved two transistor forward converter

The schematic of the two transistor forward converter is shown in Fig. 5. The converter contains two switches, Q1 and Q2 along with a transformer, T1 and an output stage similar to a buck converter.

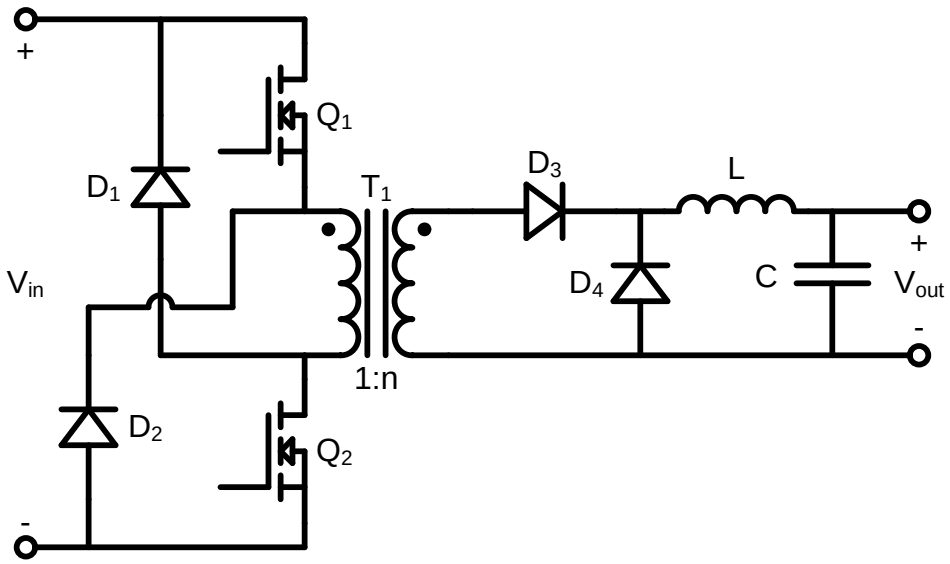

Fig. 5 Two transistor forward converter schematic

This converter has two modes of operations. These can be seen in Fig. 6. The first mode of operation occurs when the two transistors are turned on. This magnetizes the transformer and induces and positive voltage to bias the output diode and supply power to the output. The second mode of operation occurs when the transistors are switched off. During this time the primary recovery diodes conduct and any energy

stored in the magnetizing inductance is sent back to the input source. The transformer demagnetizes at the same rate as it magnetized in mode one. This limits the duty cycle to 50 percent to ensure that the transformer does not saturate.

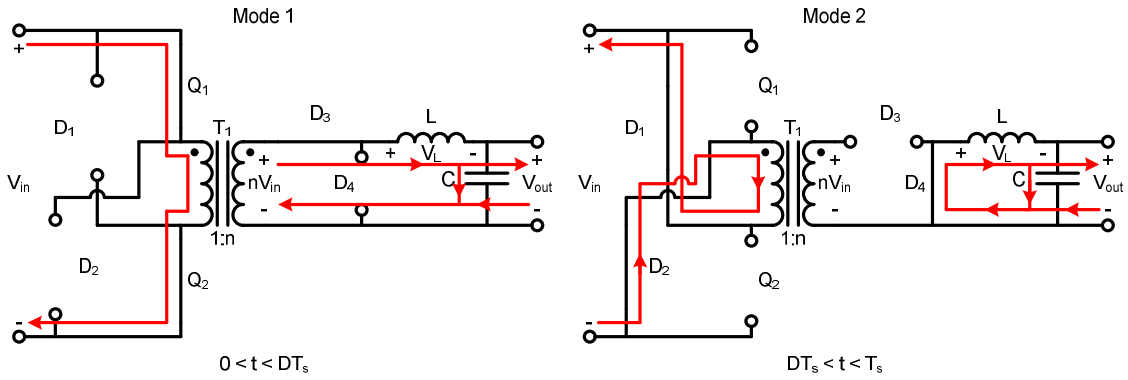

Fig. 6 Two transistor forward converter modes of operation

Solving for the gain requires volt-second analysis. During mode one, the inductor voltage is:

$$v_L = n \cdot V_{in} - V_{out} \tag{1}$$

During mode two operation the inductor voltage is given by:

$$v_L = -V_{out} \tag{2}$$

The volt-second integral for this converter is as follows:

$$\int_0^{T_s} v_L \cdot dt = D \cdot T_s \cdot \left(n \cdot V_{in} - V_{out}\right) + \left(1 - D\right) \cdot T_s \cdot -V_{out} = 0 \tag{3}$$

Solving for the output voltage results in:

$$V_{out} = n \cdot D \cdot V_{in} \tag{4}$$

The two transistor forward converter has many benefits. The voltage stress on the primary switches is a prominent feature. The maximum voltage either switch is exposed to is one half of the source voltage during turn on and the input voltage at turn off. This allows for lower drain-source voltage rated switches, which in turn reduces losses. The magnetizing energy in the forward converter is always returned to the voltage source. This improves efficiency and reliability while preventing elaborate methods to dissipate the stored energy.

Interleaving the two transistor forward converter is straight forward due to its inherent duty cycle limitation. Fig. 7 shows interleaved converters. The gate drives for the two waveforms are set 180 degrees out of phase. This prevents both from operating at the same time and doubles the effective switching frequency. The two converters share a common output filter. The interleaving allows for all of the benefits of increasing the switching frequency. These include:

- reduced output filter size
- improved transient response
- improved thermal characteristics

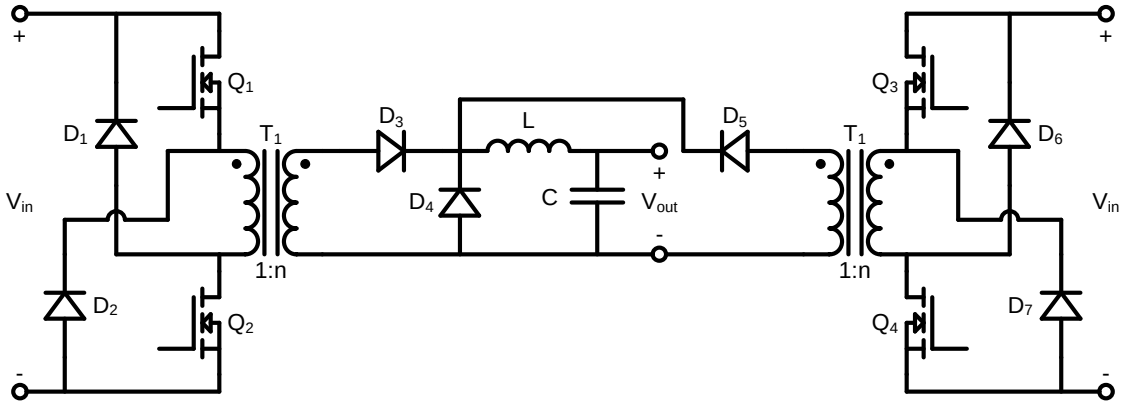

Fig. 7 Interleaved two transistor forward converter schematic

2.4 Design

The three components of the power supply have many interdependent design criteria. To address these tradeoffs, the design will begin with the DC link. Once complete the output DC to DC converter will be designed followed by the PFC boost converter design.

2.4.1 DC-link

The DC-link will provide output capacitance to the front end boost converter as well as energy storage for the power supply. The maximum input voltage for the power supply will be 240 VAC. Peak input voltage is given by:

$$V_{peak} = \sqrt{2} \cdot 240V \tag{5}$$

To ensure that the boost converter can power factor correct, the DC-link voltage must be sufficiently above the maximum rated input voltage. Traditionally, that voltage falls between 380 volts and 400 volts. The DC link voltage set point for this power supply will be a nominal 400 volts. This will determine the energy stored in the DC link capacitance.

Several factors influence the size of the DC-link capacitance for energy storage. These include:

- Output load
- Efficiency of DC to DC converter
- Total time required for hold up
- Maximum duty cycle of DC to DC converter topology
- Turn ratio of DC to DC converter transformer

The power supply's maximum specified load is 800 watts. The required input power to the output DC to DC converter at full load is given by:

$$P_{required} = \frac{P_{out}}{\eta_{DC-DC}} \tag{6}$$

The specified hold up time for the power supply is 10 milliseconds. The total energy storage requirement is given by:

$$E_{required} = P_{required} \cdot t_{holdup} \tag{7}$$

The final considerations for properly sizing the DC-link are the input voltage requirements of the DC to DC converter. As energy is removed from the DC-link capacitance, the input voltage of the DC to DC converter will decrease. The maximum duty cycle of the output converter along with its transformer turn ratio determine the minimum required input voltage to maintain voltage regulation at the output. The voltage gain for a two transistor forward converter is given by:

$$V_{out} = n \cdot D \cdot V_{in} \tag{8}$$

From this, the DC-link selection will directly influence the design of the transformer for the DC to DC converter. The holdup requirement is only for fault conditions, so minimizing design impacts on the DC to DC converter is desired. The minimum operating voltage will be limited to 80% of the nominal input voltage. This is selected to not impact the DC to DC converter too much.

The total amount of energy stored in a capacitor is given by:

$$E_{stored} = \frac{1}{2} \cdot C \cdot V^2 \tag{9}$$

The decision to maintain at least 80 percent of the voltage during fault conditions limits the available energy stored to:

$$E_{available} = \frac{1}{2} \cdot C \cdot \left(V_{no\min al}^2 - \left(0.8 \cdot V_{no\min al} \right)^2 \right) \tag{10}$$

Solving for capacitance and substituting from (6), (7) and (10) gives:

$$C_{DC-Link} = \frac{2 \cdot t_{holdup} \cdot \frac{P_{out}}{\eta_{DC-DC}}}{V_{no\min al}^2 - \left(0.8 \cdot V_{no\min al} \right)^2} \tag{11}$$

The minimum capacitance required in the DC-link for energy storage is about 330 microfarads. This capacitance will also serve as the output capacitance for the front end power factor correcting boost converter. This will be a consideration during the design of the front end converter. If needed, the capacitance will be increased for input converter.

2.4.2 DC to DC converter

Designing the DC to DC converter starts with a complete understanding of the input characteristics and output requirements. The input characteristics are determined by the design of the power factor correcting boost converter and its output capacitance, the DC link. The output voltage of the power factor correcting converter is a nominal 400 volts and the DC link energy storage is designed to store enough energy to maintain

80 percent of the nominal voltage. This sets the minimum input voltage of the converter to 320 volts. The output is specified to 12 volts.

The two transistor forward converter has an absolute maximum duty cycle of 0.5, but 80 percent of that will be used for design margin. This leaves each of the two interleaved converters with a maximum duty cycle of 0.4. Interleaving these two converters effectively doubles this available duty cycle to 0.8. Using equation (8) and solving for the required turns ratio yields:

$$n = \frac{V_{out}}{V_{in,\min} \cdot D_{\max}} \tag{12}$$

Solving for this converters required turn ratio results in a 21.3:1 primary to secondary turn ratio. Increasing to the next whole integer, the converter will require a 22:1 turn ratio.

The switching frequency of the converter is the next step in determining the required designed values for the rest of the converter. Many aspects of the converter are affected directly by the switching frequency including:

- Switching losses
- Conduction losses
- Transformers
- Output capacitance
- Inductance

The most salient tradeoff with respect to switching frequency is between switching losses and reduced output filter size. The goal is to take the switching frequency as high as possible, while maintaining a tolerable amount of switching loss.

The switching losses are mostly composed of the diode and transistor AC losses. For transistors these includes the turn on and turn off characteristics and the parasitic elements inherent from the device and its layout. The turn on and turn off delays coupled with rise and fall times can be seen in Fig. 8.

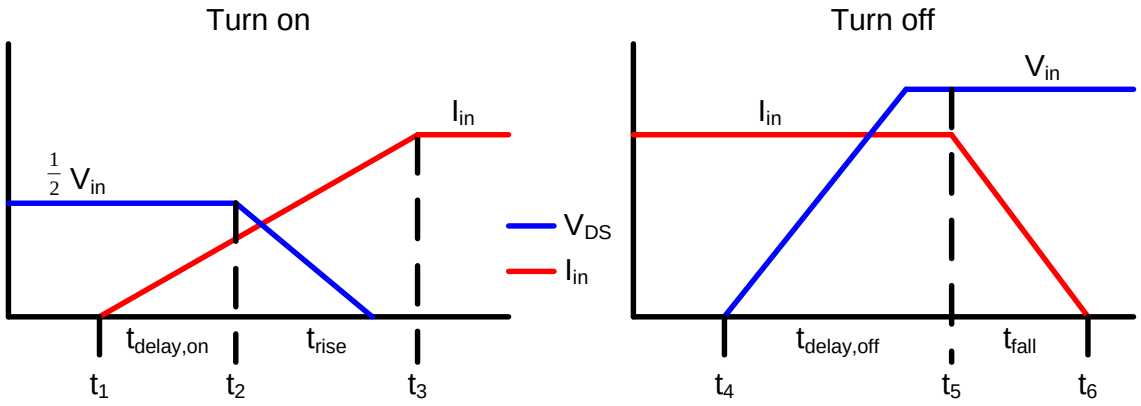

Fig. 8 Transistor turn on and turn off approximate waveforms

A fair estimate for turn on power loss is in a two transistor forward converter is given by:

$$P_{sw,on} = \left[\frac{1}{2}\cdot\left(\frac{1}{2}\cdot V_{in}\right)\cdot I_{\max}\cdot\left(t_{delay,on}+t_{rise}\right)\right]\cdot f \qquad (13)$$

Similarly, the turn off power loss is as follows:

$$P_{sw,off} = \left[\frac{1}{2} \cdot V_{in} \cdot I_{\max} \cdot \left(t_{delay,off} + t_{fall}\right)\right] \cdot f \tag{14}$$

In this application the voltage is nominally 400 volts and the current is around 2.4 amperes. Using the switching loss approximation and some timing values from a typical MOSFET the switching loss is around 30 microwatts per period. The switching losses here are linear with respect to switching frequency. Limiting the frequency to about 15 watts of switching loss per converter would result in a switching frequency of 250 kilohertz.

The size of the output inductor determines the ripple current and the continuous conduction region. The inductor current waveforms can be seen in Fig. 9.

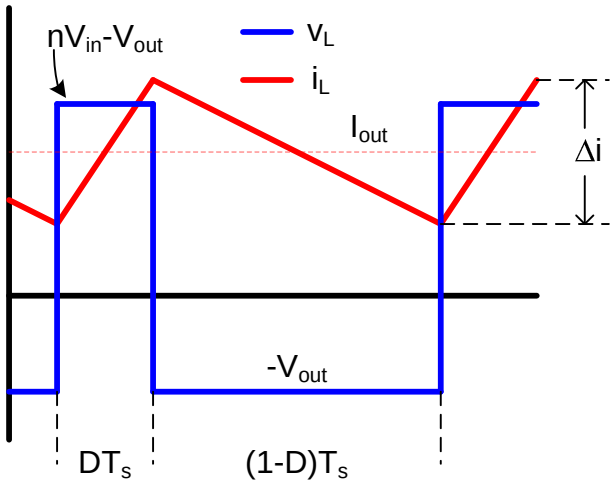

Fig. 9 Steady state interleaved two transistor forward inductor current

The current has a minimum just before the start of a new period, and peaks at the end of the duty cycle. The relationship between inductor voltage and current is given by the following:

$$v_L = L \cdot \frac{di}{dt} \tag{15}$$

During mode one the inductor voltage is equal to:

$$v_L = n \cdot V_{in} - V_{out} \tag{16}$$

The difference between the maximum current and the minimum current is the ripple current. Using a linear approximation, during mode one of operation, equation (15) becomes:

$$v_L = L \cdot \frac{\Delta i}{\Delta t} = n \cdot V_{in} - V_{out} \tag{17}$$

The change in time is the duty cycle times the switching frequency period. Solving for inductance gives:

$$L = \frac{\left(n \cdot V_{in} - V_{out}\right)}{\Delta i} \cdot D \cdot T_s \tag{18}$$

At full rated load, the output current is approximately 67 amperes. Using a 20 percent current ripple, the switching frequency of 500 kilohertz and the maximum designed duty cycle requires a minimum inductance of about 600 nanohenries.

The output ripple specification determines the minimum required output capacitance. There is also a minimum specification for output capacitance. If the minimum capacitance required exceeds the output capacitance, then more output capacitance must be added internal to the power supply. The voltage and current relationship of capacitors determines the required capacitance. This relationship is given by:

$$i_C = C \cdot \frac{dv}{dt} \tag{19}$$

The typical output voltage waveform is shown in Fig. 10. Similar to the inductor the minimum and maximum values occur during a single switching cycle.

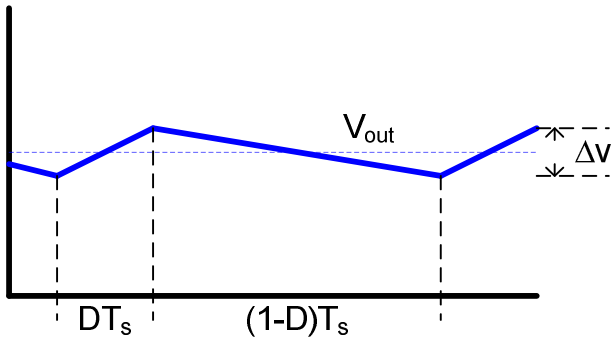

Fig. 10 Steady state interleaved two transistor forward converter output voltage

The capacitor current during both operating modes is:

$$i_C = i_L - \frac{V_{out}}{R} \tag{20}$$

The capacitor current is effectively the inductor current ripple. As the inductor current falls, the capacitor current rises to maintain a DC current. The capacitor effectively is being charged one half of the time and being discharged the other half of the time. During the discharge time, the minimum current is one half the inductor ripple current. The average current is one fourth the inductor current ripple. The change in time is exactly one half of the switching period. Using this linear approximation and solving for capacitance gives the following:

$$C = \frac{1}{2} \cdot \frac{1}{4} \cdot \Delta i \cdot \frac{\frac{1}{2} \cdot T_s}{\Delta v} \tag{21}$$

The voltage ripple is specified as 120 millivolts peak to peak. Substituting the remaining values for this converter requires at least 14 microfarads. The output capacitance is specified to be much higher than this. No internal capacitance is required to meet output voltage ripple; however, it may be required to meet specified stability margins. If this is the case, additional capacitance will be added internal to the power supply.

Everything required for the converter has been selected. Simulations will be used to determine the proper loop compensation and to test to specification.

2.4.3 Power factor correcting boost converter

To power factor correct, the boost converter must operate in a continuous mode of conduction. The inductor size determines how wide this range is. The inductor voltage during the boost converters first mode of operation, transistor is conducting is:

$$v_L = V_{in} \tag{22}$$

Likewise, the inductor voltage during the boost converter's second mode of operation, diode is conducting is:

$$v_L = V_{in} - V_{out} \tag{23}$$

Since these voltages are constant, the inductor currents are directly related to these voltages. To solve for ripple current substitute (22) into the characteristic equation of the inductor and take the linear approximation:

$$V_{in} = L \cdot \frac{\Delta i}{\Delta t} \tag{24}$$

The input voltage is variable. It is directly proportional to the inductance and inversely proportional to the duty cycle. The minimum input voltage will be used to determine the required inductance.

The switching frequency is inversely proportional to inductance. Limiting the switching frequency to well below international EMI requirements is critical to reduce EMI filter size as well as increasing efficiency. For these reasons a switching frequency of 100 kilohertz will be used.

The final criterion is the allowed ripple current. The customer's requirement for power factor is to have power factor correction during all operating loads. The ripple current will be selected as 20 percent of full operating current at the minimum input voltage. This should accommodate most typical server loads at all input voltages.

Solving (24) for inductance and substituting in the duty cycle and switching frequency gives:

$$L = V_{in} \cdot D \cdot T_s \cdot \frac{1}{\Delta i} \tag{25}$$

The required inductance for the minimum input voltage is around 400 microhenries.

The output ripple of the boost converter is not specified, but it needs to be sufficiently small to ensure proper energy storage. To check the voltage ripple the capacitor current in mode two of the boost converter is used. The current is given by:

$$i_C = -I_{out} = -\frac{V_{out}}{R} \tag{26}$$

Using this current, a linear approximation of the voltage and the capacitor characteristic equation results in:

$$-\frac{V_{out}}{R} = C \cdot \frac{\Delta v}{\Delta t} \tag{27}$$

Solving this for ripple results in the following:

$$\Delta v = -\frac{V_{out}}{R} \cdot \frac{1}{C} \cdot D \cdot T_s \tag{28}$$

Using the minimum specified DC link capacitance, the voltage ripple is at most 0.5V. This ripple is insignificant compared to the output voltage, so the minimum required DC link capacitance can be used.

2.5 Simulations

The power supply's salient component values have been designed. The next step is to analyze these converters and design the proper controller for each stage. This will be done using simulations of the converters. The converters will be operated open loop and bode plots will be generated. The controllers will be designed and implemented. Once the power supply controllers are implemented, the entire system will be simulated to meet the specification.

2.5.1 DC to DC controller design

The DC to DC converter transformer turn ratio, output inductor and output capacitance have been designed. Negative voltage feedback will be used to control the converter. The output voltage will be fed back and be forced the equal a reference voltage by implementing an error amplifier. The error amplifier will directly control the switching of both interleaved converters.

The simulated open loop bode plot with the pulse width modulator, PWM gain of the interleaved converter is shown in Fig. 11. Around 10 kilohertz the inductor and capacitance poles take effect and cause the gain to plummet and the phase to attempt to shift 180 degrees. Further along, the series resistance of the output capacitance provides a zero which slows the gain's descent and provides some phase boost.

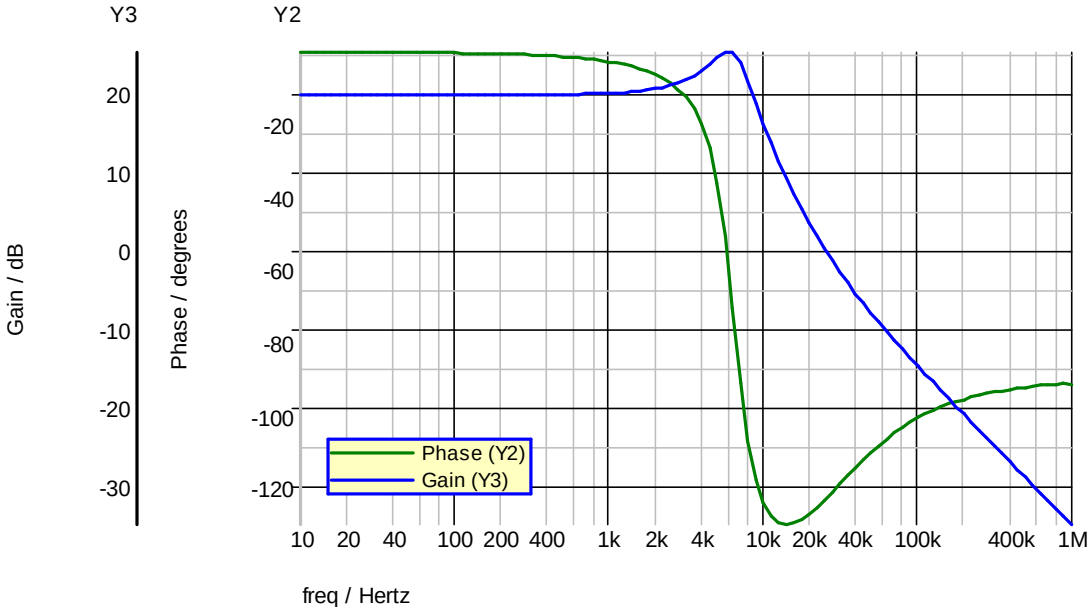

Fig. 11 Simulated interleaved two transistor forward converter open loop bode plot

The specification requires two stability criteria. The first is the phase margin of the converter and the second is the gain margin of the converter. The phase margin is the difference between negative 180 degrees and the phase at the unity gain crossover frequency. The specified phase margin is 45 degrees. The gain margin is defined as how far past unity gain the converter is when the phase reaches negative 180 degrees. The specified gain margin is 15 decibels.

To compensate the converter and to meet the required stability criteria a negative feedback error amplifier will be used. A simple type of error amplifier is an integrator. A typical implementation can be seen in Fig. 12.

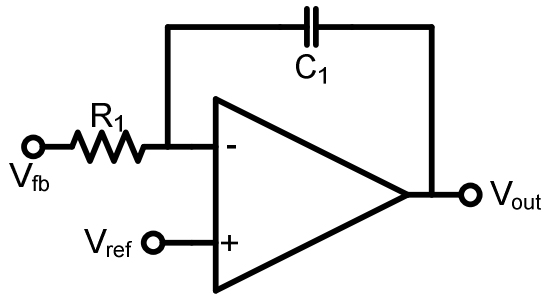

Fig. 12 Integrator error amplifier

To study the frequency response of this amplifier a Laplace transform can be taken and is shown in Fig. 13. Applying nodal analysis to this circuit gives the following:

$$-i_1 - i_2 = 0 = -\frac{v_{fb}}{R_1} - \frac{v_{out}}{\frac{1}{C_1 \cdot s}} \tag{29}$$

Solving this equation for the transfer function results in:

$$\frac{v_{out}}{v_{fb}} = -\frac{1}{R_1 \cdot C_1} \cdot \frac{1}{s} \tag{30}$$

This error amplifier has a single pole located at the origin. The values of the resistor and capacitor determine the crossover frequency of the amplifier. This single pole has a constant gain slope of minus 20 decibels per decade and a constant phase of 90 degrees. Fig. 14 has a simulated bode plot for an integrator. This type of amplifier could be used to set the crossover frequency of the converter to a desired value, but offers no phase margin adjustment.

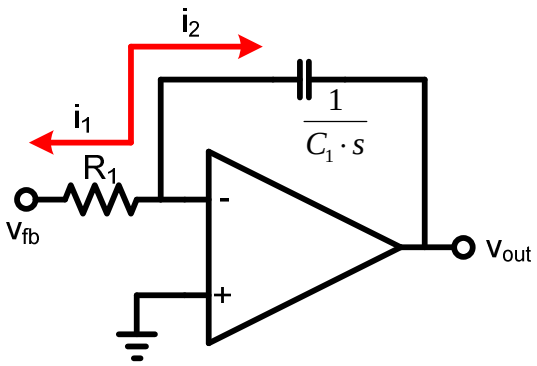

Fig. 13 Laplace transform of integrator error amplifier

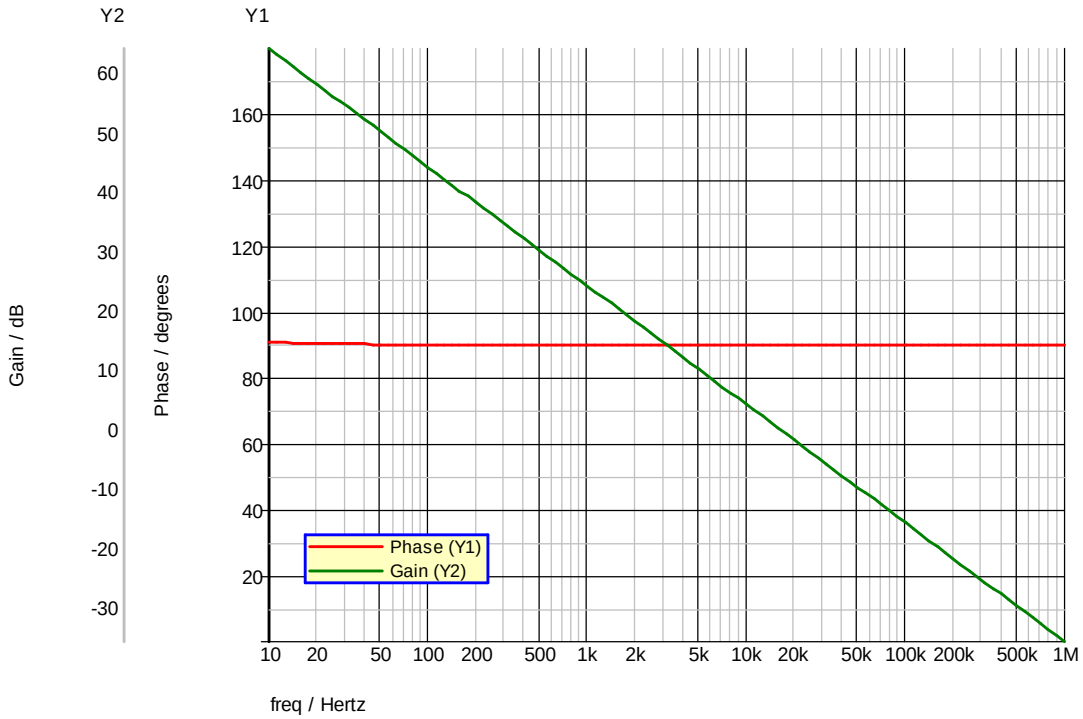

Fig. 14 Simulated bode plot for integrator error amplifier

Phase boost is required to meet the specified phase margin. To increase the phase of the error amplifier a zero must be added to the transfer function. This will increase the phase at frequencies above about one tenth of the zero frequency, but will also increase the slope of the gain by 20 decibels per decade after the zero frequency. To maintain the desired high frequency characteristics, another pole needs to be introduced above the zero frequency to lower the gain slope, so that it will tail off at higher frequencies.

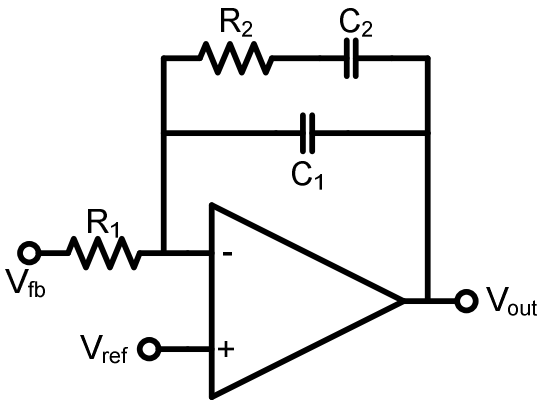

Fig. 15 Error amplifier schematic with two poles and one zero

Fig. 15 shows a practical implementation of an error amplifier meeting these criteria. Fig. 16 shows the Laplace version of the circuit and the nodal currents to solve for the transfer function.

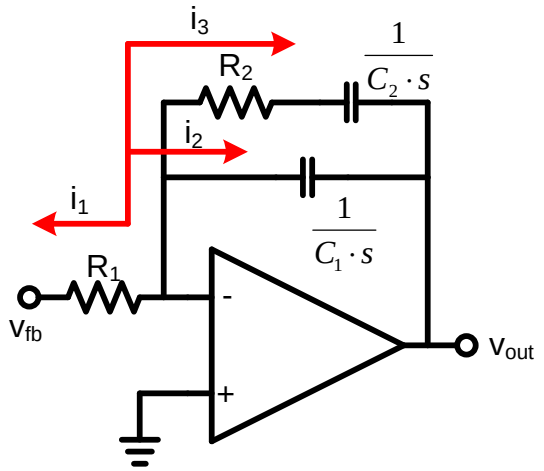

Fig. 16 Laplace transform of two pole, one zero error amplifier

Solving the nodal currents gives the following:

$$-i_1 - i_2 - i_3 = 0 = -\frac{v_{fb}}{R_1} - \frac{v_{out}}{\frac{1}{C_1 \cdot s}} - \frac{v_{out}}{R_2 + \frac{1}{C_2 \cdot s}} \tag{31}$$

Solving this for the gain results in:

$$\frac{v_{out}}{v_{fb}} = \frac{1 - C_2 \cdot R_2 \cdot s}{R_1 \cdot s \cdot \left(C_1 \cdot C_2 \cdot R_{2`} \cdot s + C_1 + C_2\right)} \tag{32}$$

This transfer function has two poles and one zero. The first pole occurs at zero frequency. The zero occurs at the following frequency:

$$f_{zero} = \frac{1}{2 \cdot \pi \cdot C_2 \cdot R_2} \tag{33}$$

The second pole occurs at:

$$f_{pole,2} = \frac{\left(C_1 + C_2\right)}{2 \cdot \pi \cdot R_2 \cdot C_1 \cdot C_2} \tag{34}$$

Selecting the component values properly results in a transfer function similar to the bode plot in Fig. 17.

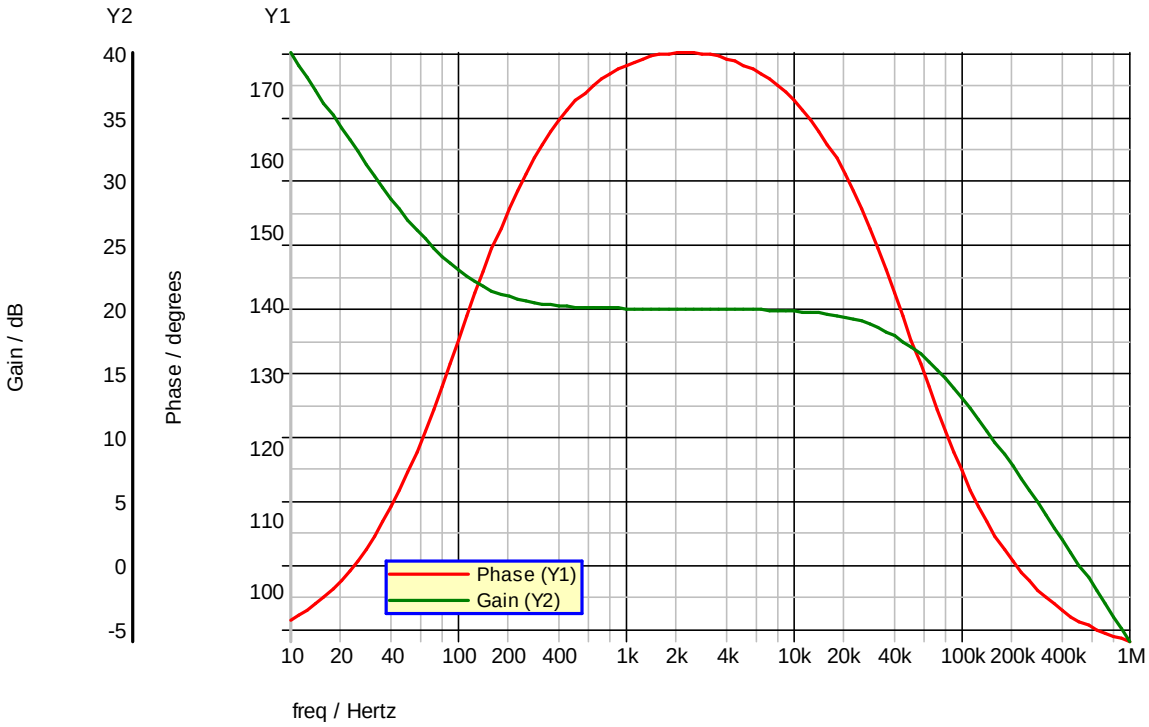

Fig. 17 Simulated bode plot for a two pole, one zero error amplifier

The adjustable pole and zero need to be selected in order to make the closed loop transfer function have the specified phase and gain margins. Setting the crossover frequency to 10 percent of the switching frequency requires the controller's gain be around 10 decibels at 50 kilohertz. Phase boost is also required from the controller at this frequency. The second pole needs to be placed such that it is as close to the crossover frequency as possible, but does not diminish the phase boost too much at the desired crossover frequency.

The error amplifier, whose characteristics are shown in Fig. 18 appear to meet the requirements needed to meet the specified stability criteria.

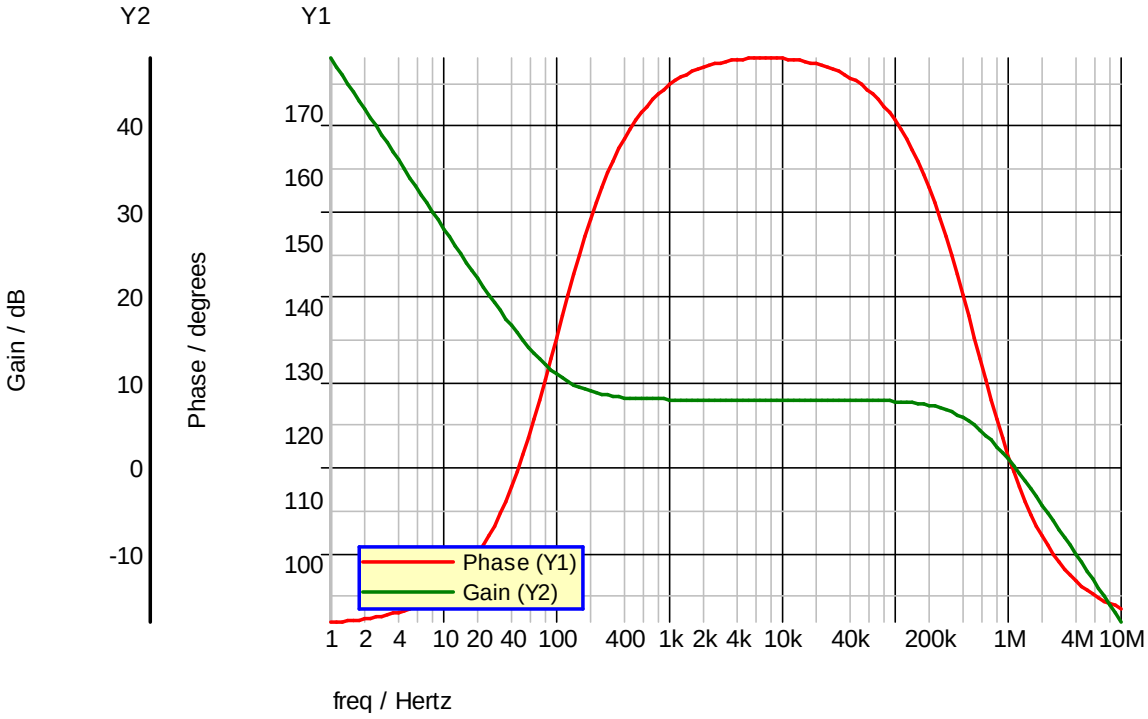

Fig. 18 Simulated proposed DC to DC error amplifier bode plot

Applying the error amplifier with characteristics shown in Fig. 18 stabilizes the DC to DC converter. The closed loop bode plot is shown in Fig. 19. The overall phase margin is around 60 degrees, comfortably above the 45 degrees requirement. The gain margin is more than 20 decibels, well beyond the specification of 15 decibels. This compensation loop, while stable may not be sufficient to meet all of the specifications. If this is the case, the compensation loop would need to be altered to bring the power supply into its specified ranges.

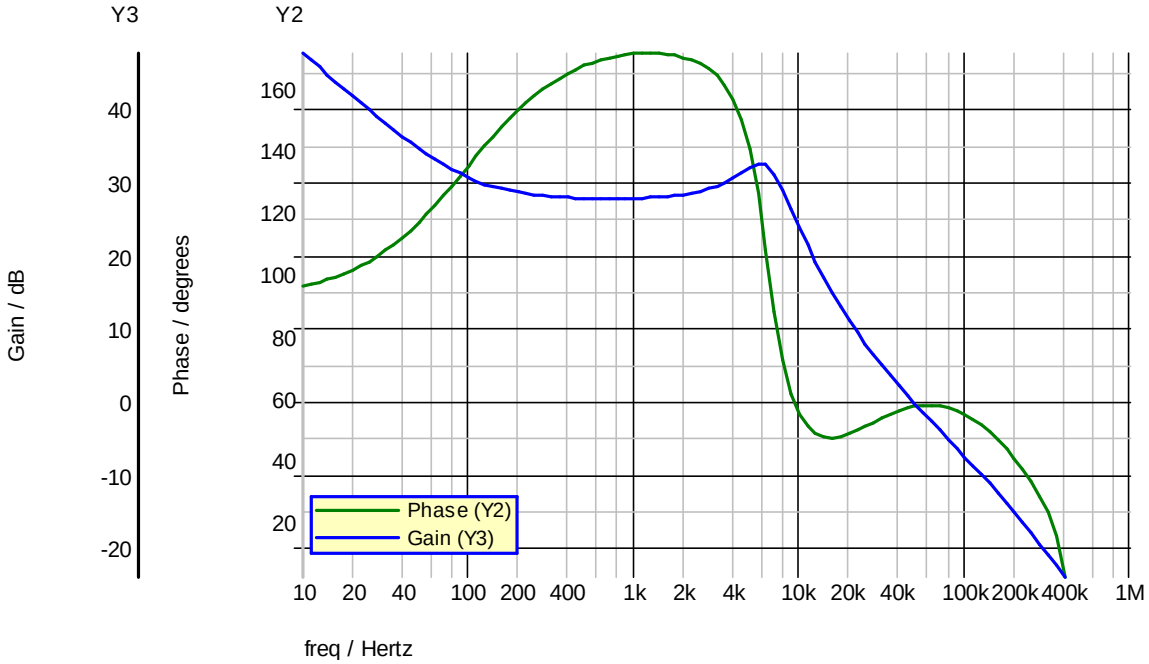

Fig. 19 Simulated closed loop bode plot of DC to DC converter

2.5.2 Power factor correcting boost converter controller design

The power factor correcting boost converter requires two error amplifiers to stabilize the system. The open loop bode plot for the designed boost converter, with the PWM gain can be seen in Fig. 20.

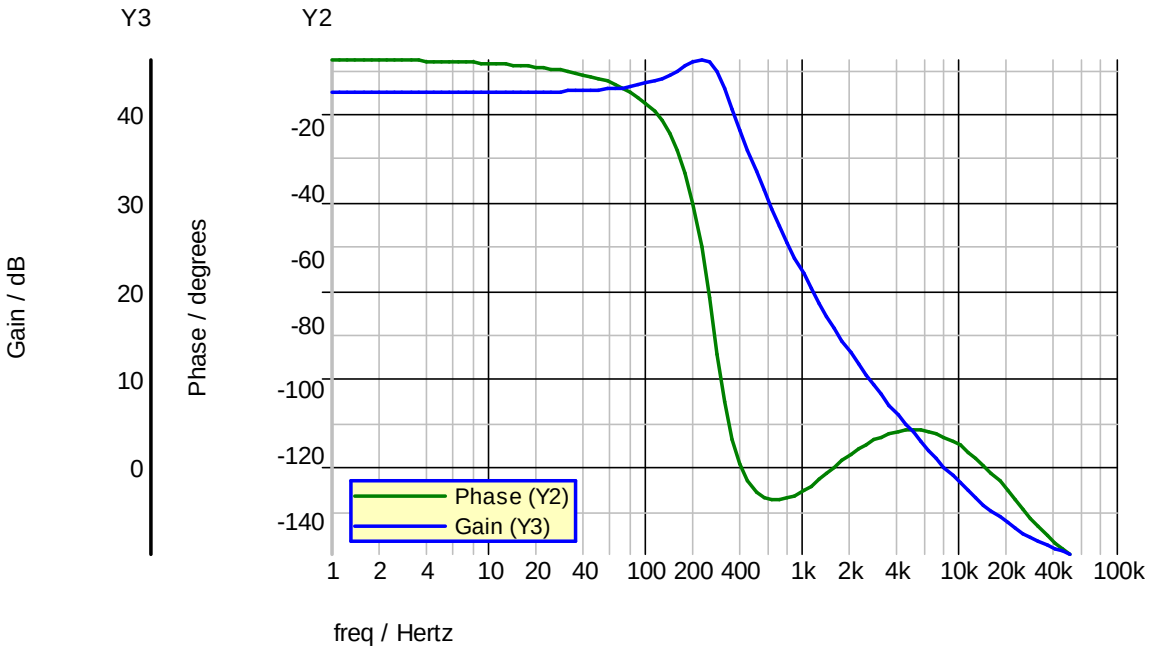

Fig. 20 Simulated boost converter open loop bode plot

The two error amplifiers required represent the output voltage and input current regulation. The input current shaping is the most critical for power factor correction, so that is the faster, inner loop. The output voltage regulation will be an outer slower control loop. This will create large voltage ripple with a frequency of twice the input AC frequency. This ripple is from the rectification and input current shaping.

The slower outer loop needs to have low gain with respect to both the switching frequency and the input AC frequency. This requirement means a crossover frequency in the range single digits of hertz is desirable. The boost converter has a gain of about 42 decibels in this range. This is also an ideal location to add some phase boost to the converter. The bode plot in Fig. 21 is the designed amplifier for this slow, outer error

amplifier. This error amplifier has the correct gain around 5 hertz and has a significant phase boost at the desired crossover frequency.

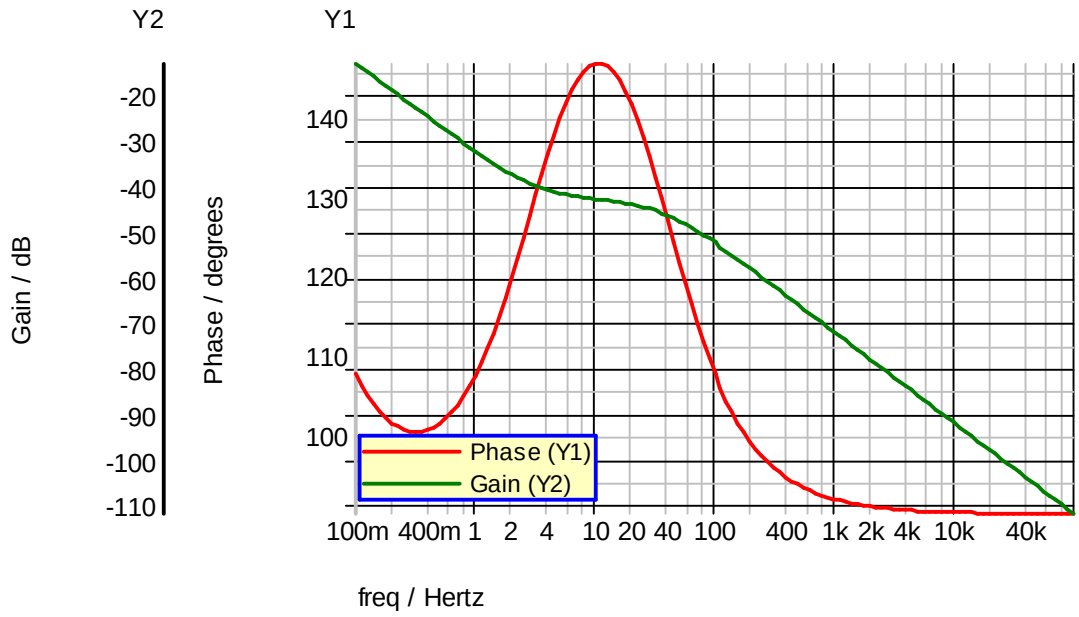

Fig. 21 Simulated frequency characteristics of error amplifier for output voltage feedback

The current shaping error amplifier requires significant gain at the AC frequencies in order to be able to shape the current. Fig. 22 shows a simple integrator with a zero allowing for a high gain around the input frequency and diminishing off at higher frequencies before the gain flattens out from the zero.

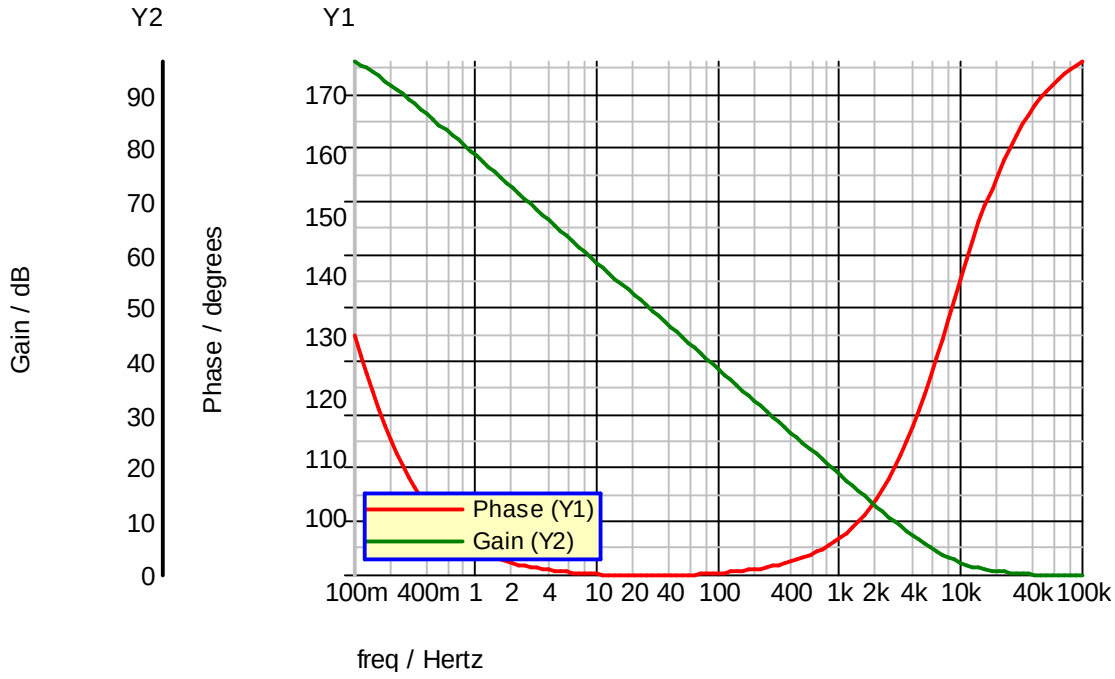

Fig. 22 Frequency characteristics for the current shaping error amplifier

These two error amplifiers should sufficiently stabilize the boost converter. The multiplier in the control scheme prevents simulated frequency analysis of the converter in closed loop. The converter will be simulated with the power supply to show its characteristics.

2.6 Specification simulations

The entire power supply is now designed. Simulation must be carried out in order to test this design to the specification. Certain simulated waveforms will also be compared to an actual server power supply to ensure the simulated result is an accurate representation of a mass produced server power supply. The manufactured power supply is a 1200 watt power supply.

2.6.1 Input specification simulations

The power supply is required to run at all line voltages from 100 volts AC to 240 volts AC and from 50 hertz to 60 hertz. It also must maintain a power factor greater than 0.95 at any valid input condition at full rated load. The power supply successfully operated at all line voltages and frequencies. Fig. 23 shows the input voltage and current operating at full rated load at 240 volts AC 50 hertz. This operating condition yields the lowest power factor. The simulation shows a power factor much larger than the specified full load minimum of 0.95.

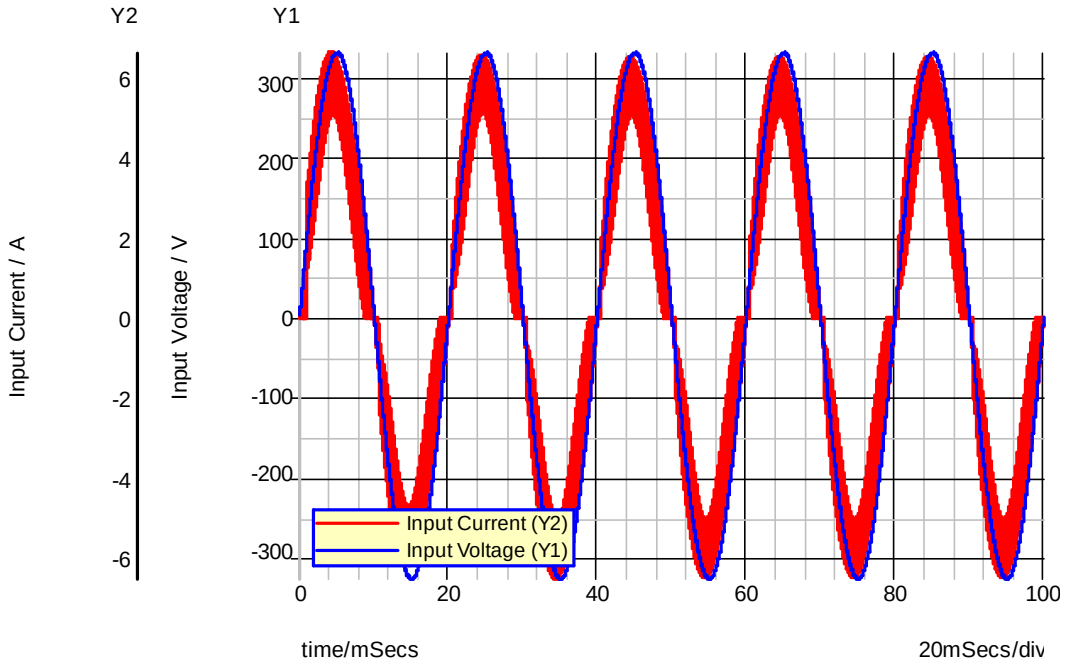

Fig. 23 Simulated input voltage and current at 240 volts AC 50 hertz

2.6.2 Output specification simulations

The first output specification is the voltage set point. It is specified as 12 volts at ampere of load with a tolerance of 30 millivolts. Fig. 24 shows this result. The power supply does meet this requirement.

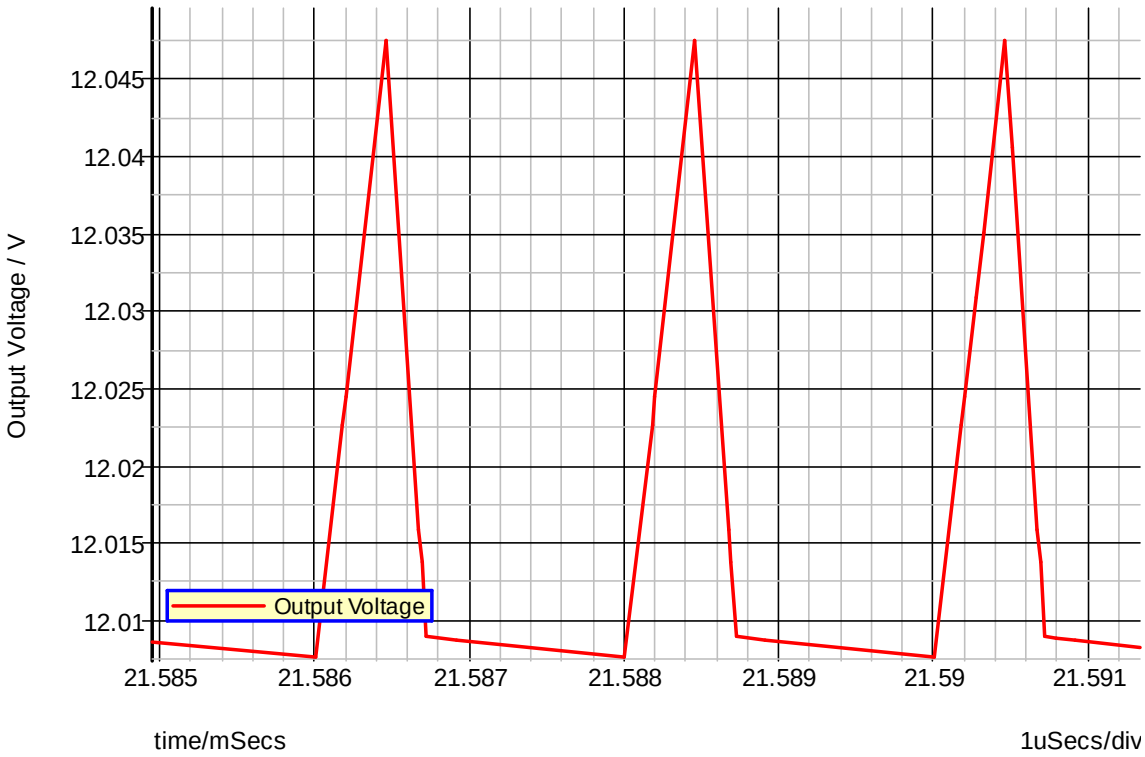

Fig. 24 Simulated output voltage at 1 A output load

The static load voltage regulation is the next specified power supply characteristic. The output voltage under any static load is specified to be within the range of 11.90 volts and 12.10 volts. Fig. 25 shows the simulated output voltage with static no

load and static full load. The power supply does remain within the limits specified. The full load voltage has a significant 120 hertz component. This does not create a specification violation, but could be reduced with added output capacitance or a lower controller gain at 120 hertz.

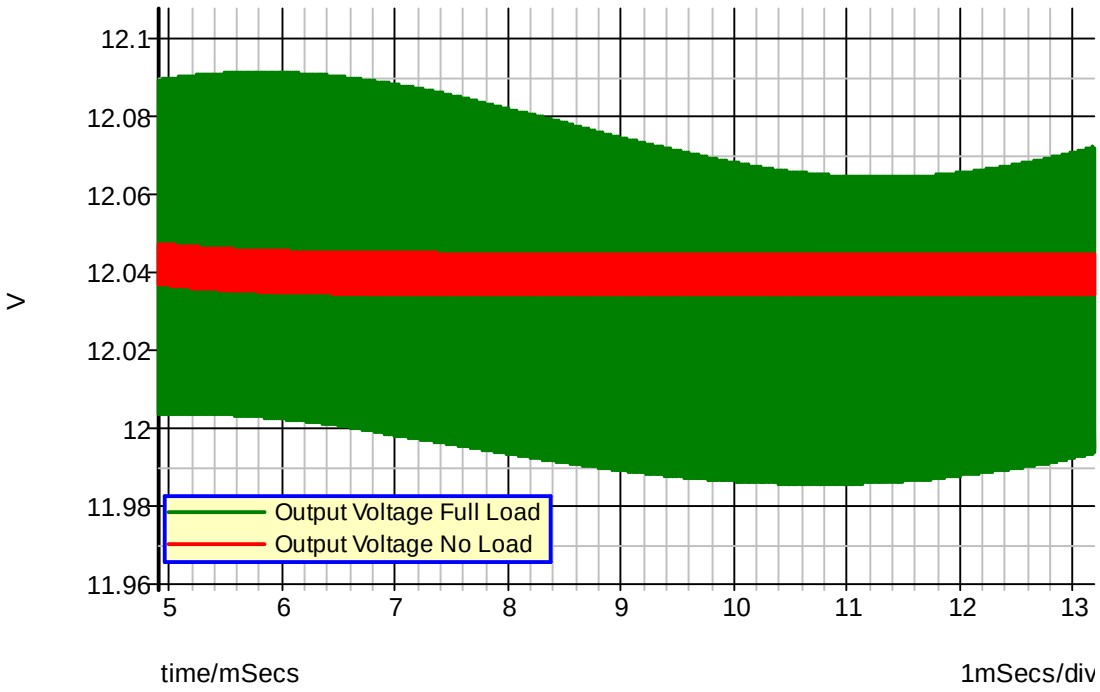

Fig. 25 Simulated static output voltage regulation

The dynamic voltage regulation requirements are the allowable voltage range for and specified transient load change. The maximum specified load change is 50 percent. During any load change of up to 50 percent the allowed voltage range is 10.8 volt to 13.2 volts. Fig. 26 shows the output voltage with zero to 50 percent load changes and 50 to

100 percent load changes. The simulated power supply passes this requirement with the minimum specified output capacitance.

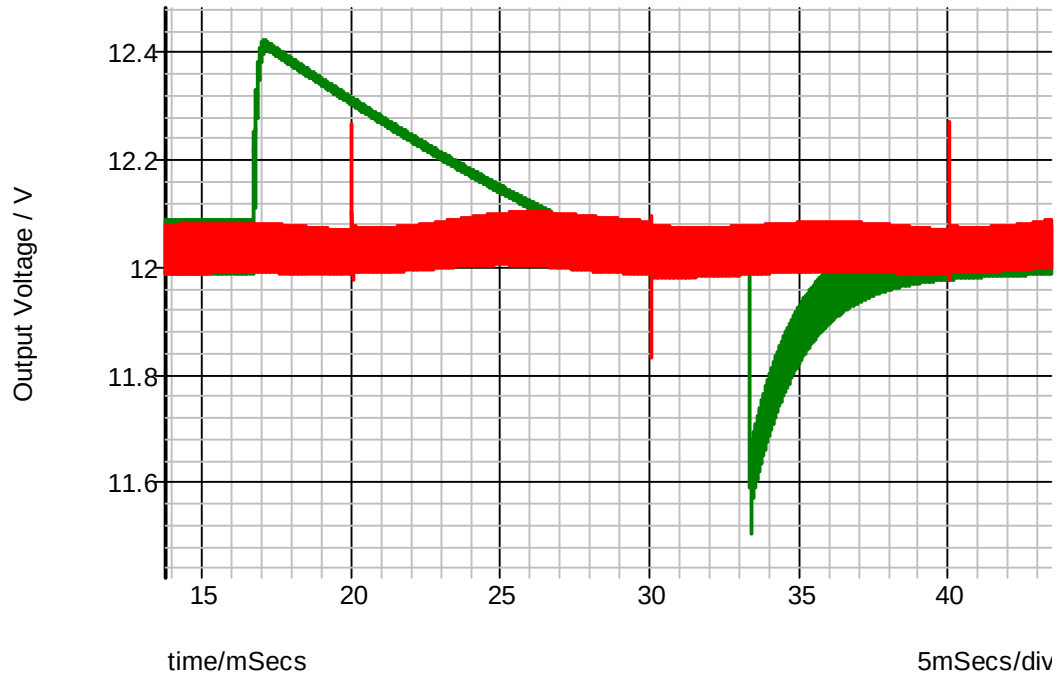

Fig. 26 Simulated transient load output voltage

Fig. 27 shows the output voltage of the manufactured power supply with the worst case load transient from the simulations. The manufactured power supply has a minimum specified output capacitance larger than the simulated power supply. This greatly improves the dynamic response; however, the waveforms are very similar.

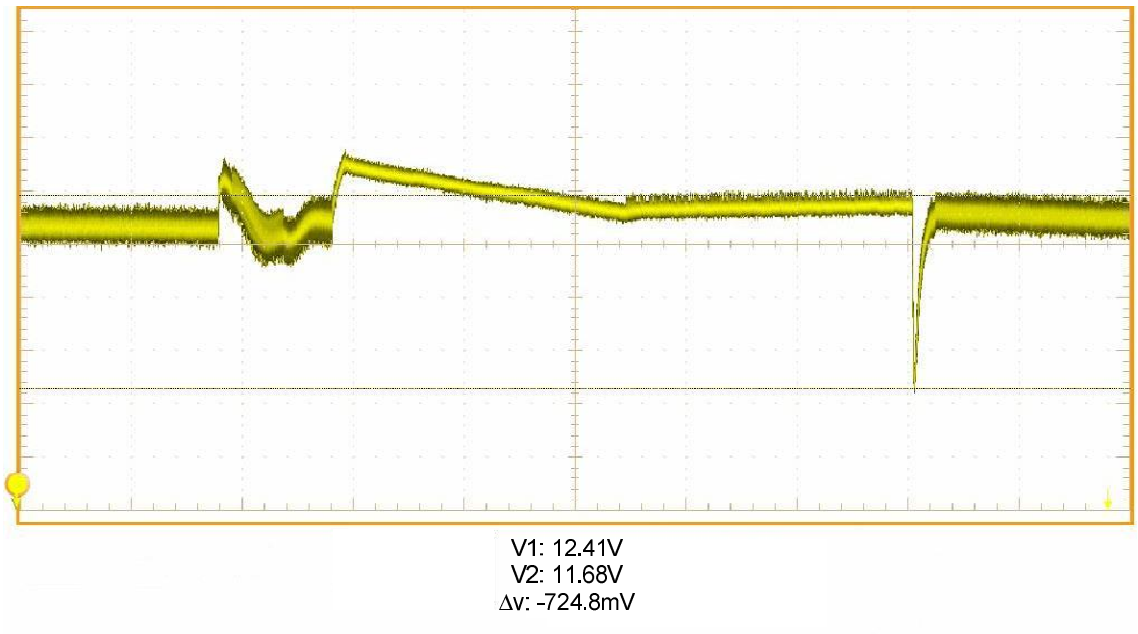

Fig. 27 Measured output voltage of manufactured power supply with zero to 50 percent load transient

The power supply is required to supply power for a duration no less than 10 milliseconds. Fig. 28 shows an AC dropout and the time in which the power supply exceeds the specified minimum voltage for greater than 10 milliseconds. The shown waveform turns off the AC voltage at the worst possible time, the peak.

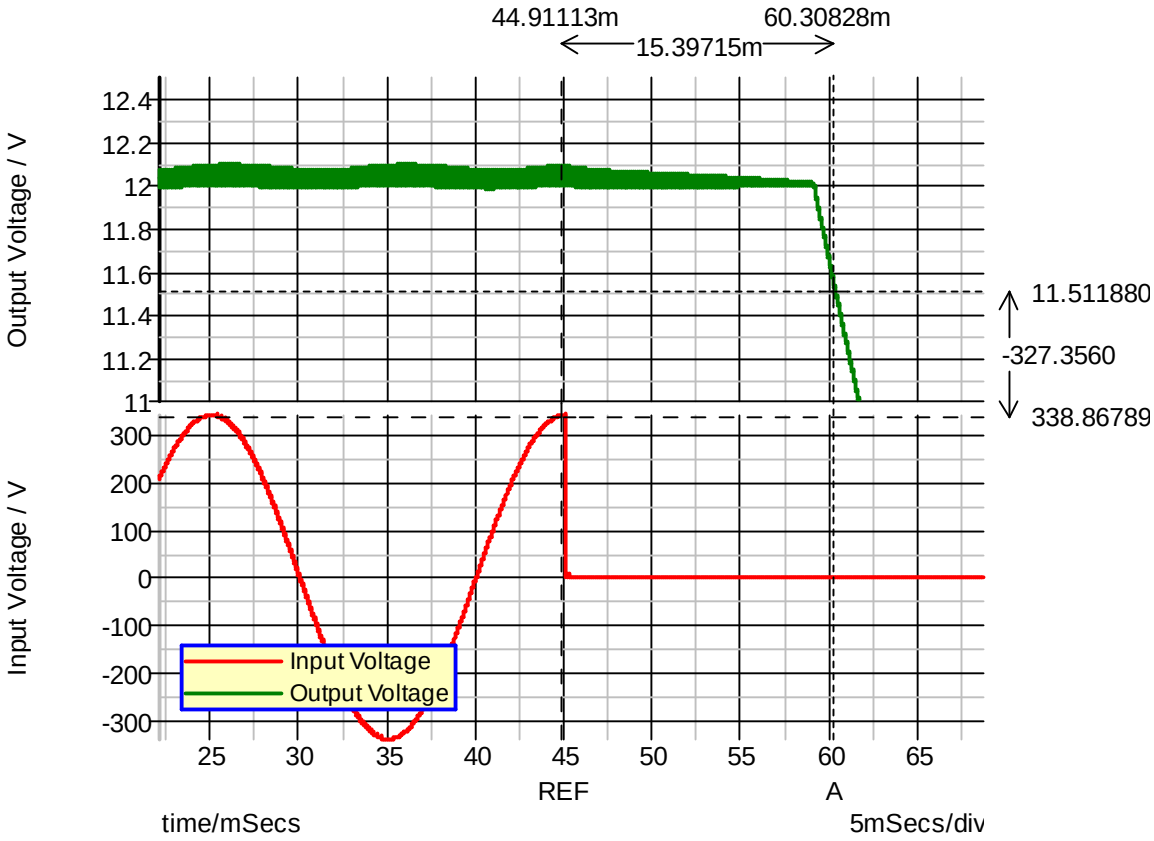

Fig. 28 Simulated voltage dropout hold up time

Fig. 29 shows the same plot for the manufactured power supply. The power supply contains significantly more DC link capacitance and has a much longer holdup time.

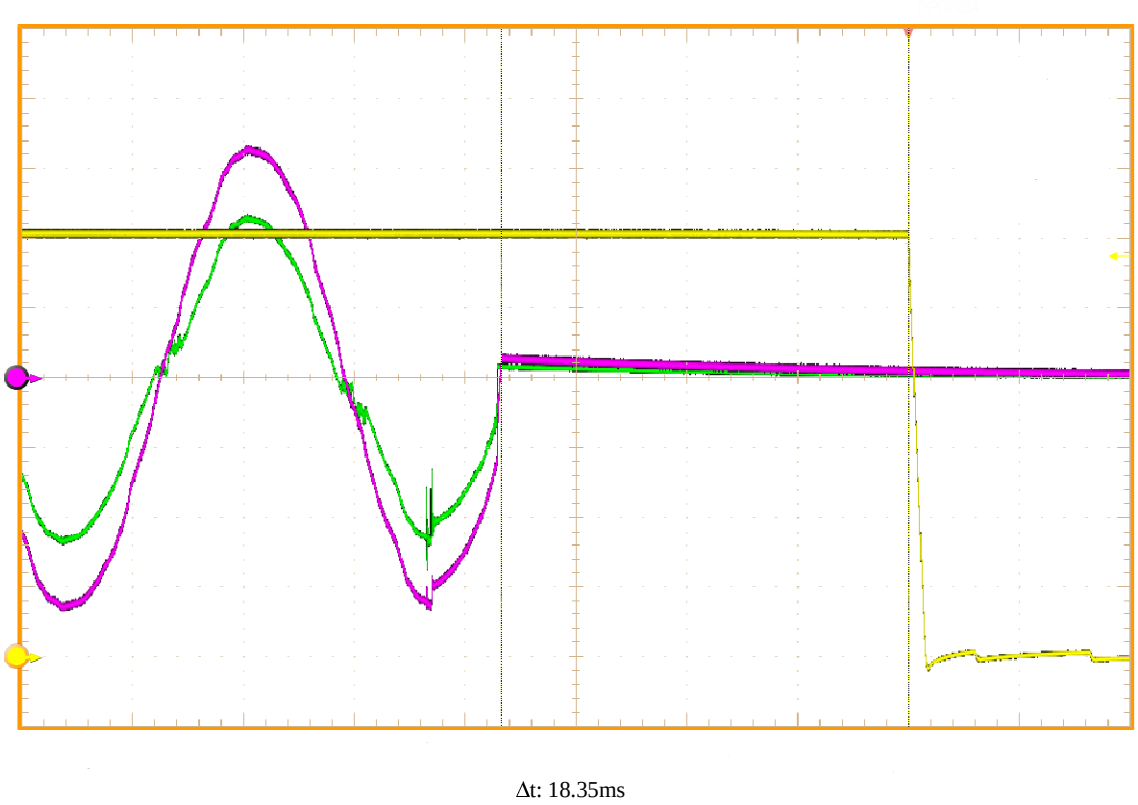

Fig. 29 Measured hold up time from AC dropout

The final simulation is the output voltage ripple. This is specified as 120 millivolts peak to peak at any operating point. The worst case is a fully loaded power supply. Fig. 30 shows this for the simulated power supply. It does meet the minimum requirement.

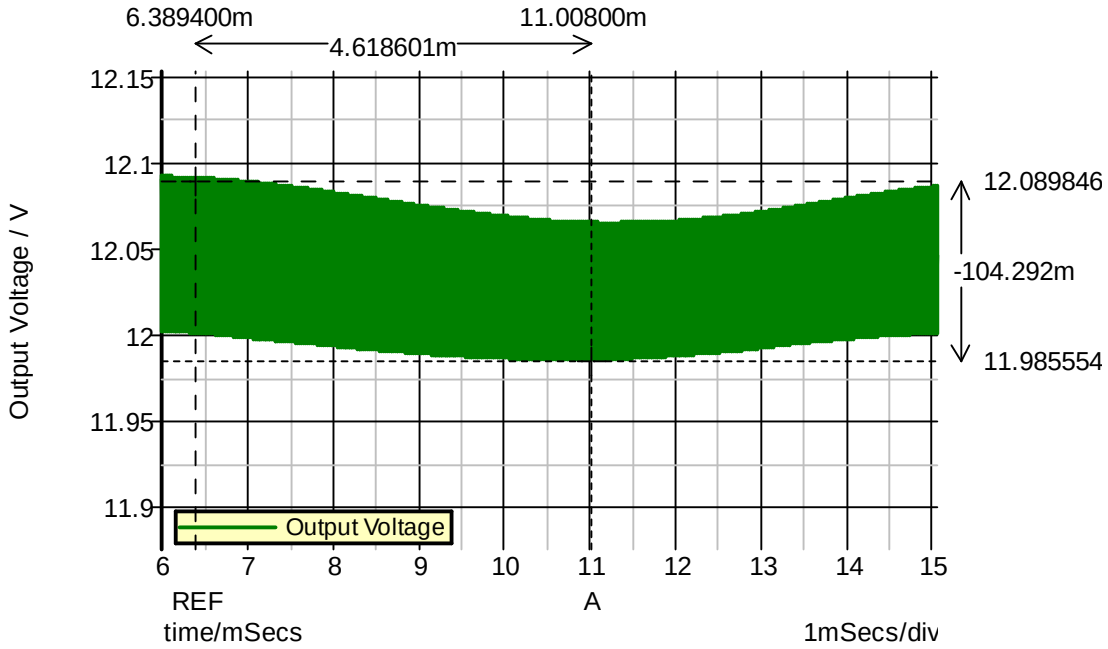

Fig. 30 Simulated output voltage ripple at full load

Fig. 31 is the same output with the manufactured power supply. The output ripple in the manufactured power supply is aided by larger minimum output capacitance. The voltage spikes are not counted. They were introduced due to where the measurement was taken.

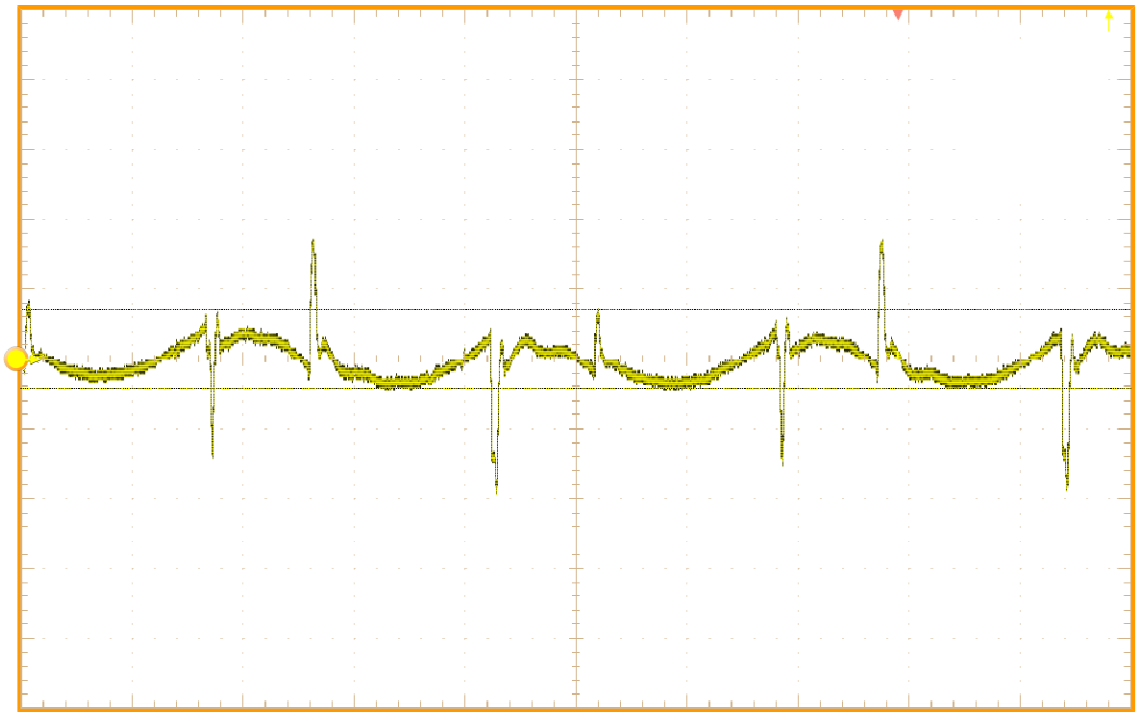

ΔV: 56.35mV

Fig. 31 Measured output voltage ripple

2.7 Summary

An AC to DC server power supply has been specified, designed and simulated to meet all specifications. This model will be used to test, via simulation the use of a PEM fuel cell as a backup energy source for network servers. That UPS is required to maintain the output specifications in the event of a utility failure of unknown duration.

CHAPTER III

FUEL CELL CONVERTER

3.1 Introduction

To begin the design of the fuel cell converter, the fuel cell's electrical characteristics must be understood. All fuel cells have their own unique electrical characteristics which are derived from their chemistry. There have been many proposed solutions to the fuel cell converter problem [4]-[11]. This sample of solutions offer unique perspectives to the issues faced with fuel cells and will be important in ensuring a robust design results.

3.2 Fuel cell modeling

The Ballard Nexa fuel cell power module is a 1200 watt rated fuel cell stack. This is an ideal power level to power one fully utilized server, or two to three lightly configured servers. W. Choi extensively tested and modeled this fuel cell stack along with a couple other fuel cell stacks of differing voltages and power ratings. Fig. 1 [3] shows the voltage and current characteristics of the Ballard Nexa fuel cell stack. W. Choi also modeled the AC characteristics of fuel cell stacks and determined a linear model to be used for modeling a PEM fuel cell stack [3]. Fig. 32 shows the model [3].

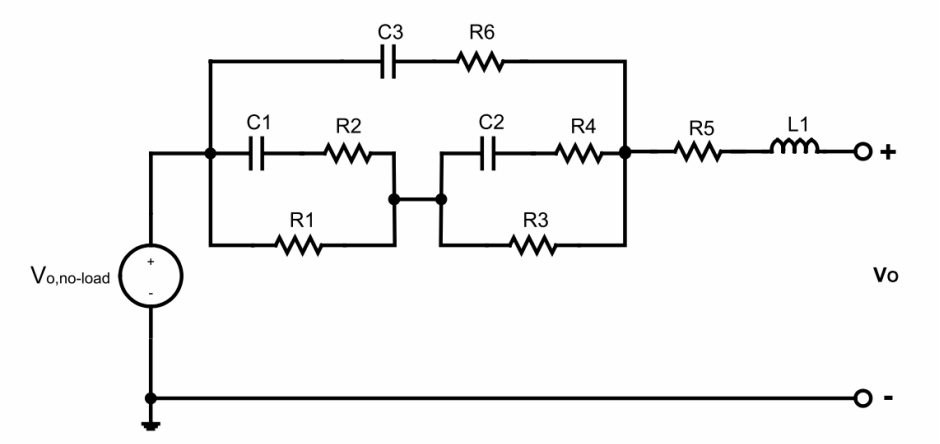

Fig. 32 Fuel cell linear model [3]

The experimentally derived values for the different components were also given in [3]. The simulated transfer function for the Nexa fuel cell stack is shown in Fig. 33.

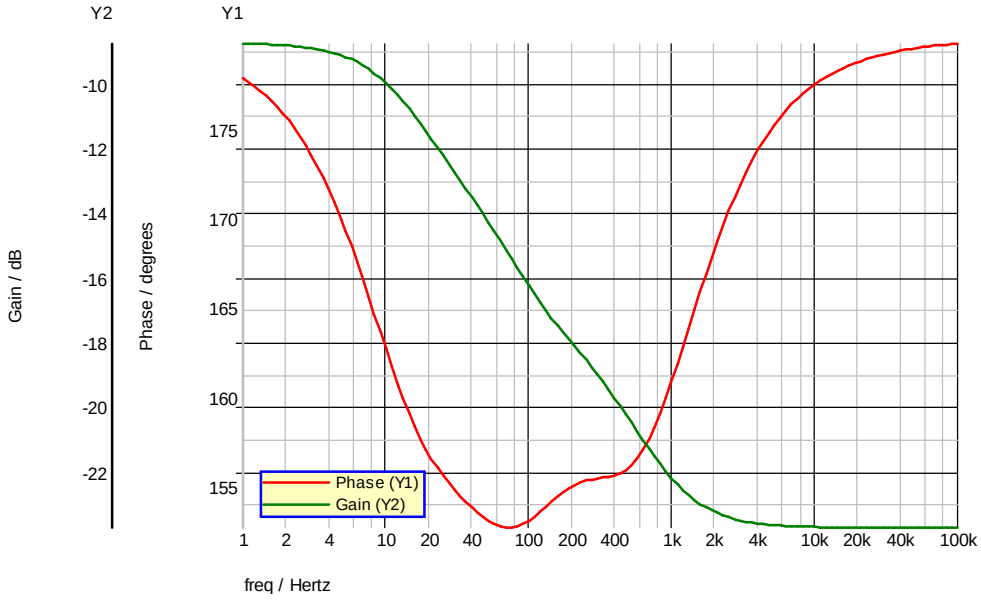

Fig. 33 Ballard Nexa fuel cell modeled impedance

This is the model that will be used as a power source when simulating the fuel cell DC to DC converter. Observing the gain of the fuel cell impedance suggests that an input filter is not required for stabilization. The switching frequency should be high enough to not be noticed by the fuel cell; however, a capacitance may be desirable to reduce current ripple.

3.3 Topology review

Any DC to DC converter which boosts the input voltage is a possible solution for the fuel cell converter. Certain requirements exist for this converter which limits the choices available. Some of these include:

- Size
- Manufacturability
- Reliability
- Power level
- Efficiency
- Cost

Many people have offered solutions to the fuel cell step up converter, and they all have their merits. Some of these will be looked at and a conclusion determined for this specific application [4]-[11]. No single topology exists to meet every criterion, so tradeoffs must be made.

3.3.1 Current fed half bridge converter

J.-T. Kim *et al.* proposed a modified current fed half bridge converter for use with fuel cells [4]. The basic schematic is shown in Fig. 34.

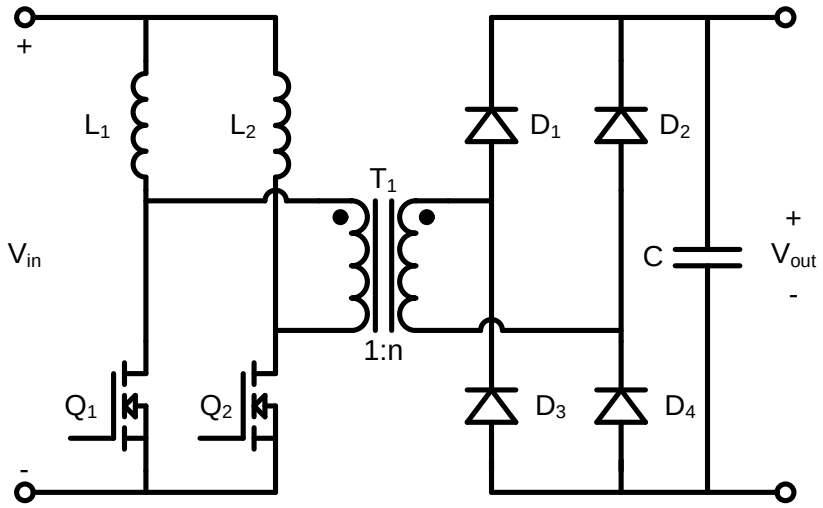

Fig. 34 Current fed half bridge converter schematic

The converter has four modes of operation. These can be seen in Fig. 35. Mode one turns on both transistors to store energy in the inductors. Next, transistor Q1 turns off, forcing the inductor current in L1 through the transformer, inducing a positive output voltage across the secondary of the transformer. Mode three turns Q1 back on storing energy in both inductors. Mode four occurs when Q2 turns off and the current in L2 is forced through the transformer the other direction, inducing a negative voltage on the secondary.

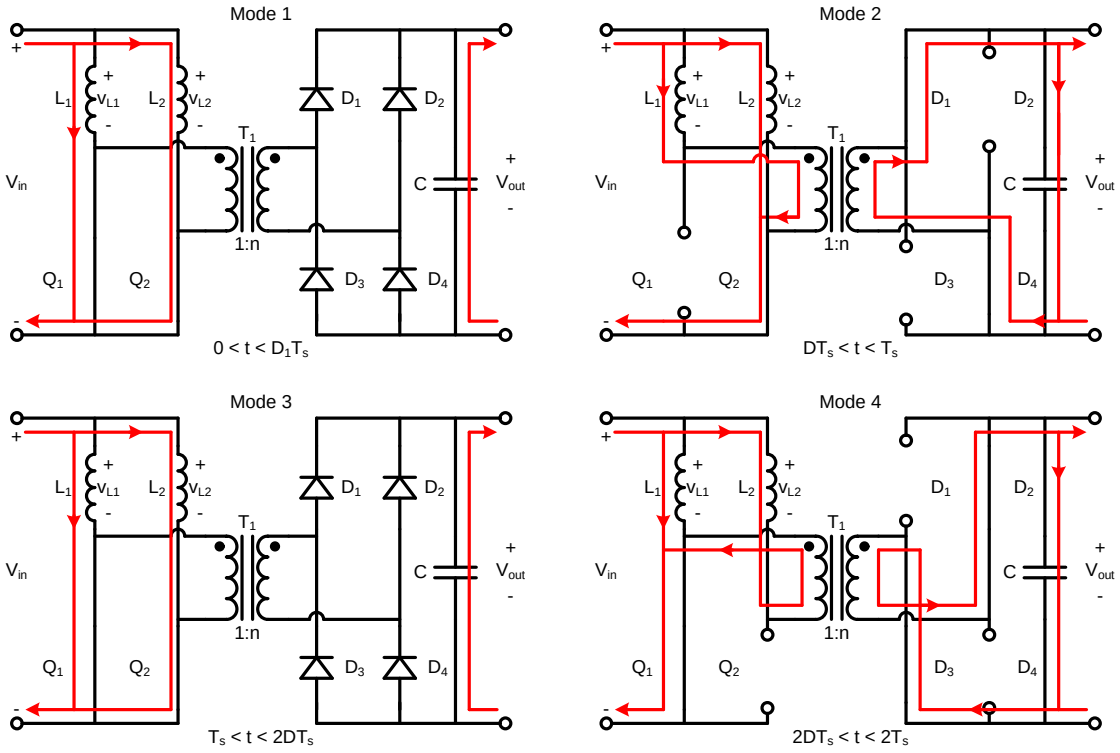

Fig. 35 Current fed half bridge converter modes of operation

The converter has many properties conducive to use with fuel cells. It is suitable for moderate power levels due to the amount of silicon available for heat dissipation. The inductors allow the input current to remain continuous, which is a benefit to many types of fuel cells. Another desired characteristic is the boosting effect by the inductors before the transformer. This can reduce the required turn ratio of the transformer.

The current fed half bridge does have a few drawbacks for this application. Significant voltage stress is generated across the transistors due to the magnetizing inductance of the transformer among other things. These voltage transients would need

to be reduced in order to make the converter viable for this application. This topology also requires two inductors, which adds complexity.

3.3.2 Voltage and current fed full bridge converters

M. Mohr and F.-W. Fuchs wrote about using full bridge converters for fuel cell applications [5]. This converter is well suited for both step up and step down DC to DC converters. The basic schematic for the voltage fed full bridge converter is shown in Fig. 36.

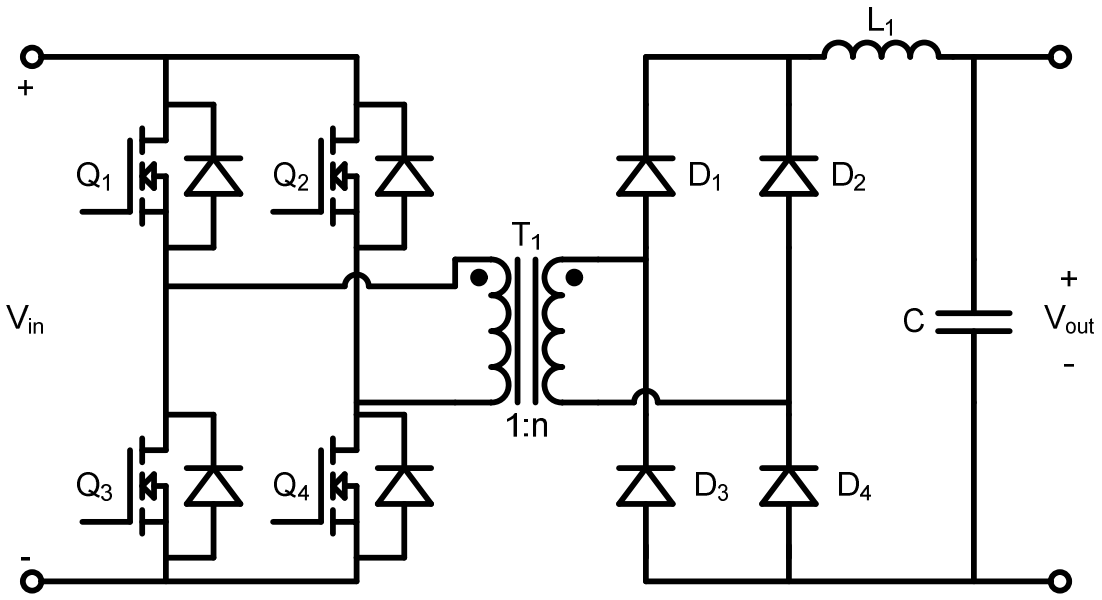

Fig. 36 Schematic of voltage fed full bridge converter

The voltage fed converter has four modes of operation. These can be seen in Fig. 37. During mode one, transistors Q1 and Q4 are switched on, applying the input voltage

across the transformer. This will induce a current on the secondary biasing the full bridge rectifier, where a standard buck output filter is located. Mode two occurs directly after the two transistors turn off. The anti-parallel diodes in Q2 and Q3 allow the energy stored in the magnetizing inductance to return to the voltage source. Once the energy is returned, mode three can begin. Here, Q2 and Q3 are turned on and minus the input voltage is placed across the transformer. This biases the other half of the rectifier on the primary and feeds power through the output filter. Mode four is the demagnetizing time for mode three.

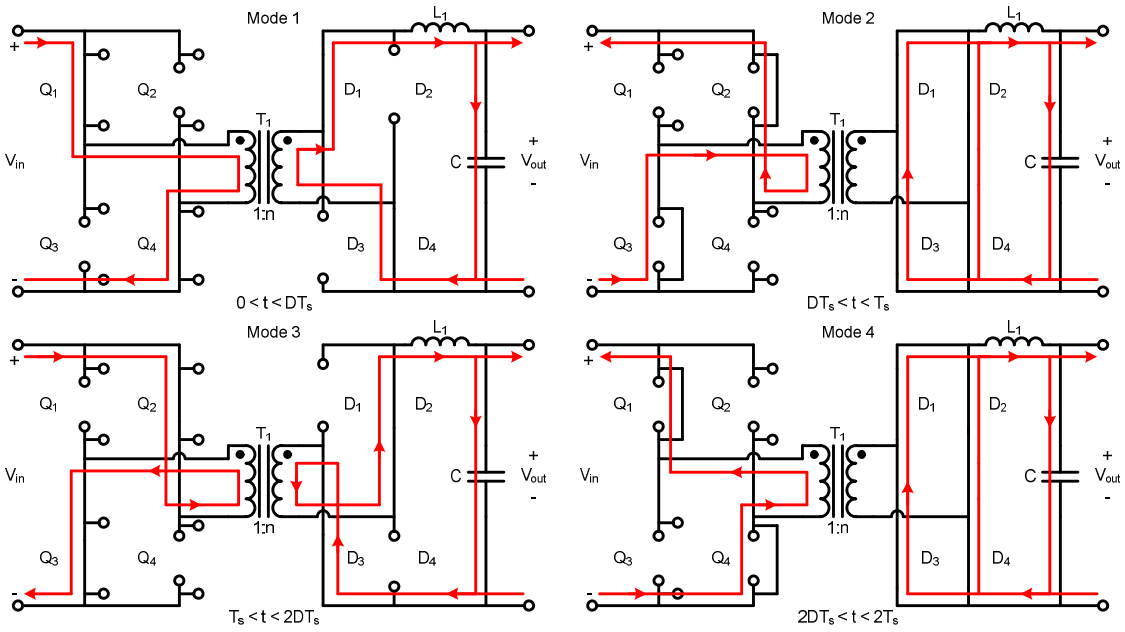

Fig. 37 Modes of operation for voltage fed full bridge converter

The current fed full bridge converter is similar to the half bridge converter from [4], except only one inductor is required since there are twice as many transistors. The basic schematic is shown in Fig. 38.

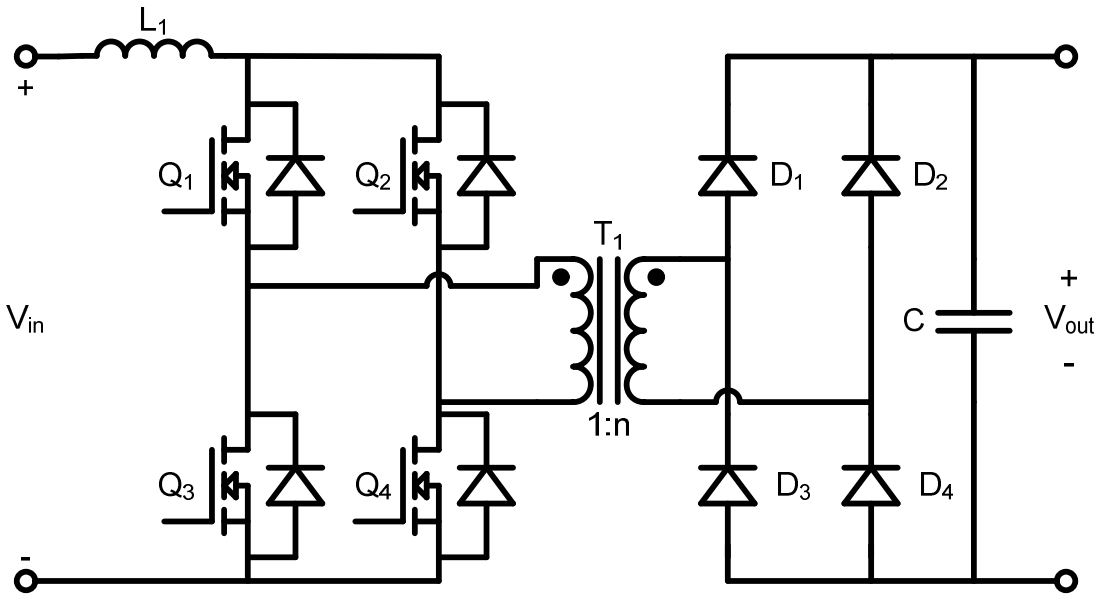

Fig. 38 Schematic of current fed full bridge converter

There are four modes of operation for the converter. They are shown in Fig. 39. Mode one occurs when all four transistors are conducting. This charges the inductor and allows the transformer to reset since there is zero voltage across the primary. Once the transformer has reset, mode two can occur. During this time, transistors Q2 and Q3 are switched off. The current is directed through the transformer and the secondary rectifier is biased transmitting power to the output. Mode three is another reset stage with all four

transistors conducting. Mode four turns off Q1 and Q4 to force the current back through the transformer, biasing the other half of the output rectifier.

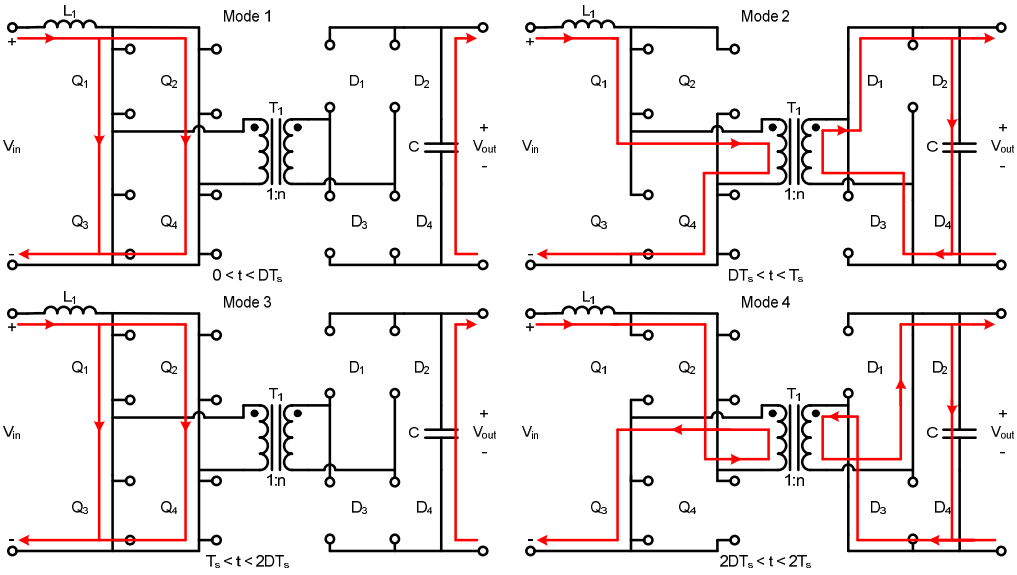

Fig. 39 Modes of operation for current fed full bridge converter

The full bridge converter scales very nicely to large amounts of power. This is due to many factors including the amount of silicon available for power dissipation and the full use of the transformers magnetic curve. The voltages are less stressful on the transistors than with single switch topologies. The current fed version is realized with only a single inductor, saving space and cost.

The full bridge converter has more switching losses than other topologies. The current fed version requires a primary inductor, which is less desirable than a secondary side inductor due to the large conduction differences.

S.-R. Moon and J.-S. Lai proposed interleaving full bridge converters for fuel cell applications [6]. This would allow an even greater ability to scale, and offers more flexibility in the design of the individual converters. Fig. 40 shows one of their proposed implementations of an interleaved full bridge converter. This type of implementation is for loads far exceeding the requirements of this fuel cell powered UPS.

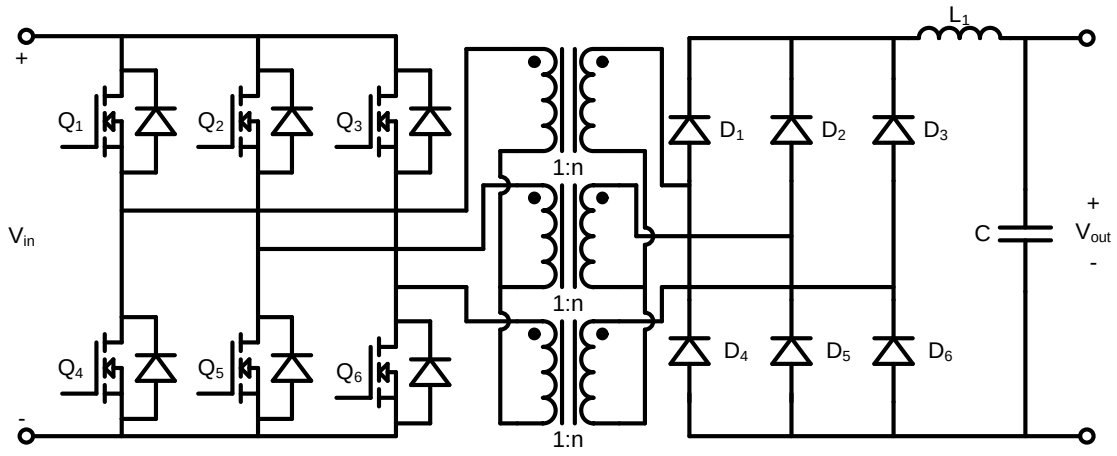

Fig. 40 Schematic of a proposed interleaved full bridge converter [6]

3.3.3 SEPIC-flyback converter

S.-J. Jing *et al.* proposed a hybrid converter for use with low voltage fuel cells. The primary is set up as a flyback converter, with a traditional flyback secondary

winding, along with another winding in a SEPIC type configuration [7]. This SEPIC-flyback hybrid converter has a basic schematic shown in Fig. 41.

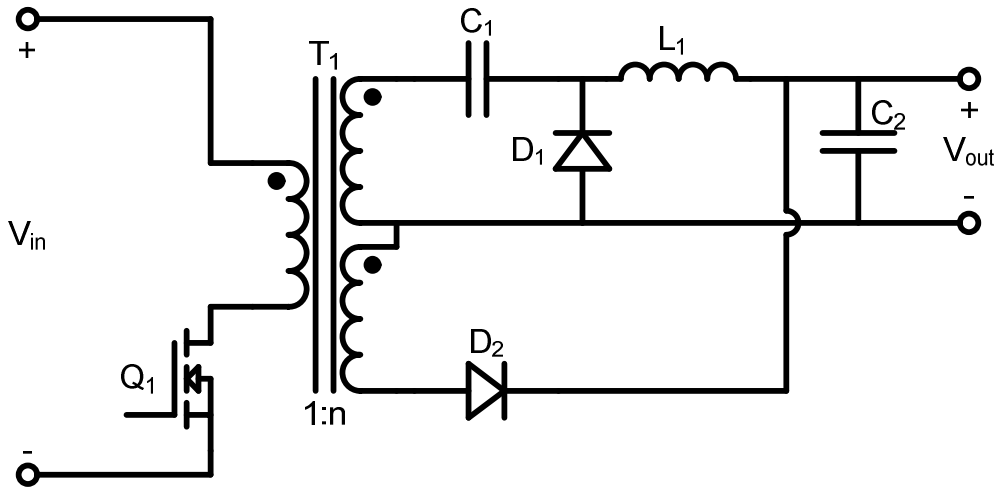

Fig. 41 Basic schematic of SEPIC-flyback hybrid converter [7]

This converter has two fundamental modes of operation. Mode one occurs when transistor Q1 is conducting. During this time, the SEPIC winding conducts increasing the current through the inductor. Mode two occurs when the transistor is opened. This is the flyback mode. The flyback secondary winding conducts and transfers the stored energy in the transformer to the output. The SEPIC inductor continues conducting during this time. Fig. 42 shows the modes of operation.

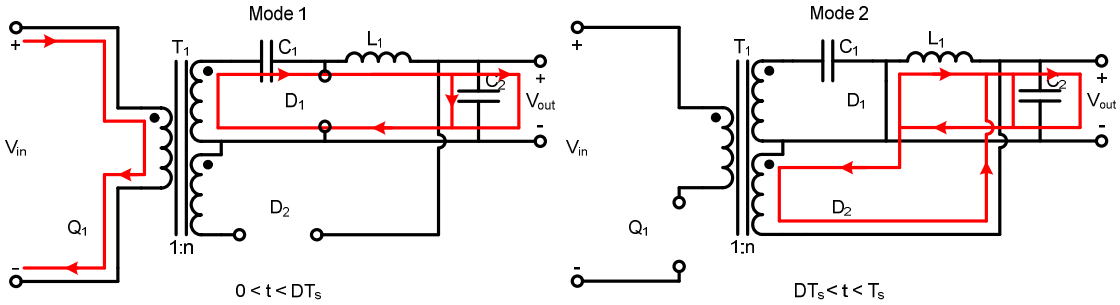

Fig. 42 SEPIC-flyback converter modes of operation

This converter uses less silicon than the other converters. This can limit the power scalability. It does have the ability to transfer energy during most of the cycle. The topology does not fully utilize the transformer's magnetic capabilities. The primary transistor requires a clamping circuit to aid with inductive voltage spikes inherent to single switch isolated converters. The converter is a viable option when lower overall efficiencies are acceptable. It would be an improvement to any application where a standard flyback is considered. This topology also does not scale well and is suited for higher power levels.

3.3.4 Two stage step up converter topologies

Another approach to the step up converter problem is using two converters. The first converter would typically be used to stabilize the fuel cell voltage, followed by a second step up converter that operates at the constant input DC voltage.

M. Harfman-Todorovic *et al.* proposed a topology of this type [8]. They proposed a three level boost converter followed by a two inductor boost converter. The

topology schematic is shown in Fig. 43. The three level boost converter operates such that the inductors are much smaller than a traditional boost converter [8].

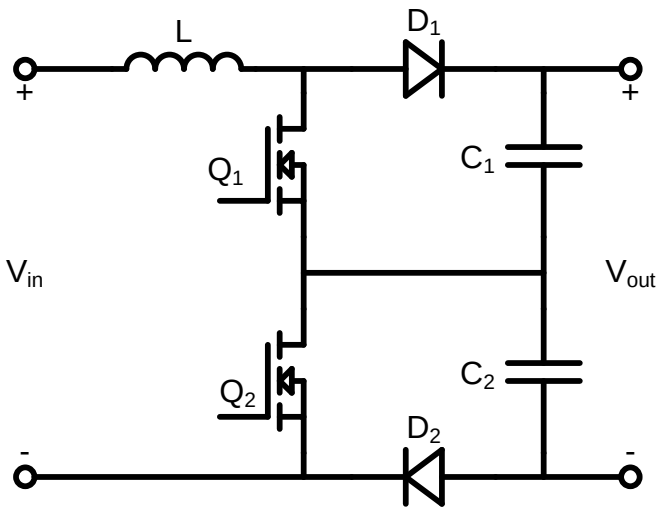

Fig. 43 Three level boost converter basic schematic

The three level boost converter has four operating modes. Fig. 44 shows these operating modes. During mode one, transistor Q1 turns on charging the inductor and raising the voltage of the bottom capacitor C2, while draining the capacitor C1. Entering mode two, Q1 opens and the current is redirected to the capacitor C1, the output load and the output capacitance if required. Mode three occurs when the bottom transistor Q2 is switched on. This mode charges the inductor by making the voltage across the capacitor, C1 less than half of the input voltage. Diode D2 blocks Q2 from discharging

the capacitor C2. Mode four again releases the stored energy into the output stage by turning off Q2.

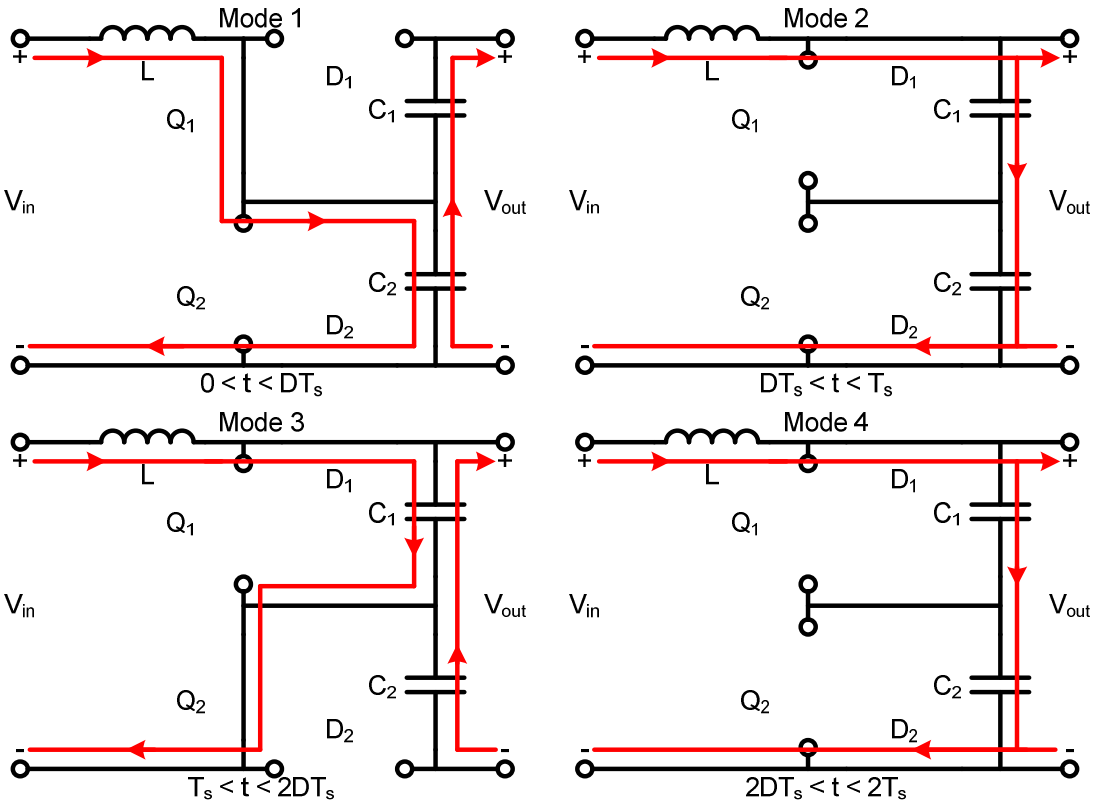

Fig. 44 Three level boost converter modes of operation

The second converter in [8], the two inductor boost converter is similar to the half bridge topology studied earlier. The schematic can be seen in Fig. 45. The secondary of the transformer here has two windings, allowing the elimination of a full bridge rectifier.

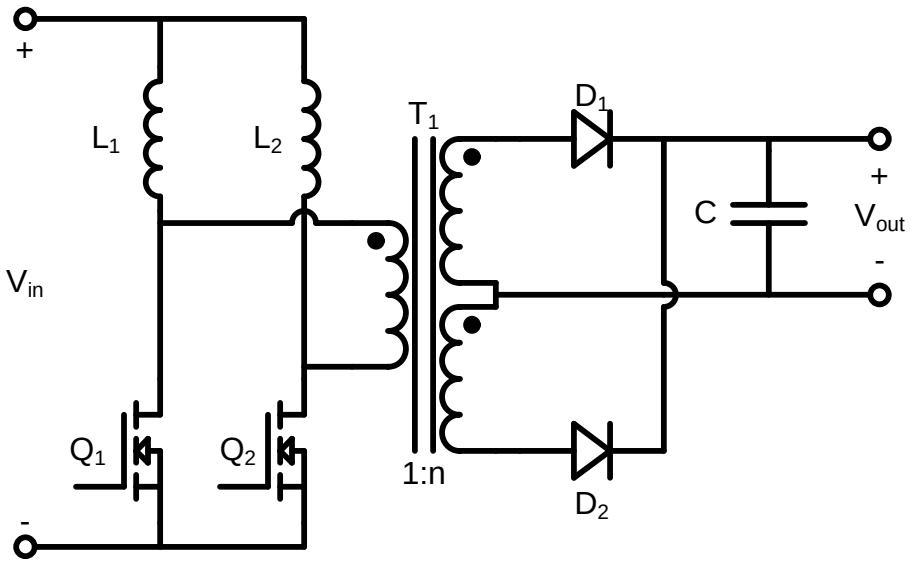

Fig. 45 Basic schematic for two inductor boost converter

There are four modes of operation for this converter. Mode one has both transistors conducting, charging their respective inductors. Mode two occurs when transistor Q1 opens, forcing current through the transformer. This induces a current to the output. Mode three turns Q1 back on and resumes charging the inductors. Mode four opens transistor Q2 and forces current through the transformer the opposite way. This again induces current on the output. Fig. 46 shows these modes of operation.

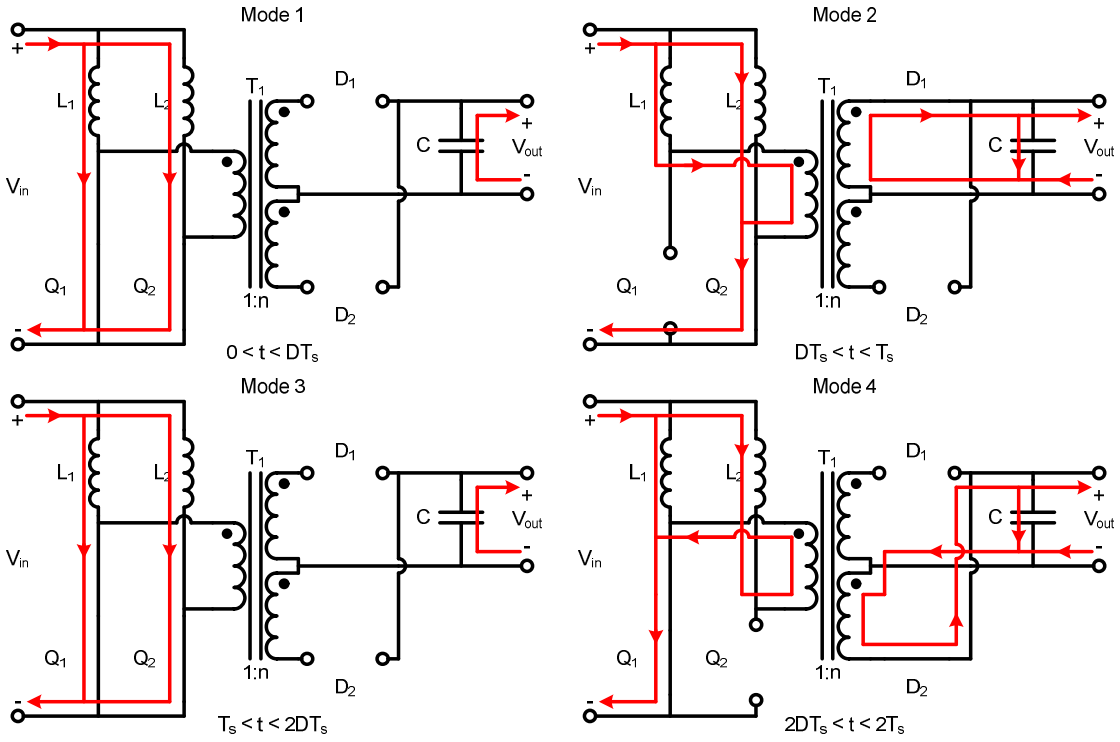

Fig. 46 Two inductor boost converter modes of operation

This two converter topology allows for much easier control of the system. The output converter can be a constant duty cycle if the first converter is well regulated. Using two converters has the potential to have lower efficiency than a single converter, so it must be optimized very well. To counter the potential efficiency loss, the system would need to be cheaper, which is possible with the smaller magnetic and transistor sizing inherent with this topology. This is a very good way to divide the issues converters have with fuel cells into more tractable pieces. The size of this solution likely places it out of the running to fit within the required power densities of server power supplies. There are also potentially large drain voltage spikes in the second converter.

Another two converter topology is offered by S.-G. Song *et al*. [9]. They propose the use of a buck converter feeding a current fed push pull converter. In [9], the buck converter switching frequency is set to twice that of the push pull converter, allowing the inductor to be shared between the converters, and for the elimination of a DC link capacitance.

Fig. 47 shows the basic schematic for the current fed push pull converter. The inductor shown is the output inductor of the buck converter. The converter has four basic modes of operation. These are shown in Fig. 48. During mode one, transistor Q1 and Q2 are on, allowing for the shared inductor to store energy. During mode two, Q1 opens forcing current through the Q2 side of the transformer. This transfers power to the secondary. Mode three turns transistor Q1 back on and recharges the inductor and resets the transformer. Mode four opens Q2 and forces current the Q1 turns of the transformer. This is another stage transferring power to the output.

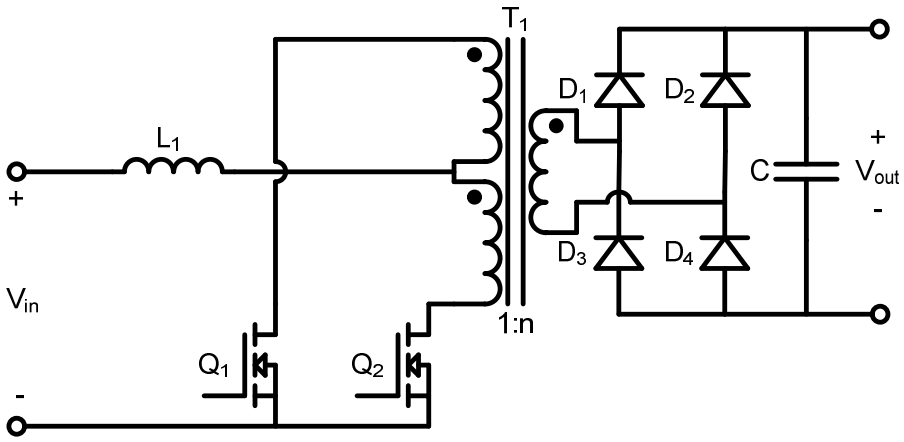

Fig. 47 Basic schematic for a current fed push pull converter

This two stage converter places a greater burden on the transformer than the other two stage converter that was studied. The number of inductors is reduced to two, but the amount of silicon is increased. The buck converter give the push pull converter the ability to operate at a full 50 percent duty cycle. This is due to a current fed topology's remedy to the flux balance issue common to push pull converters.

This topology is likely too large to fit into a server power supply's form factor. It also can have significant drain voltage spikes. Reducing the fuel cell voltage below its minimum voltage would increase the turn ratio and reduce the efficiency of the push pull converter. This topology is best suited for higher voltage fuel cells than the current selected stack.

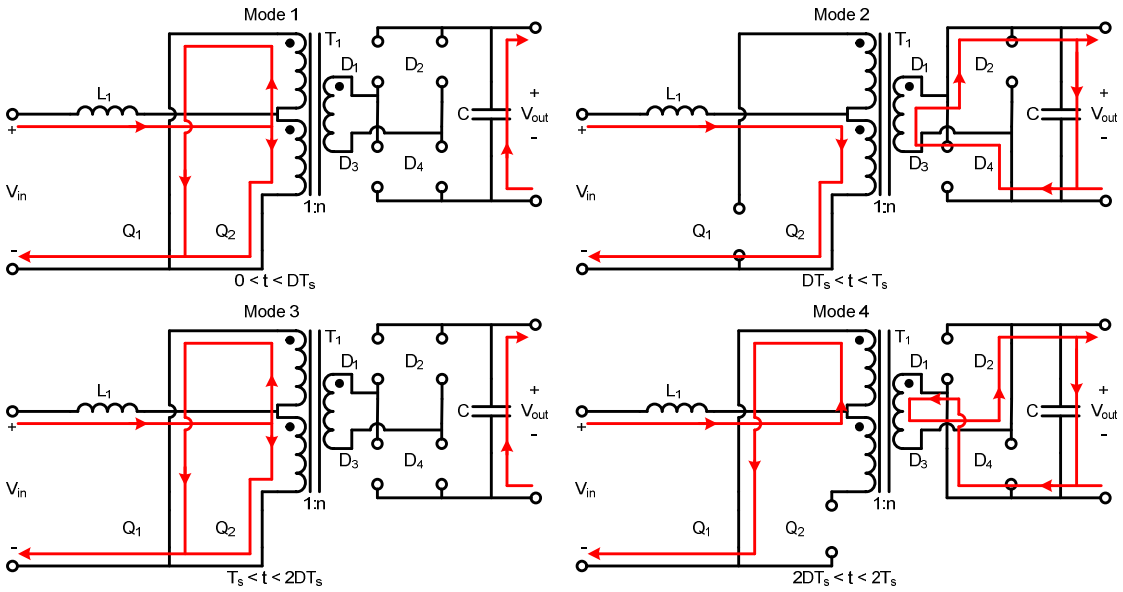

Fig. 48 Current fed push pull converter modes of operation

3.3.5 Topology selection

Two types of solutions have been reviewed, a single converter or two converters in parallel. The form factor limitation of servers requires the use of a single converter. Server power supplies require additional circuitry to meet international agency standards which occupies valuable real estate. Using two converters would be very difficult to cool effectively in the confined form factor.

The converter needs to fully utilize the transformer, to maximize the duty cycle and reduce the transformer turn ratio. The push pull, half bridge and full bridge converters qualify. The push pull has a serious flux imbalance issue when it is not current fed, and it requires more primary windings. The half bridge converter tends to have very large drain spikes on the transistors, requiring elaborate soft switching methods and increased voltage ratings on transistors. The full bridge converter requires more silicon, but has a lower component stress than the two switch topologies. Also, the other two topologies likely would required additional transistors in parallel to lower the conduction losses with higher voltage rated transistors. This can negate the full bridge converter's increased silicon requirement. No perfect topology exists, but a voltage fed full bridge converter fits the requirements well and will be used for this converter.

The researched two converter solutions leveraged a common feature. This was the use of a very simple control scheme for the isolated step up converter. In [8] the second converter was able to operate with a constant duty cycle. This specific application has the unique characteristic that the input voltage changes dramatically with load and the output voltage has a very wide range of operation due to the hold up time

requirements of the AC power supply. This characteristic will be utilized in the design of the fuel cell DC to DC converter.

3.4 Design and simulations

The fuel cell converter design will begin by determining the required values of the magnetic components, along with the required input and output capacitance values. The magnetic components will then be designed. Once the components are selected and designed, the converter will be simulated and stabilized. Then, the converter will be simulated to test the characteristics of its operation with the fuel cell linear model.

3.4.1 Fuel cell converter component value design

The basic schematic for a voltage fed full bridge converter is shown in Fig. 36. The first required design value is the transformer turn ratio. To determine this value, the converter gain function must be determined. To find this, inductor volt-second balance will be applied. While operating in either mode one or mode three, the inductor voltage is given by:

$$v_L = n \cdot V_{in} - V_{out} \tag{35}$$

During operation in either mode two or mode four, the inductor voltage is:

$$v_L = -V_{out} \tag{36}$$

Applying volt second balance gives the following:

$$\int_0^{T_s} v_L\,dt = D\cdot\left(n\cdot V_{in} - V_{out}\right) - \left(1-D\right)\cdot\left(-V_{out}\right) = 0 \tag{37}$$

From this, the gain of the full bridge converter is:

$$V_{out} = n\cdot D\cdot V_{in} \tag{38}$$

During the design of the server power supply, the holdup time of the power supply was simulated. The results are shown in Fig. 49. The power supply is able to provide output with input voltages down to a little below 300 volts. The fuel cell converter needs to maintain an output voltage of at least this. Adding a 5 percent margin increases the required minimum voltage to be around 315 volts.

The output voltage of the fuel cell falls to about 26 volts at full rated load. This is the minimum input voltage for the fuel cell converter. The maximum duty cycle used will be 0.8 for design purposes. Using the formula from equation (38) the required turn ratio is 1:15.

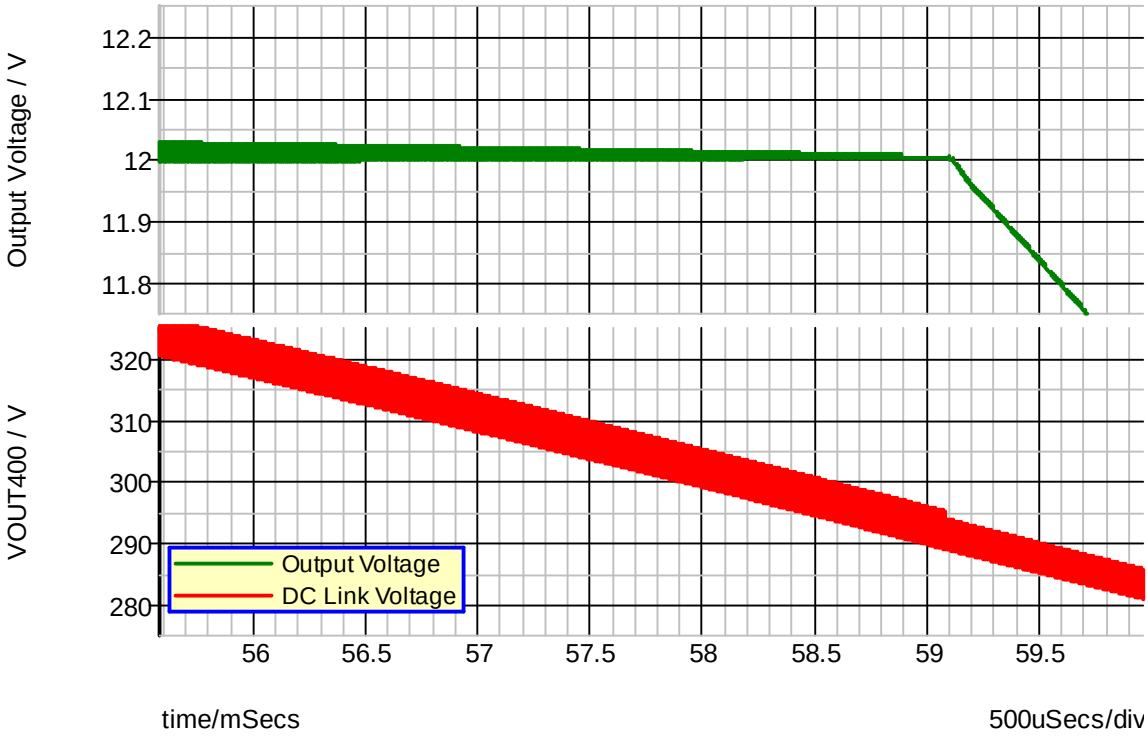

Fig. 49 Simulation showing required input voltage for the AC power supply DC to DC converter

To determine the input and output filter values a switching frequency must be determined. The switching frequency needs to be sufficiently large to reduce component sizes, but low enough to keep switching losses at a manageable level. The two transistor forward converter and the full bridge converter have the same switching loss characteristics. Equations (13) and (14) can be used to estimate the full bridge switching losses. Estimating 90 percent efficiency for the fuel cell converter and the power supply DC to DC converter yields a total required input power of about 990 watts. The approximate voltage and current operating points for the fuel cell at this level are around 28 volts and 35 amperes. This can be seen in Fig. 1 for the Ballard Nexa [3]. Using

transistor characteristics for 80 volt rated MOSFETs, the switching losses can be estimated as 83 microwatts for each transistor cycle. At a switching frequency of 250 kilohertz the switching losses are approximately 42 watts. Adding conduction losses, this would be approximately 14 watts per transistor. To reduce the total power per transistor to 10 watts, the switching frequency needs to be set at 150 kilohertz. This will be the converter switching frequency.

The output waveforms are identical to the two transistor forward outputs. The same formulas can be used to determine output inductance and capacitance. Equation (18) yields the required inductance value to maintain a desired ripple current. Using 20 percent ripple current, 315 volt output, 28 volt input, 90 percent power supply DC to DC converter efficiency and a desired 20 percent current ripple the minimum required inductance is 990 microhenries.

Equation (21) determines the output capacitance. With 1 percent voltage ripple, a 315 volt output, a duty cycle of 0.8 and 20 percent current ripple, the required capacitance for this converter is at least 75 microfarads. This will be this initial amount used. If additional capacitance is needed to stabilize the system or to better provide back up power, more will be added.

The final component value required is the input capacitance for the fuel cell converter. This capacitor is only used to reduce current ripple for the fuel cell, since this will be a voltage mode converter. A capacitance of 100 uF rated at 60V will be used for this purpose.

3.4.2 Inductor and transformer design

The minimum required output inductance was determined to be 990 millihenries. The inductor design method described by R. Erickson and D. Maksimovic in [12] will be used for core selection. In [12] they begin by defining a geometric constant for any particular core. This is given by:

$$K_g = \frac{A_c^2 \cdot W_A}{(MLT)} \tag{39}$$

The required parameters are:

A_c	Core cross sectional area
W_A	Core window area
MLT	Mean length per turn

The selected core must have a geometric constant which satisfies the following inequality:

$$K_g \geq \frac{\rho \cdot L^2 \cdot I_{\max}^2}{B_{\max}^2 \cdot R \cdot K_u} \cdot 10^8 \tag{40}$$

The utilized parameters are:

ρ	Wire resistivity
L	Inductance

$I_{\max}$	Peak current
$B_{\max}$	Maximum operation flux density
R	Winding resistance
K_u	Winding fill factor

The core material will be Magnetics Inc MPP. This has a saturation flux density of 0.75 torr. This inductor will be limited to 80 percent of that value. The winding resistance will be targeted to limit conduction losses to around 500 milliwatts. A winding fill factor of 0.4 will be used. Substituting all of the values, and known values from earlier design steps, the core geometric constant must be greater than or equal to 0.285. The Magnetics-Inc 55322 has a geometric constant of 0.385, which is the closest value above 0.285 in their standard sized MPP cores.

R. Erickson and D. Maksimovic next determine the required 1000 turn inductance for the core [12]. This is given as:

$$A_L = \frac{10 \cdot B_{\max}^2 \cdot A_c^2}{L \cdot I_{\max}^2} \tag{41}$$

This inductance per 1000 turn ratio required is at least 146 millihenries per 1000 turns. Looking at this core's characteristics a ratio of 150 mH per 1000 turns is listed as nominal.

Next, the number of turns needs to be determined [12]. This is done with the following relationship:

$$n = \frac{L \cdot I_{\max}}{B_{\max} \cdot A_c} \cdot 10^4 \tag{42}$$

This inductor requires 83 turns. The final step is to determine the wire gauge [12]. The wire area must be as large as possible to reduce losses, but is limited by the desired winding fill factor. This tradeoff is given as:

$$A_W \leq \frac{K_u \cdot W_A}{n} \tag{43}$$

From this, 15 gauge wire can be used for this inductor.

Two characteristics of the transformer have been determined. The required turn ratio is 1:15 and the output power needs to be around 950 W. The method described by A. Pressman in [13] will be used to size the transformer. This method determines the output power for any given core based on various parameters. It begins with the output power as [13]:

$$P_{out} = \eta \cdot P_{in} \tag{44}$$

The input power is then substituted for its voltage and current components [13]:

$$P_{out} = \eta \cdot \left(V_{DC,\min} \cdot I_{avg,DC\min} \right) \tag{45}$$

The average current at this point is equal to the average of the current when the converter is transferring power times the maximum duty cycle. Substituting this in for current gives [13]:

$$P_{out} = \eta \cdot V_{DC,\min} \cdot \left(D_{\max} \cdot I_{avg,ontime}\right) \tag{46}$$

The RMS value for the current is given by:

$$I_{RMS} = \sqrt{D} \cdot I_{avg,ontime} \tag{47}$$

Substituting (47) into (46) yields the following:

$$P_{out} = \eta \cdot V_{DC,\min} \cdot D_{\max} \cdot \left(\frac{1}{\sqrt{D_{\max}}} \cdot I_{RMS}\right) \tag{48}$$

The next step is to substitute in for the voltage from Faraday's law. This substitution is given as [13]:

$$V_{DC,\min} = N_p \cdot A_e \cdot \frac{\Delta B}{\Delta T} \cdot 10^8 \tag{49}$$

The following terms are defined for above [13]:

N_p	Number of primary turns
A_e	Transformer core area
ΔB	Change in flux density
ΔT	Total on time

Substituting Faraday's law into the output power equation gives [13]:

$$P_{out} = \eta \cdot \left(N_p \cdot A_e \cdot \frac{\Delta B}{\Delta T} \cdot 10^8 \right) \cdot D_{\max} \cdot \frac{1}{\sqrt{D_{\max}}} \cdot I_{RMS} \tag{50}$$

The final series of steps is replacing the current with some parameters relating to current density [13]. The following definitions are required [13]:

A_b	Bobbin area
A_p	Primary winding area
A_s	Secondary winding area
A_{ti}	One primary turn area
A_{tcm}	Primary winding area in circular mils
D_{cma}	Circular mils current density

Two assumptions are made based on practical limitations. The first is the space factor, percentage of winding area used will be 40 percent and that area will be shared equally between the primary and the secondary [13]. These assumptions lead to the following relationships [13]:

$$A_p = 0.2 \cdot A_b = N_p \cdot A_{ti} \tag{51}$$

Solving for the single primary turn area gives [13]:

$$A_{ti} = \frac{0.2 \cdot A_b}{N_p} \tag{52}$$

Substituting for the bobbin area and doing a unit conversion to circular mils by multiplying by a constant gives the primary winding area in circular mils [13]:

$$A_{tcm} = \frac{(c) \cdot (0.2 \cdot A_b)}{N_p} \tag{53}$$

The current density per circular mil is expressed as:

$$D_{cma} = \frac{A_{tcm}}{I_{RMS}} \tag{54}$$

The final step to determining the core available output power is to solve for the RMS current and substitute back into the output power equation [13]. This gives the following [13]:

$$P_{out} = \eta \cdot N_p \cdot A_e \cdot \frac{\Delta B}{\Delta T} \cdot 10^8 \cdot D_{\max} \cdot \frac{1}{\sqrt{D_{\max}}} \cdot \left(\frac{c \cdot 0.2 \cdot A_b}{D_{cma} \cdot N_p} \right) \tag{55}$$

The number of primary turns does disappear, leaving an expression for the power based on the converter's desired characteristics. Pressman recommends a circular mil current density of 500 circular mils per ampere [13]. He also recommends at frequencies above 50 kilohertz reducing the maximum flux density to a value between 800 and 1400 Gauss [13]. For designing this transformer, a maximum flux density of 1000 Gauss will be used.

The Ferroxcube ETD39 core looks to be a good selection. Solving for the output power with the characteristics required for this converter gives an estimated output power of around 980 watts. The number of primary turns is the next step in the transformer design. Pressman uses Faraday's law to determine this value [13]. The equation is given as:

$$N_p = \frac{(V_{\min} - 1) \cdot t_{on,\max} \cdot 10^8}{A_e \cdot \Delta B} \tag{56}$$

All of these values are already known. Substituting these values and rounding up to the nearest whole turn gives a minimum requirement of 3 primary turns. The final consideration is the wire size required to give the designed current density [13]. The number of circular mils required is:

$$A_{cm,\min} = \frac{D_{cma}}{I_{RMS}} \tag{57}$$

From this it is determined that the primary requires 7 gauge wire and the secondary winding requires 19 gauge wire. This sized wire generates a power loss of approximately 500 to 600 milliwatts on the primary and secondary from conduction losses. This is determined by multiplying the mean turn length from the core data sheet and the number of turns to get the total amount of wire. Multiplying this by the resistivity gives the copper resistance for the primary and secondary windings.

3.4.3 Converter simulations

This converter requires a rating of about 900 watts at a possible minimum input of 26 volts from the fuel cell. The first simulated critical feature is the current going through the magnetic components. This is done with magnetic models which can saturate. The transformer and output inductor current should exhibit nice linear increases in current due to the constant DC input voltage. Fig. 50 shows the steady state current through the simulated output inductor.

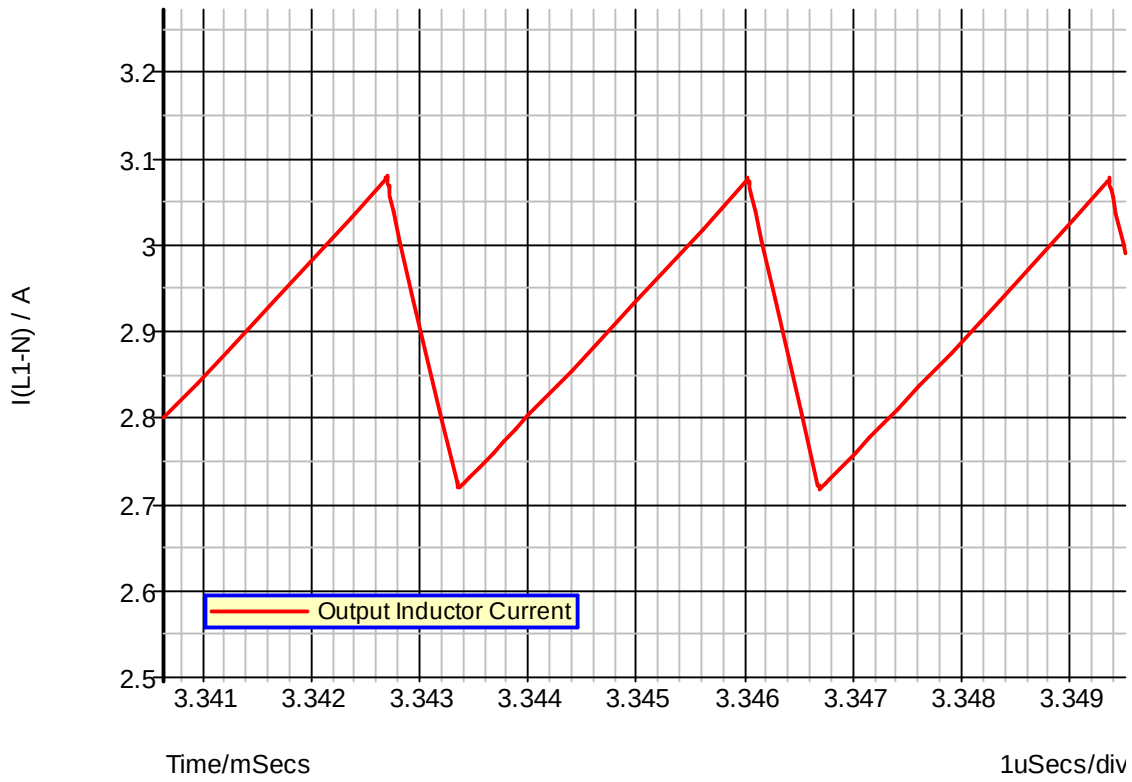

Fig. 50 Simulated output inductor current

The inductor current shows no signs of saturation at maximum load, minimum input voltage. Fig. 51 shows the primary current through the transformer. This waveform also shows no sign of saturation at full rated load, maximum current.

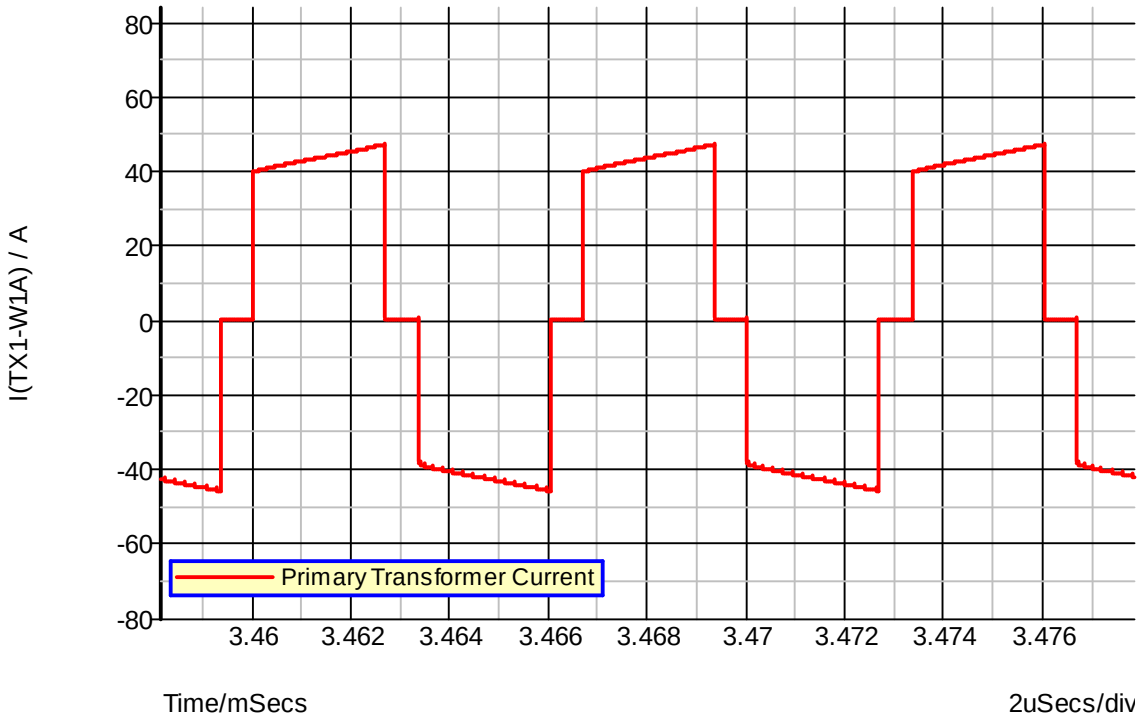

Fig. 51 Simulated primary transformer current

The load was increased until obvious signs of saturation appeared on both the inductor and transformer. The load was increased enough to believe that the transformer and inductor should not saturate during normal operation. Fig. 52 shows the simulated saturation of the converter.

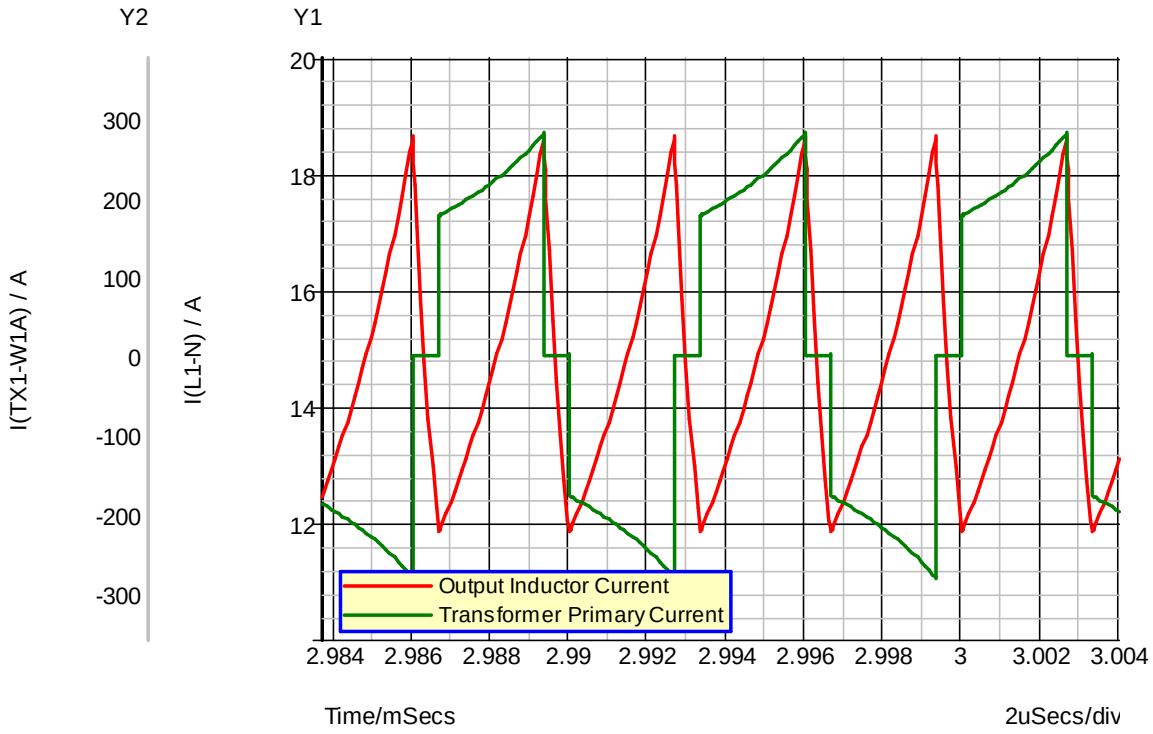

Fig. 52 Simulated saturation current waveforms

This simulation estimated an efficiency of about 88 percent. This simulation did not account for switching losses in the transistors. Adding the previously calculated estimate into the equation results in an efficiency of 85 percent, this is in line with expectations.

The power supply DC to DC converter operates at a nominal voltage of 400 volts. The silicon is sized for this voltage, so the fuel cell converter must not output voltage above this level. The voltage will be regulated to a voltage of 380 volts to ensure the output does not exceed these requirements. The maximum duty cycle will be limited such that the converter operates open loop at higher loads. A constant load of

approximately 20 watts has been added to the output of the converter to account for housekeeping circuits and fans. This will also ensure that the fuel cell is always providing some power and allow for better transient responses.

Fig. 53 shows the open loop frequency characteristics of the converter and the PWM gain with a 900 watt load. The target crossover frequency needs to be past the zero introduced by the output capacitor's series resistance. The crossover frequency also needs to be much lower than the switching frequency. The series resistance zero occurs around 4 kilohertz, so 10 kilohertz will be selected as the target crossover frequency. This is less than 10 percent of the switching frequency.

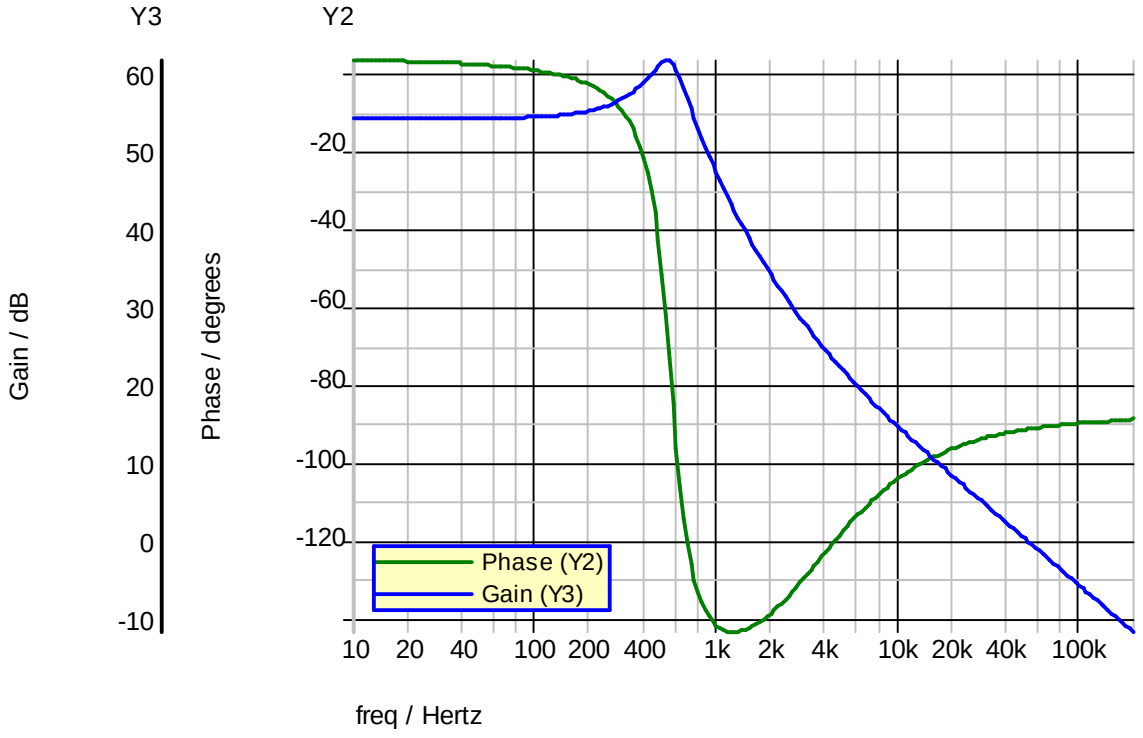

Fig. 53 Simulated fuel cell converter open loop bode plot

Fig. 54 shows the error amplifier characteristics designed to provide feedback and stability to the system. At the crossover frequency of 10 kilohertz, the gain of this amplifier is low enough to bring the total gain down to unity. There is also a significant phase boost since the pole and zero are more than a decade away from the crossover frequency.

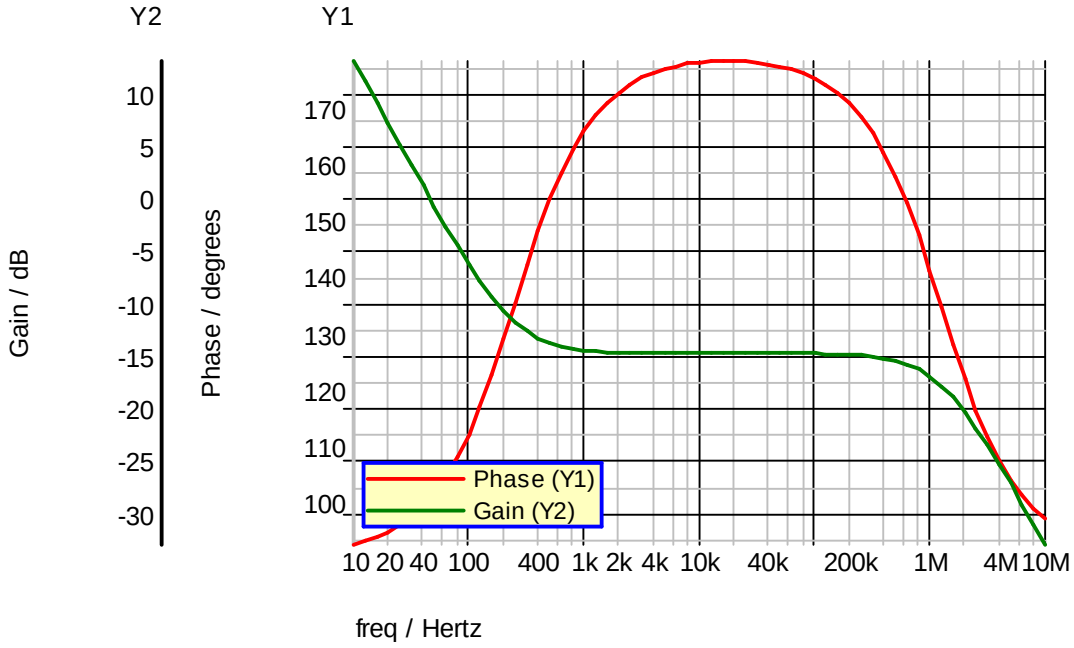

Fig. 54 Simulated proposed error amplifier characteristics

Applying the designed error amplifier to the converter yields the transfer characteristics in Fig. 55. The crossover frequency occurs at 10 kilohertz as designed. There is approximately 55 degrees of phase margin at the crossover frequency. The

phase boost from the error amplifier is very prominent at the crossover frequency. The gain margin is approximately 40 dB. This converter looks to be stable.

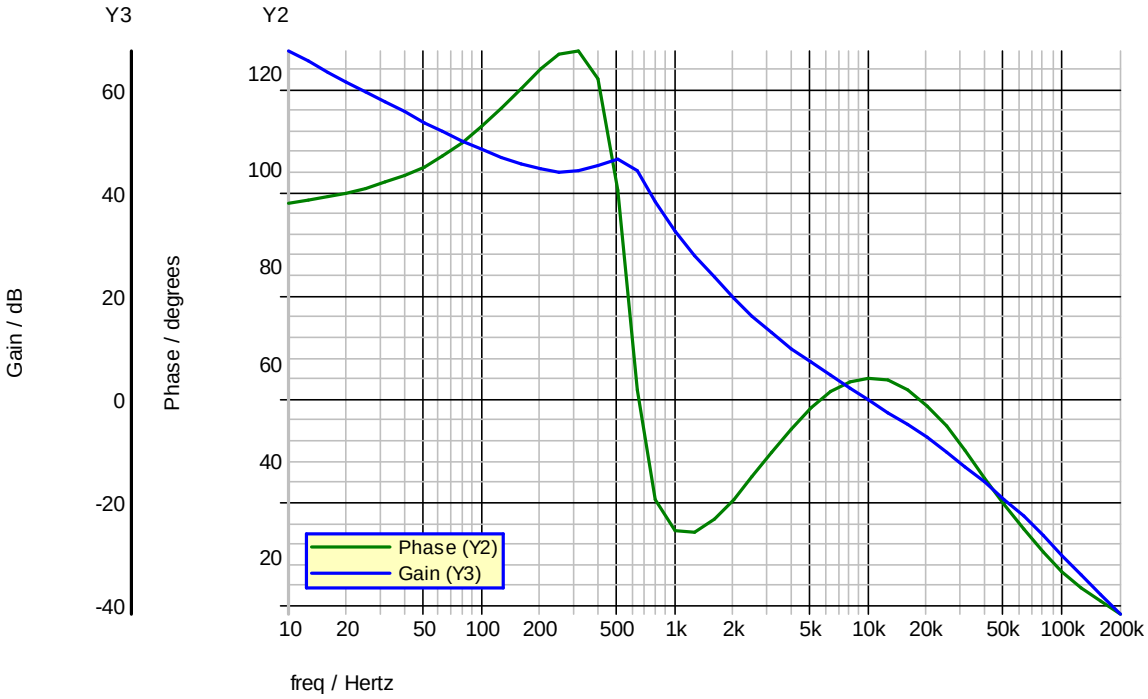

Fig. 55 Simulated closed loop frequency response

Now that the system is stable, the final design change is reducing the maximum duty cycle such that at maximum load, the output voltage is 315 volts and the converter is ostensibly operating open loop. This duty cycle is approximately 68 percent. Fig. 56 shows the simulated output voltage ripple at full rated load. The total voltage ripple is much less than the target one percent ripple.

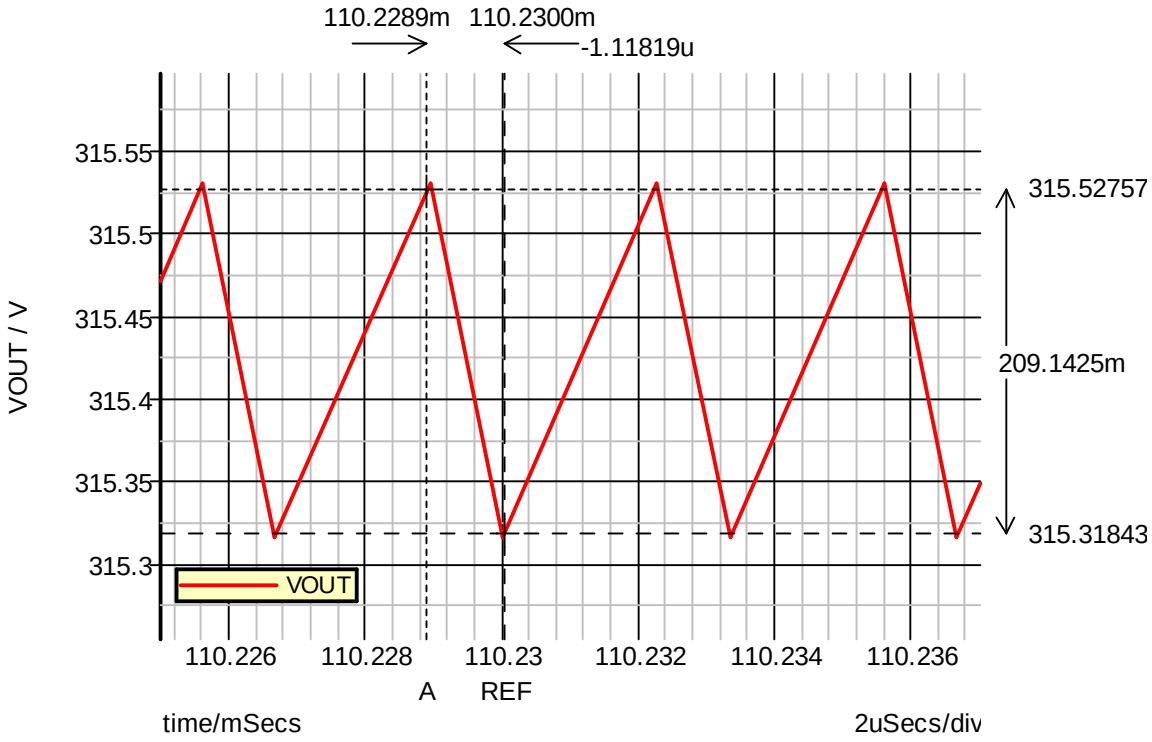

Fig. 56 Simulated output voltage ripple at full load

Two extreme load conditions can occur with this converter. The first is from zero to full rated load. This would occur if there is a failure in the server power supply's front end DC to DC converter. If that is the case, the DC link bulk capacitance in the server power supply would be shorted and no stored energy would be available. This would force the fuel cell converter to support 100 percent of the load. Fig. 57 shows this simulated transient condition. The simulation shows that the output capacitance is more than enough to give the fuel cell and its converter enough time to take over the load.

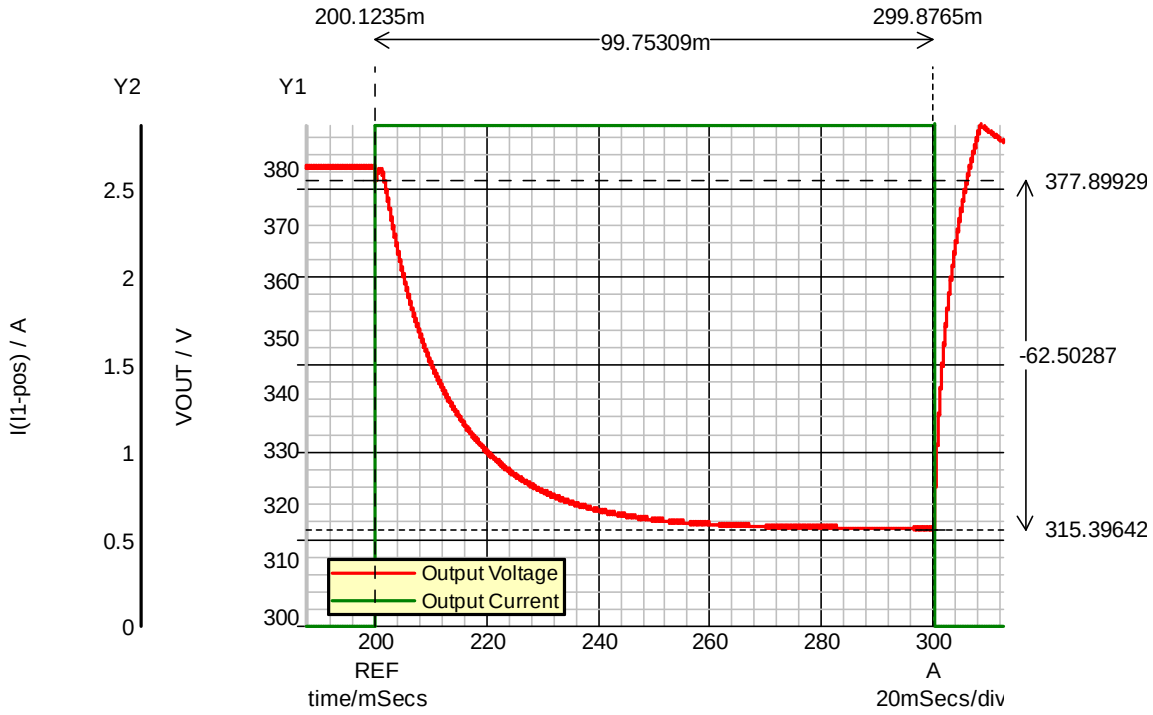

Fig. 57 Simulated no load to full load transient

The second large dynamic load that may occur for the converter is full to zero load. This would occur when there has been a loss of power to the server power supply, followed by the input power returning. Fig. 58 simulates this transient. There is a slight voltage overshoot up to about 387 volts. This peak voltage is significantly below the 400 volt nominal boost converter output voltage. This simulation is also a bit worse than what would occur with the power supply. The DC link voltage would rise, and when it increases above 315 volts, it would start taking load in a much slower manner than this simulation. This slight overshoot should be acceptable.

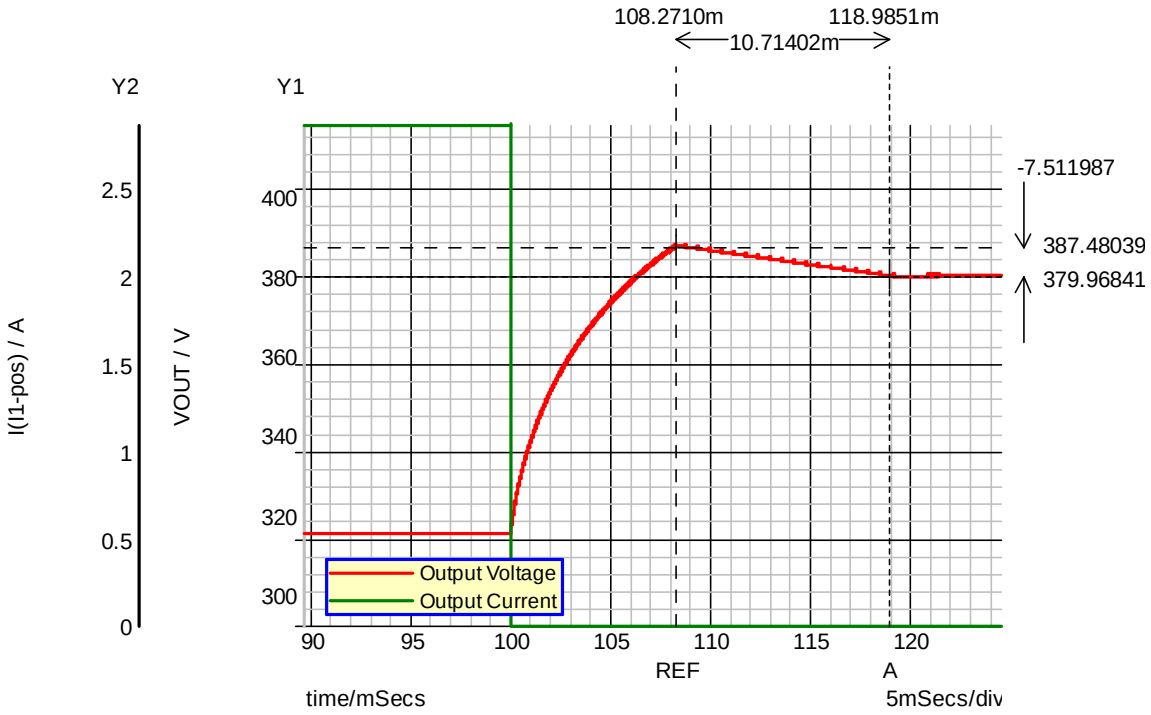

Fig. 58 Simulated full to no load transient

Fig. 59 shows the fuel cell outputs during the two extreme transient conditions. The waveforms suggest that the fuel cell would easily survive these load transients.

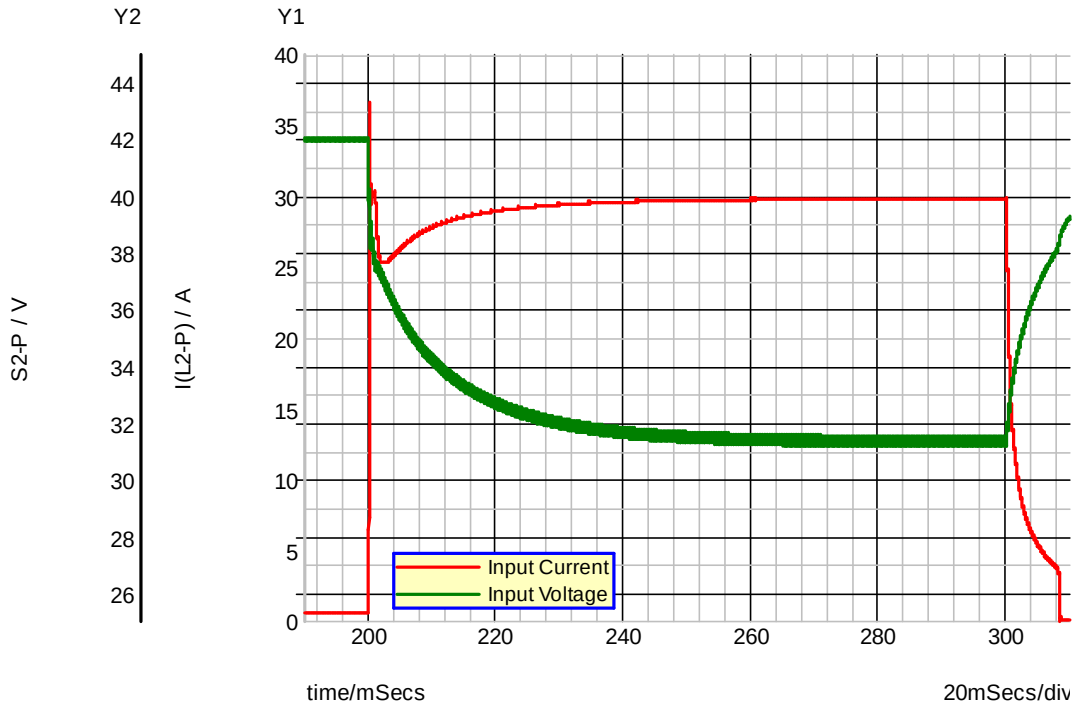

Fig. 59 Simulated worst case fuel cell transients

3.5 Summary

A step up DC to DC converter has been designed to regulate a fuel cell's output power to a usable form for the output converter of the server power supply. The extreme transients have been simulated and analyzed with no issues observed. The converter utilized a common theme from some of the studied previous work and incorporated open loop operation during much of the converter's load range. This aided in ensuring stable operation of the converter at higher loads without excessive output capacitance.

CHAPTER IV

BACKUP POWER CONTROL STRATEGY

4.1 Introduction

To be a consideration for use as a back up power source, any fuel cell UPS system must protect at least as well as a traditional battery powered system. The UPS must protect during an interruption from the primary power source, and it must also relinquish the load gracefully when the primary power source returns. These two criteria will be key in determining the proposed UPS system topology.

4.2 Topology

Traditional UPS systems with fuel cell energy sources have been studied. W. Choi *et al.* proposed a line interactive fuel cell powered UPS [10]. Fig. 60 shows their proposed system topology. They propose using two boost converters for separate fuel cells and a two direction converter to store transient energy in super capacitors [10]. This topology requires two conversions and the overhead of a third converter to provide backup power to its load. AC loads require such a UPS, but if the load converts the AC back to DC, an extra power conversion stage exists. This extra power conversion diminishes efficiency and adds a single point of failure to the system, which is not necessary.

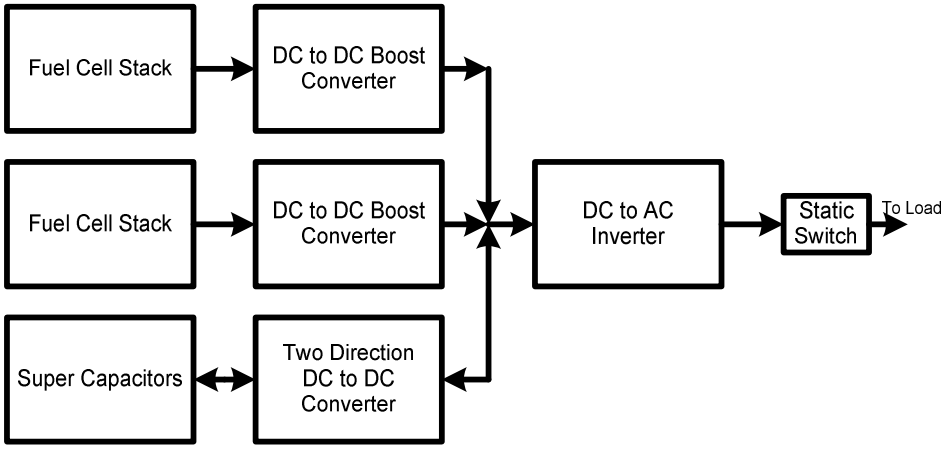

Fig. 60 Adapted illustration of proposed fuel cell powered UPS [10]

Q. Zhao *et al.* proposed a dual input power supply for a network server [11]. Their proposal is seen in Fig. 61. They suggest using standard 48 VDC telecom batteries interfaced directly with the network server power supply as a UPS [11]. The converter proposed was for a bank of batteries, but the idea of interfacing directly with the power supply's DC link is introduced, but not explored. This idea will be used and studied.

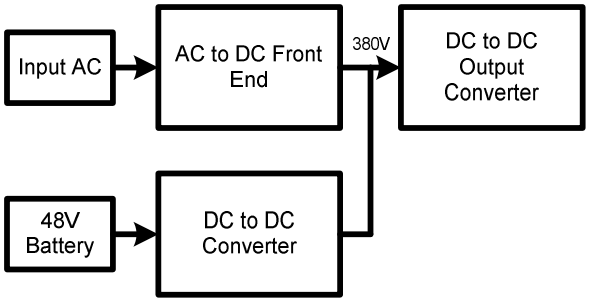

Fig. 61 Adapted illustration of proposed dual input server power supply application [11]

The proposed UPS topology is shown in Fig. 62. The fuel cell and its DC to DC converter interface directly with the DC link inside the server power supply. The basic sharing scheme can be seen in Fig. 63. During normal operation, the fuel cell converter will only consume housekeeping power loads as well as perhaps some standby constant loads from the network server. The output voltage from the fuel cell converter is regulated lower than the PFC boost converter, meaning the PFC boost converter will provide all power.

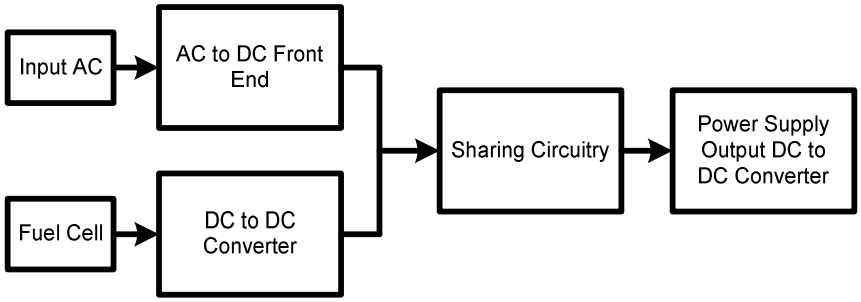

Fig. 62 Proposed UPS topology

The diodes should be ORing diodes, which can handle the stresses required for its blocking function and keep losses down. One key added benefit to this topology is the additional protection from failures in the PFC boost converter. Traditional UPS systems provide AC to the power supply, and can do nothing about a failure in the PFC boost circuitry. This topology can keep the server running indefinitely with a PFC boost failure. The output capacitance is added to allow the stored energy in the transformer to be returned when the converter resets the transformer. There would be excessive voltage spikes without a place to return the magnetizing energy from the two transistor forward converters.

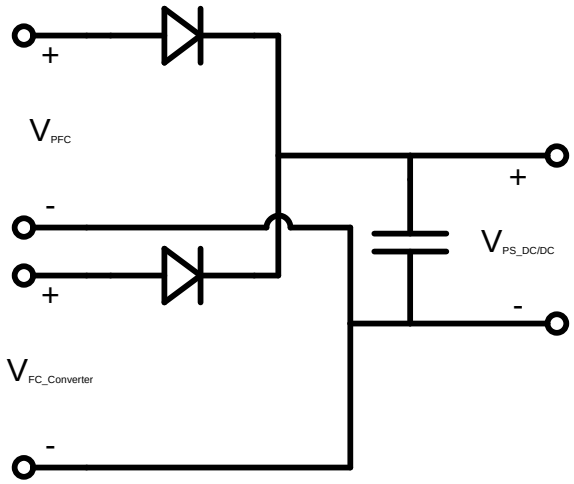

Fig. 63 Basic schematic for proposed sharing circuitry

4.3 Simulations

Two sets of simulations will be performed to study the proposed UPS topology. The first tests will simulate the output requirements of the server power supply's DC to DC converter while being powered by the fuel cell. Following these tests, the UPS system's ability to prevent server outages will be simulated. An AC dropout, an AC recovery and a PFC boost converter failure will be simulated to study the server power supply's output responses to these failure modes.

4.3.1 Fuel cell converter with server power supply

The first output specification simulated was the output voltage set point. Fig. 64 shows this result. The average output voltage is within the specified 60 millivolt window.

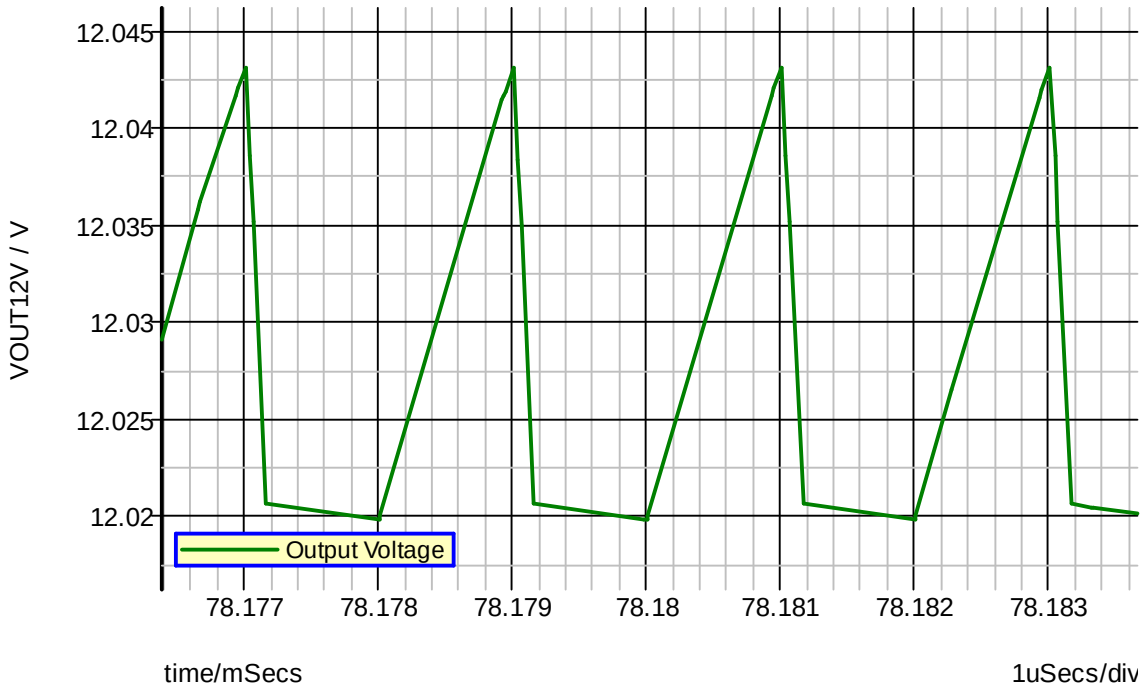

Fig. 64 Simulated output voltage set point with fuel cell power source

The maximum specified transient responses were the final simulations performed. Fig. 65 and Fig. 66 show the half to full load dynamic responses. The output voltage remains very comfortably within the specified dynamic voltage window.

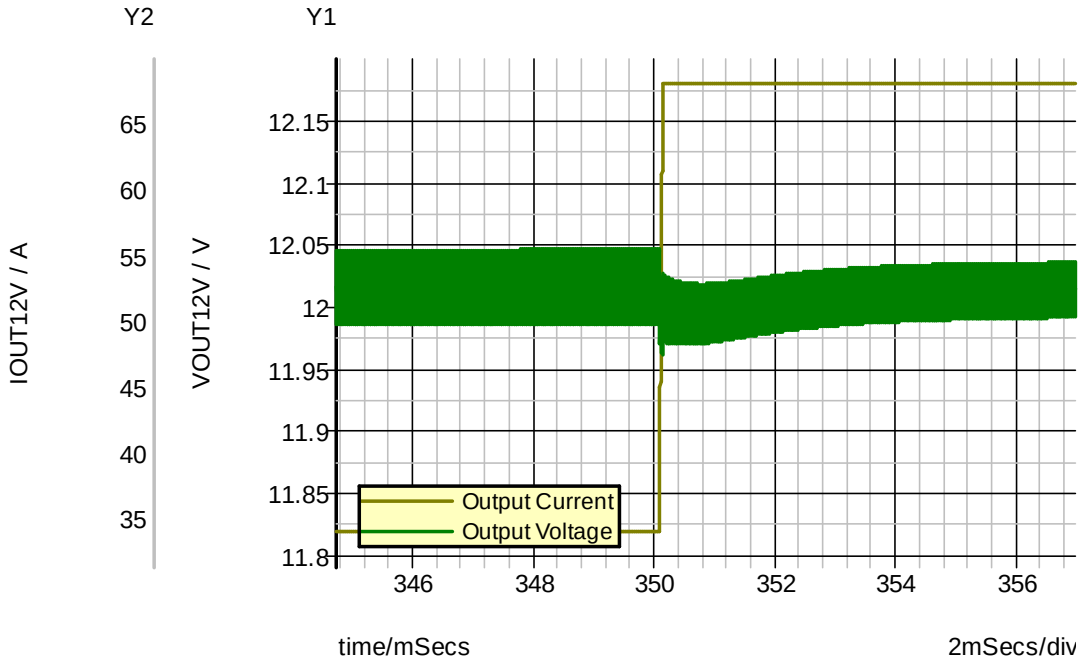

Fig. 65 Simulated output transient response with fuel cell half to full load

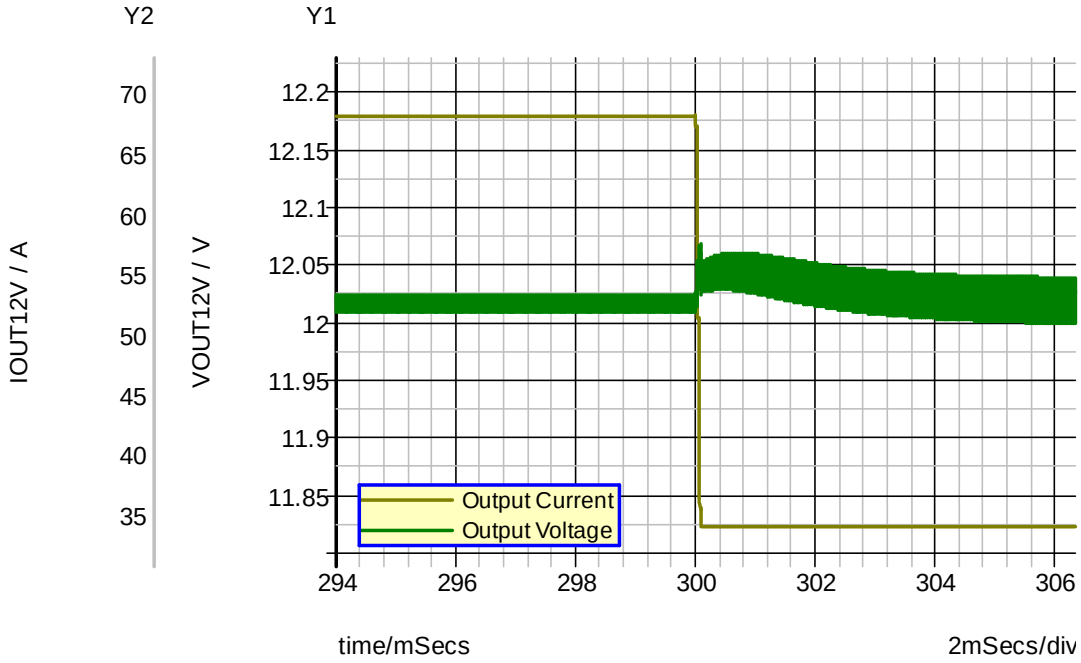

Fig. 66 Simulated output transient response with fuel cell full to half load

Fig. 67 shows the no load to half load transient response. The large drop in voltage is directly related to the series resistance in the output capacitance. The resistance here was low enough to safely keep the output voltage within the transient specification.

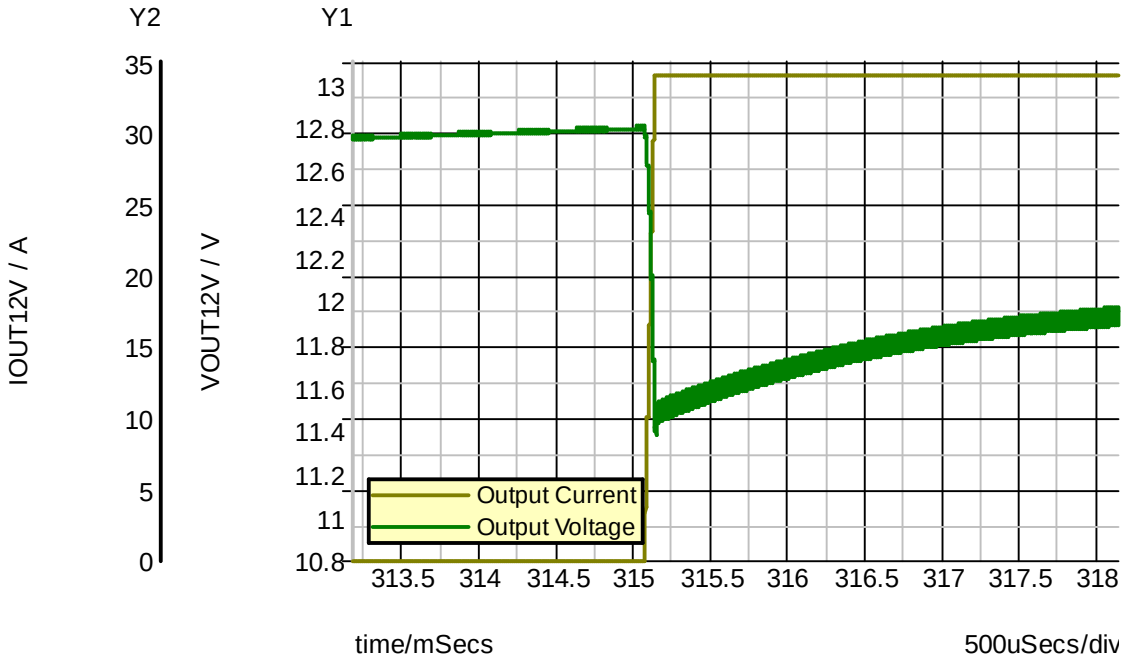

Fig. 67 Simulated no load to half load transient with fuel cell

Fig. 68 shows the half to zero load voltage transient. The output voltage remained well within the specified voltage window during this simulation.

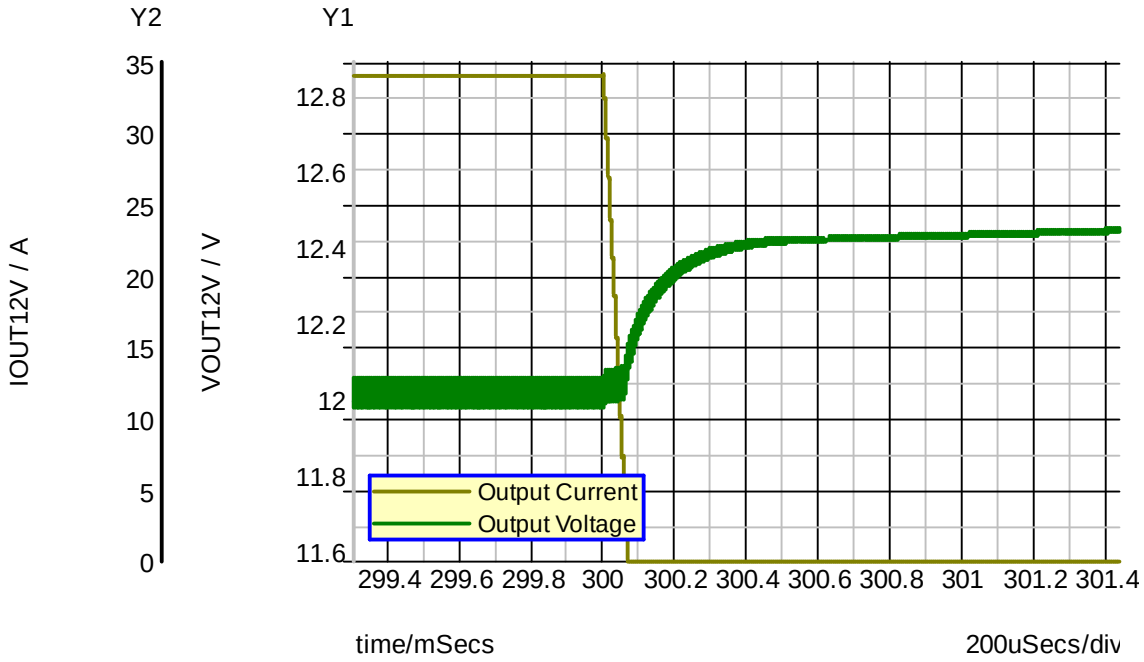

Fig. 68 Simulated half to zero load transient with fuel cell

The server power supply's DC to DC converter operates within specification with the fuel cell converter as its input source.

4.3.2 Fuel cell converter as a UPS

The first power loss scenario to simulate is an AC dropout. This occurs when the input power to the server power supply faults. This type of failure is very common and is not very tractable. When the AC faults, the fuel cell converter needs to provide up to 100 percent of the output power rating within a matter of milliseconds. Fig. 69 shows the fuel cell's reaction and the output voltage during this failure mode. The output voltage remains within its static regulation specifications. The 120 hertz noise on the output also

disappears when the AC fails. The fuel cell was allowed a transient time on the order of tens of milliseconds. This is a very acceptable transient for the fuel cell.

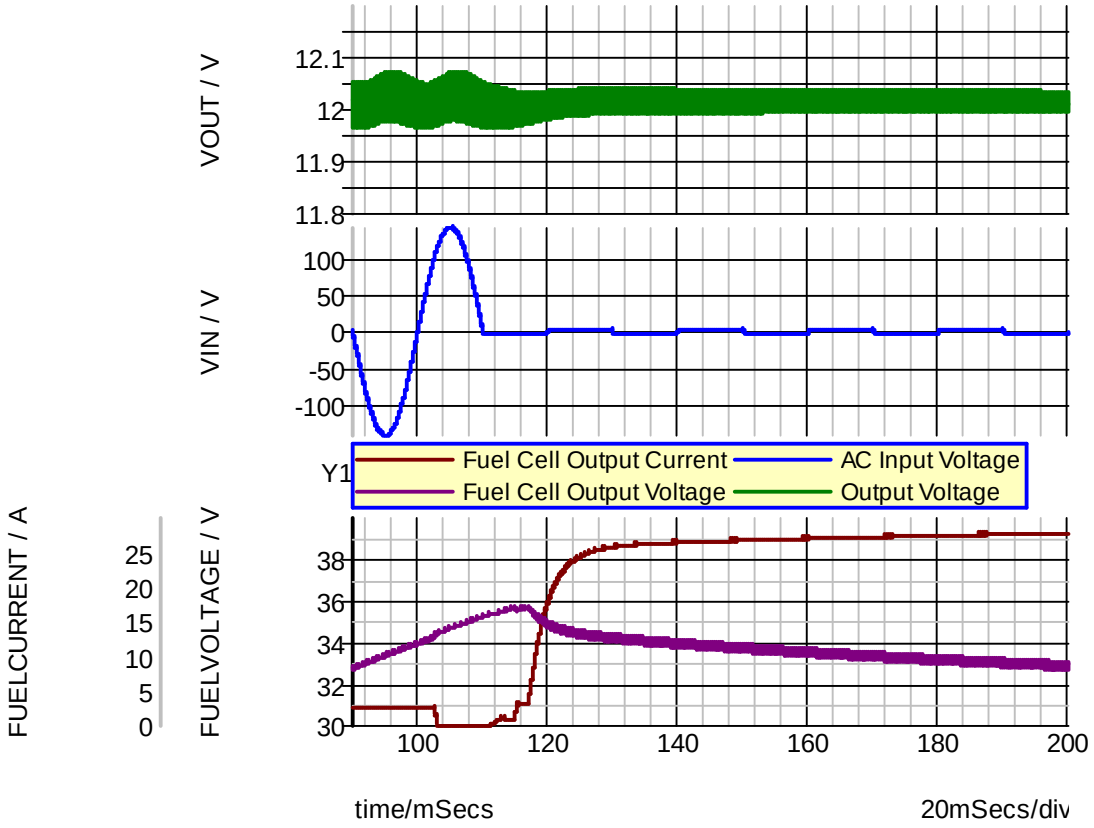

Fig. 69 Simulated UPS response to an AC dropout

After the AC dropout occurs, the AC will return once a repair has been made. This event is known as an AC recovery. The fuel cell should relinquish the full load back to the AC utility once it is available to conserve fuel. This event was simulated and is shown in Fig. 70. The output voltage does show a slight transient, but it is well within

specifications. The fuel cell relinquishes the load much faster than it took it over. This is due to the large output capacitance of the PFC boost converter, and the voltage droop on the fuel cell converter. The capacitance and the converter essentially share the load until the fuel cell converter's output voltage regulates to a voltage below the PFC boost converter's output.

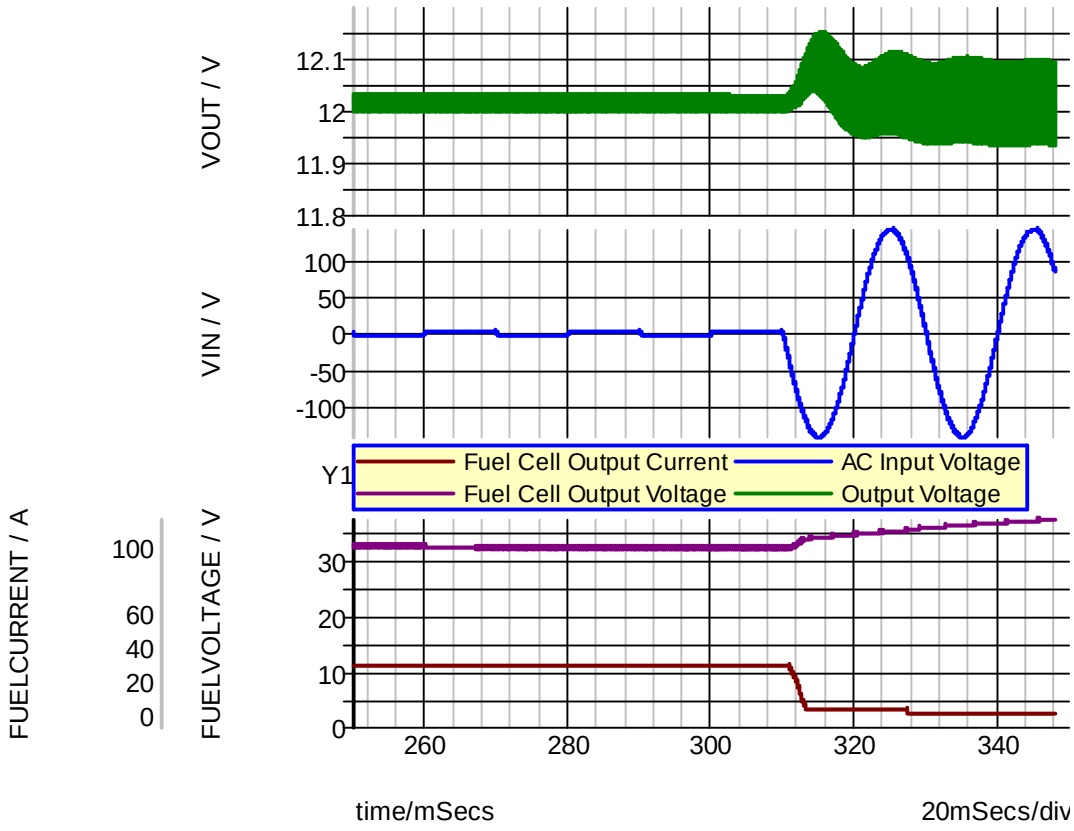

Fig. 70 Simulated UPS response to AC recovery

Typical UPS systems only protect from certain failure modes to the main input power source. If the PFC converter fails in the power supply, no typical UPS can maintain the server's availability. This proposed UPS interfaces with the power supply beyond the PFC converter. This enables for an added layer of protection. Fig. 71 simulates a PFC transistor failure to a short circuit. The sharp drop around 120 milliseconds is where the failure occurs. There is a slight transient on the output voltage, but it stays within the specified operating range. The fuel cell and its converter required a few milliseconds to respond. This is well within the fuel cell's transient capabilities.

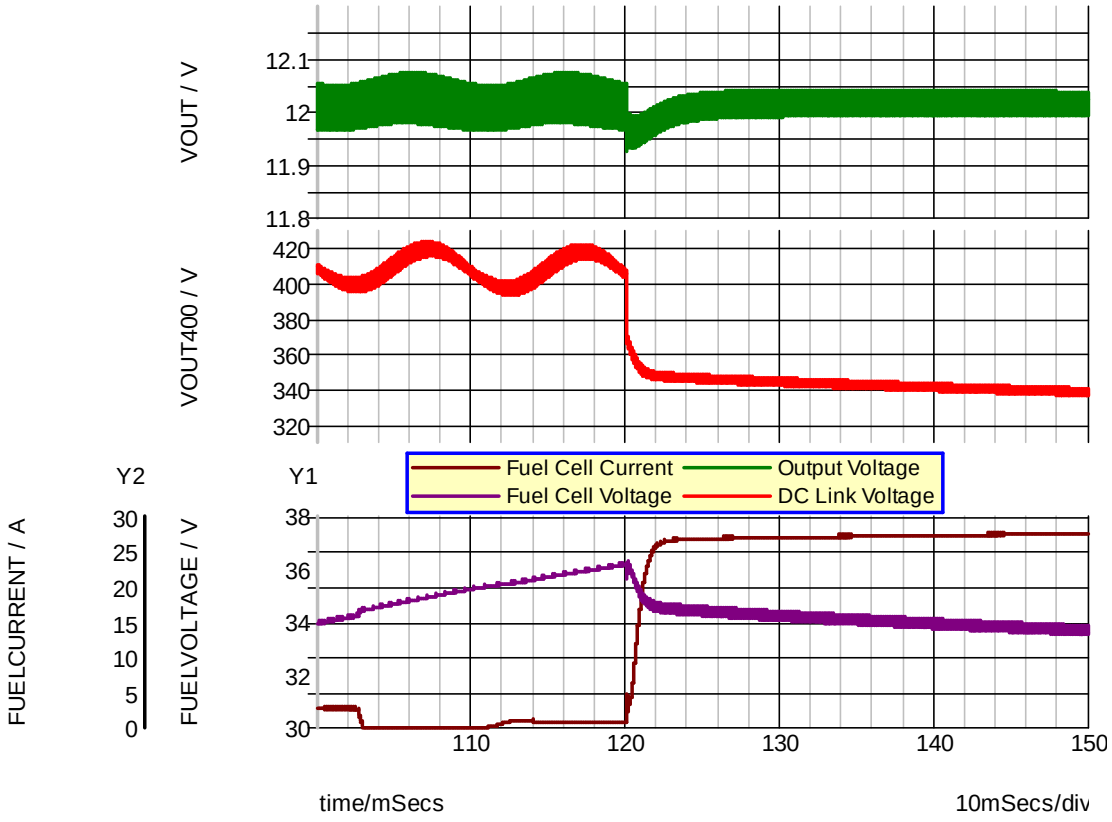

Fig. 71 Simulated UPS response to PFC converter failure to short circuit

4.4 Summary

A UPS which derives it backup energy from a fuel cell has been designed and simulated to operate with a server power supply. Standard input fault protection was simulated and found to give satisfactory results for maintaining the server's availability. An additional feature to the UPS was simulated. This enhanced mode of protection maintained availability during a PFC converter hard failure. This enhancement is a byproduct of the proposed UPS topology.

CHAPTER V

CONCLUSIONS

5.1 Summary

Data centers are tasked with maximizing availability of their servers. This normally involves some type of UPS system. Typical UPS systems use large banks of batteries as an energy source. Fuel cells have some marked advantages to batteries. The cells are sized for the output load and energy stored is related to the amount of fuel, instead of battery size. This gives the potential to run indefinitely with a constant fuel feed. The fuel cell is also a much more environmentally friendly alternative to batteries.

To determine the best implementation of a fuel cell UPS the server power supply must be understood. Chapter II was dedicated to the design and specifications of a server power supply and simulating the design for use in testing the fuel cell UPS.

Chapter III explored the responses of the fuel cell and studied many proposed step up converters for fuel cells. There is definitely no clear cut topology for fuel cell usage. The total requirements of the application must be kept in mind during the selection and design. From the information presented a topology was selected and a step up converter for this specific application was designed wholly and simulated.

The UPS topology was determined in Chapter IV. Two proposed UPS systems were analyzed and a topology with this specific application in mind was selected. The previously designed server power supply and fuel cell powered step up converter were simulated together and shown to protect during normal failure modes in which a UPS

should protect. An enhanced protection mode was also simulated and shown to be an advantage over existing UPS topologies.

5.2 Future work

The next step is to construct a prototype. This would allow for testing on a fuel cell simulator, followed by testing with the actual fuel cell. A server power supply would require some minor modification for the testing to occur.

After the prototypes are built, the fuel cell converter control loop should be optimized to layout and real circuit characteristics. Efficiency improvements should also be explored. This would include alternate magnetic components, changing transistors and adding synchronous output transistors to replace the diodes. After optimization, extensive tolerance simulations would be performed to ensure all manufactured power supplies would meet all specified requirements.

The final tests would be powering the server and testing the different failure modes under real world loads.

REFERENCES

[1] T. Sels, C. Dragu, T. Van Craenenbroeck and R. Belmans, "Overview of new energy storage systems for an improved power quality and load managing on distribution level," in *16th Int. Conf. and Exhibition Electricity Distribution*, Amsterdam., 2001, vol. 4, pp. 5.

[2] Curtis Ashton, "Ultra™ capacitors for short duration backup of DSL cabinets," in *28th Annu. Int. Telecommunications Energy Conf*., 2006, vol. 15, pp. 1-7.

[3] Woojin Choi, "New approaches to improve the performance of the PEM based fuel cell power systems," Ph.D dissertation, Dept. Elect. Eng., Texas A&M Univ., College Station, TX, 2004.

[4] J.-T. Kim, B. Lee, T.-W. Lee, S.-J. Jang, S. Kim, C.-Y. Won, "An active clamping current fed half bridge converter for fuel cell generation systems," in *35th Annu. IEEE Power Electronics Specialists Conf*., 2004, vol. 6, pp. 4709-4714.

[5] M. Mohr and F.-W Fuchs, "Voltage fed and current fed full bridge converter for use in three phase grid connected fuel cell systems," in *5th Int. Power Electronics and Motion Control Conf*., 2006, vol. 1, pp. 1-7.

[6] S.-R. Moon and J.-S. Lai, "Mulitphase isolated DC-DC converters for low-voltage high-power fuel cell applications," in *22nd Annu. Applied Power Electronics Conf*., Anaheim, CA, 2007, pp. 1010-1016.

[7] S.-J. Jang, T.-W. Lee, K.-S. Kang, S.-S. Kim and C.-Y. Won, "A new active clamp sepic-flyback converter for a fuel cell generation system," in *32nd Annu. Conf. IEEE Industrial Electronics Society*, 2005, pp. 2538-2542.

[8] M. Harfman Todorovic, L. Palma and P. Enjeti, "Design of a wide input range DC-DC converter with a robust power control scheme suitable for fuel cell power conversion," in *19th Annu. Applied Power Electronics Conf*., 2004, vol. 1, pp. 374-379.

[9] S.-G. Song, F.-S. Kang, S.-J. Park, C.-J. Moon and G.-J. Son, "Zero-voltage and zero current switched fuel cell powered DC-to-DC converter," in *Int. Symp. Signals, Circuits and Systems*, 2007, pp. 1-4.

[10] W. Choi, P. Enjeti and J.W. Howze, "Fuel cell powered UPS systems: design considerations," in *34th Annu. Power Electronics Conf*., 2003, vol. 1, pp. 385-390.

[11] Q. Zhao, F. Tao and F.C. Lee, "A front-end DC/DC converter for network server applications," in *32nd Annu. Power Electronics Specialists Conf*., 2001, vol. 3, pp. 1535-1539.

[12] R. Erickson and D. Maksimovic, “Inductor Design,” in *Fundamentals of Power Electronics*, 2nd ed. Norwell Massachusetts: Kluwer Academic Publishers, 2001, pp. 543-545.

[13] A. Pressman, “Transformer and Magnetics Design,” in *Switching Power Supply Design*, 2nd ed. New York: McGraw-Hill, 1998, pp. 277-300.

VITA

Name:	Daniel Alan Humphrey
Address:	Hewlett-Packard Company 11445 Compaq Center Dr W MS:M0702-704 Houston, TX 77070
Education:	B.S., Electrical Engineering, Texas A&M University, 2004 M.S., Electrical Engineering, Texas A&M University, 2008